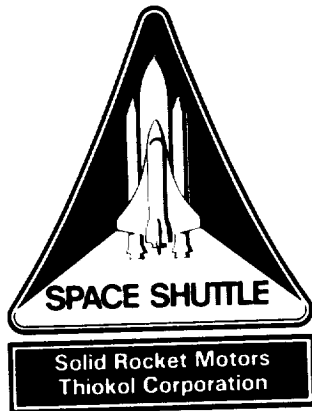


CR-184186



TWR-61561

TECHNICAL EVALUATION MOTOR NO. 7 (TEM-07)
INTERIM REPORT (60 day)

8 February 1991

Prepared for:

**NATIONAL AERONAUTICS AND SPACE ADMINISTRATION
GEORGE C. MARSHALL SPACE FLIGHT CENTER
MARSHALL SPACE FLIGHT CENTER, ALABAMA 35812**

Contract No. NAS8-30490
DR. No. 5-3
WBS.No. HQ601-20-10
ECS No. 1028

***Thiokol* CORPORATION**
SPACE OPERATIONS

P.O. Box 707, Brigham City, UT 84302-0707 (801) 863-3511

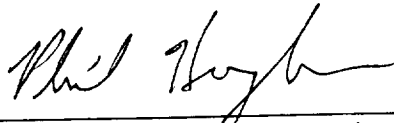
(NAS8-30490) TECHNICAL EVALUATION MOTOR
NO. 7 (TEM-07) INTERIM REPORT (Thiokol
CORP.)

N01-30461

03/20 005774
unclass

Technical Evaluation Motor No. 7 (TEM-07)
Interim Report (60 day)

Prepared by:

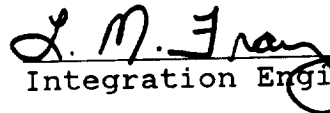


Certification Planning
Systems Engineer

Approved by:



Certification Planning
Supervisor



Integration Engineer



Program Manager



Data Management/Release

ECS# SS1028

Major contributors to this report were:

Instrumentation:	D. South
Case/Leak Check/Seals:	T. Swauger, R. Ash, G. Abawi
Insulation:	J. Passman, S. Manz
Nozzle:	R. George, R. Lange, F. Weiler
Joint Protection Systems:	C. Prokop, K. Rees
Ballistics/Mass Properties:	A. Drendel
Aero/Thermal:	R. Buttars, E. Mathias, D. Ruddell
Structural Analysis:	M. Fairbourn, D. Bright
Postfire Hardware Evaluation:	J. Curry
Photo Instrumentation:	C. Larsen

ABSTRACT

Technical Evaluation Motor No. 7 (TEM-7) was a full scale, full-duration static test firing of a high performance motor (HPM) configuration solid rocket motor (SRM) with nozzle vectoring. The static test fire occurred on 11 December 1990 at the Thiokol Corporation Static Test Bay T-97.

This interim test report documents the procedures, performance and results available through 22 January 1991. Critical post test hardware activities and assessment of test data are not complete in time to support a complete final test report submittal 60 days after the test date. A complete final test report will be submitted no later than 19 April 1991.

Included are a presentation and discussion of the TEM-7 performance, anomalies, and test result concurrence with the objectives outlined in CTP-0107 Revision A, Space Shuttle Technical Evaluation Motor No. 7 (TEM-07) Static Fire Test Plan.

CONTENTS

<u>Section</u>	<u>Page</u>
1.0 INTRODUCTION	1
1.1 TEST ARRANGEMENT AND FACILITIES	3
1.2 TEST ARTICLE DESCRIPTION	3
1.2.1 Case/Seals	4
1.2.2 Internal Insulation/Liner/Inhibitor	12
1.2.3 Propellant	13
1.2.4 Ignition System	13
1.2.5 Nozzle/TVC	13
1.2.6 Leak Check Port Plugs	19
1.2.7 Adjustable Vent Port Plugs	19
1.2.8 Joint Protection System	19
2.0 TEST OBJECTIVES	20
3.0 EXECUTIVE SUMMARY	22
4.0 INSTRUMENTATION	23
4.1 INTRODUCTION	23
4.1 OBSERVATIONS	23
5.0 PHOTOGRAPHY	24
5.1 STILL PHOTOGRAPHY	24
5.2 MOTION PICTURES	24
6.0 TEST RESULTS	27
6.1 CASE PERFORMANCE	27
6.1.1 Introduction	27
6.1.2 Observations	27
6.2 CASE INTERNAL INSULATION PERFORMANCE	29
6.2.1 Introduction	29
6.2.2 Observations	29
6.3 SEALS/LEAK CHECK PERFORMANCE	36
6.3.1 Introduction	36
6.3.2 Observations	37
6.4 NOZZLE ASSEMBLY PERFORMANCE	43
6.4.1 Introduction	43
6.4.2 Observations	43
6.4.3 TEM-07 Nozzle Strain Gage Response Summary	46
6.4.4 Nozzle TVC Performance	47
6.5 IGNITION SYSTEM PERFORMANCE	48
6.5.1 Introduction	48
6.5.2 Observations	48
6.6 JOINT PROTECTION SYSTEMS PERFORMANCE	52
6.6.1 Introduction	52
6.6.2 Observations	52

CONTENTS (cont)

<u>Section</u>	<u>Page</u>
6.7 BALLISTICS/MASS PROPERTIES PERFORMANCE	53
6.7.1 Introduction	53
6.7.2 Objectives	53
6.7.3 Conclusions/Recommendations	53
6.7.4 Observations	54
6.8 STATIC TEST SUPPORT EQUIPMENT	80
6.8.1 Introduction	80
6.8.2 Observations	80
7.0 APPLICABLE DOCUMENTS	81

FIGURES

<u>Figure</u>		<u>Page</u>
Figure 1-1.	TEM-7 Test Article	5
Figure 1-2.	Stiffener Stub Outer Ligament Cracks and Instrumentation	6
Figure 1-3.	Stiffener Stub Outer Ligament Cracks and Instrumentation	7
Figure 1-4.	Stiffener Stub Outer Ligament Cracks and Instrumentation	8
Figure 1-5.	TEM-07 Field Joint Configuration	9
Figure 1-6.	TEM-7 (HPM Modified) Nozzle-to-Case Joint Configuration	10
Figure 1-7.	Cowl Liner/Flex Bearing Thermal Protector Area Configuration Changes	15
Figure 1-8.	Improved Nose Cowl Assembly Method	16
Figure 1-9.	Fixed Housing and Boot Cavity Instrumentation	17
Figure 1-10.	Thrust Vector Actuation (TVA) System	18
Figure 5-1.	T-97 Photography Coverage - TEM-07	26
Figure 6-1.	HPM Field Joint	30
Figure 6-2.	Clevis Joint Filler Putty Layup	31
Figure 6-3.	Assembled HPM Field Joint	32
Figure 6-4.	TEM-7 (HPM Modified) Case-to-Nozzle Joint Configuration - Putty Layup	33
Figure 6-5.	Ignition System Components and Seals	49
Figure 6-6.	Standard HPM Igniter System	50
Figure 6-7.	S&A Device Configuration	51
Figure 6-8.	TEM-7 Predicted and Measured Pressure at 65 Deg. F	61
Figure 6-9.	TEM-7 Reconstructed and Measured Pressure at 65 Deg. F	62
Figure 6-10.	Reconstructed Vacuum Thrust at 65 Deg. F	63
Figure 6-11.	Comparison of Reconstructed and Measured Aft-End Pressure	64
Figure 6-12.	Measured Head-End Pressure Transients	69
Figure 6-13.	TEM-7 Igniter Reconstructed at 80 Deg. F within Specification Limits	70
Figure 6-14.	TEM-7 Igniter Pressure vs. Head-End and Nozzle Stagnation Pressure	71
Figure 6-15.	TEM-7 Measured Head-End and Nozzle Stagnation Pressure Time Histories	72
Figure 6-16.	TEM-7 Waterfall Plot for PNCAC001	74
Figure 6-17.	TEM-7 Maximum Oscillation Amplitudes for PNCAC001 1-L Acoustic Mode	75
Figure 6-18.	TEM-7 Maximum Oscillation Amplitudes for PNCAC002 2-L Acoustic Mode	76
Figure 6-19.	TEM-7 Reconstructed Thrust Compared to CEI Specification Limits	77

TABLES

<u>Table</u>		<u>Page</u>
Table 1-1.	TEM-07 Segment History	3
Table 5-1.	Photography and Video Coverage	25
Table 6-1.	TEM-7 Seal Leak Testing	37
Table 6-2.	TEM-7 Case Field Joint Leak Test Results	38
Table 6-3.	TEM-7 Igniter and S & A Leak Test Results	38
Table 6-4.	TEM-7 Nozzle-to-Case Leak Test Results	39
Table 6-5.	TEM-7 Nozzle Internal Joint Leak Test Results	39
Table 6-6.	Summary of Measured Ballistic and Nozzle Performance Data	55
Table 6-7.	Burn Rate Data Comparison Subscale to Full-Scale	66
Table 6-8.	Historical Three Point Average Thrust and Pressure Rise Rate Data	67
Table 6-9.	Measured SRM Ignition Performance Data at 65 °F	68
Table 6-10.	Maximum Pressure Oscillation Amplitude Comparison	78

1.0 INTRODUCTION

Technical Evaluation Motor No. 7 (TEM-7) was successfully static test fired at 1300 hours on 11 December 1990 at the Thiokol Corporation Static Test Bay T-97. The ambient temperature at the time of the test was 43.7 °F and the propellant mean bulk temperature was 65 °F. Ballistics performance values were within the specified requirements.

TEM-7 was a full scale, full-duration static test fire of a high performance motor (HPM) configuration solid rocket motor (SRM). TEM-7 was the first full scale test motor on which all segments were more than five years old and the first TEM static test motor with nozzle vectoring. The TEM-8 static test motor will also be vectored. The TEM-7 test arrangement included the Modified Aft End Heating System (MAEHS) normally used for static tests with vectored nozzles plus a nozzle to case joint heater normally used for TEM static tests.

The primary purpose of TEM static tests is to recover SRM case and nozzle hardware for use in the RSRM flight program; however, TEM static tests also provide windows of opportunity to evaluate or certify various design, process, and supplier issues for the RSRM flight program. Accordingly, TEM-7 was the first full scale static test for qualification of North American Rayon Corporation (NARC) rayon in all nozzle carbon cloth phenolic (CCP) liners. Two additional full scale nozzles will be statically tested for qualification of the NARC rayon as outlined in the second source rayon program plan, TWR-18965. Low cost nozzle improvements, previously incorporated into the TEM-6 static test, to be qualified on TEM-7 included a change in the carbon cloth phenolic (CCP) liner ply angle of the cowl, improved inner and outer boot ring phenolic cure cycles, and an extended belly band flexible bearing protector design.

Inspection and instrumentation data indicate that the TEM-7 static test firing was successful. Instrumentation measurements consisted of forward and aft end chamber pressure; igniter chamber pressure; forward and aft pressure chamber pressure oscillations; stiffener stub strains; nozzle components temperatures and strain; temperature for deluge control; nozzle deflections; nozzle boot cavity temperature and pressure; plume radiation measurements; test stand water deluge pressure; and timing.

Overall, the postburn condition of the NARC rayon nozzle liners was very good (TWR-61490). Only two small, shallow wash areas were found on the aft exit cone liner, but no surface ply lifting was observed. The erosion of the throat and throat inlet rings was smooth with the typical rippled erosion pattern occurring on the aft 6 inches of the throat ring (0.1 inch deep maximum). The post burn mean throat diameter was 56.07 inches.

This is within the historical database of RSRM/HPM throat diameters. The preliminary throat erosion rate was 9.17 mils/sec. Typical minor wash areas (0.1 inch deep maximum) were observed on the forward portions of the nose cap. The cowl ring erosion was smooth and did not exhibit the typical wash areas seen on RSRM (0 degree ply wrap) cowls.

All postfire flow surface gaps between phenolic components were uniform around the circumference and were within the historical database. There was no indication of movement of the nose cap and the bondline between the cowl and outer boot ring was still intact.

TEM-7 was instrumented with four (4) aft end chamber pressure transducers installed through special instrumentation holes drilled through the fixed housing and phenolic insulation. TEM-6 also contained this arrangement. The objective of this instrumentation was to obtain aft end chamber pressures for ballistics modelling and pressure oscillations.

On TEM-7, aft end pressure plots showed spikes shortly after ignition. Upon removal of the pressure transducers, the ends were found charred and heat effected. After removal of the nozzle, the fixed housing phenolic insulation was found to be shifted forward (unbonded) approximately 0.20 inch from the metal fixed housing. After nozzle disassembly, the fixed housing phenolic insulation was found to be almost 100% adhesive unbonded from the metal.

By comparison, TEM-6 aft end pressures were as predicted, with slag plugging the holes randomly after T+20 sec. Plugging of the instrumentation holes was expected. The TEM-6 pressure transducers were found to be in excellent condition upon removal with no indications of leakage or gas flow.

TEM-7 was configured with a bearing protector in which the belly band was lengthened and thickened. The belly band was extended to place the region of maximum erosion in the thickened portion of the bearing protector. On TEM-7 the belly band was additionally thickened to accomodate potential for increased erosion due to enlarged cowl vent holes. After removal of the TEM-7 fixed housing from the bearing, the bearing protector was found to be deeply eroded in the areas where gas impinged from the cowl vent holes. Maximum erosion was centered in this lengthened and thickened belly band region of the bearing protector.

Preliminary observations indicate that performance of the improved cowl assembly process (Joint #2) was excellent.

TEM-7 postfire inspection procedures followed TWR-60273 and TWR-61209.

1.1 TEST ARRANGEMENT AND FACILITIES

The TEM-7 static test arrangement was assembled in accordance with Drawing 2U129760. T-97 was equipped with a water deluge system and a CO₂ quench. The test motor included an SRB aft skirt assembly which contains the TVC subsystem and the heat shield installation. The Thrust Vector Actuation (TVA) System is comprised of two SRB actuators and two Hydraulic Power Units (HPU) located in the aft skirt. The HPU Ground Test Controller, HPU Manual/ Automatic Panel (MAP) and the Ascent Thrust Vector Control units (ATVC) serve as the control units for the TVC subsystem.

1.2 TEST ARTICLE DESCRIPTION

The TEM-7 test assembly was in accordance with Drawing 7U76879. The motor was instrumented to provide data to satisfy the test objectives. An overall view of the test article is shown in Figure 1-1. A TEM-7 drawing tree is included in Appendix A.

TEM-7 consisted of HPM-configuration motor segments which were fabricated and loaded with propellant more than five years before the static test fire on 11 December 1990. A listing of each segment, segment flight identification, cast date, and storage and transportation history is shown in Table 1-1.

Table 1-1. TEM-07 Segment History

TEM-07 Segment	Forward	Fwd Ctr	Aft Ctr	Aft
Flight Identification	SRM 28B	SRM 28B	SRM 28B	SRM 26A
Casting Date	24 Sep 85	21 Oct 85	14 Oct 85	17 Jul 85
Shipped to KSC	31 Jan 86	10 Jan 86	7 Jan 86	26 Dec 85
Shipped to Thiokol	27 Mar 87	18 Jan 89	25 Jul 89	24 Mar 88
Arrived at Thiokol	10 Apr 87	25 Jan 89	31 Jul 89	10 Apr 88
Shipped to KSC	10 Jun 87	-	-	-
Shipped to Thiokol	22 Feb 89	-	-	-
	29 Feb 89	-	-	-

The High Performance SRM static test motor consisted of a lined, insulated, segmented rocket motor case loaded with solid propellant; an ignition system complete with electro-mechanical safety and arming device, initiators and loaded igniter; movable nozzle with flexible bearing and exit cone. For this test, the nozzle was vectored.

The assembled static test motor was approximately 116 feet in length and 12 feet in diameter. The test item configuration was controlled by released engineering drawings (reference TEM-7 Drawing Tree) and the test plan, CTP-0107, Revision A. Deviations to this configuration were processed through the normal configuration control system and approved by the Integration Engineer, Program Manager and NASA, and will be documented in the final test report.

1.2.1 Case/Seals

The Case consisted of 11 individual weld-free segments: the forward dome, six cylinder segments, the ET attach segment, two stiffener segments and the aft dome. The 11 segments were preassembled into four subassemblies to facilitate propellant casting.

The four loaded assemblies were the forward segment assembly (Drawing 7U76899), the forward center segment assembly (Drawing 1U52566), the aft center segment assembly (Drawing 1U52566), and the aft segment assembly (Drawing 7U76882). These segments were joined by means of tang and clevis field joints, which in turn, were held in place by pins.

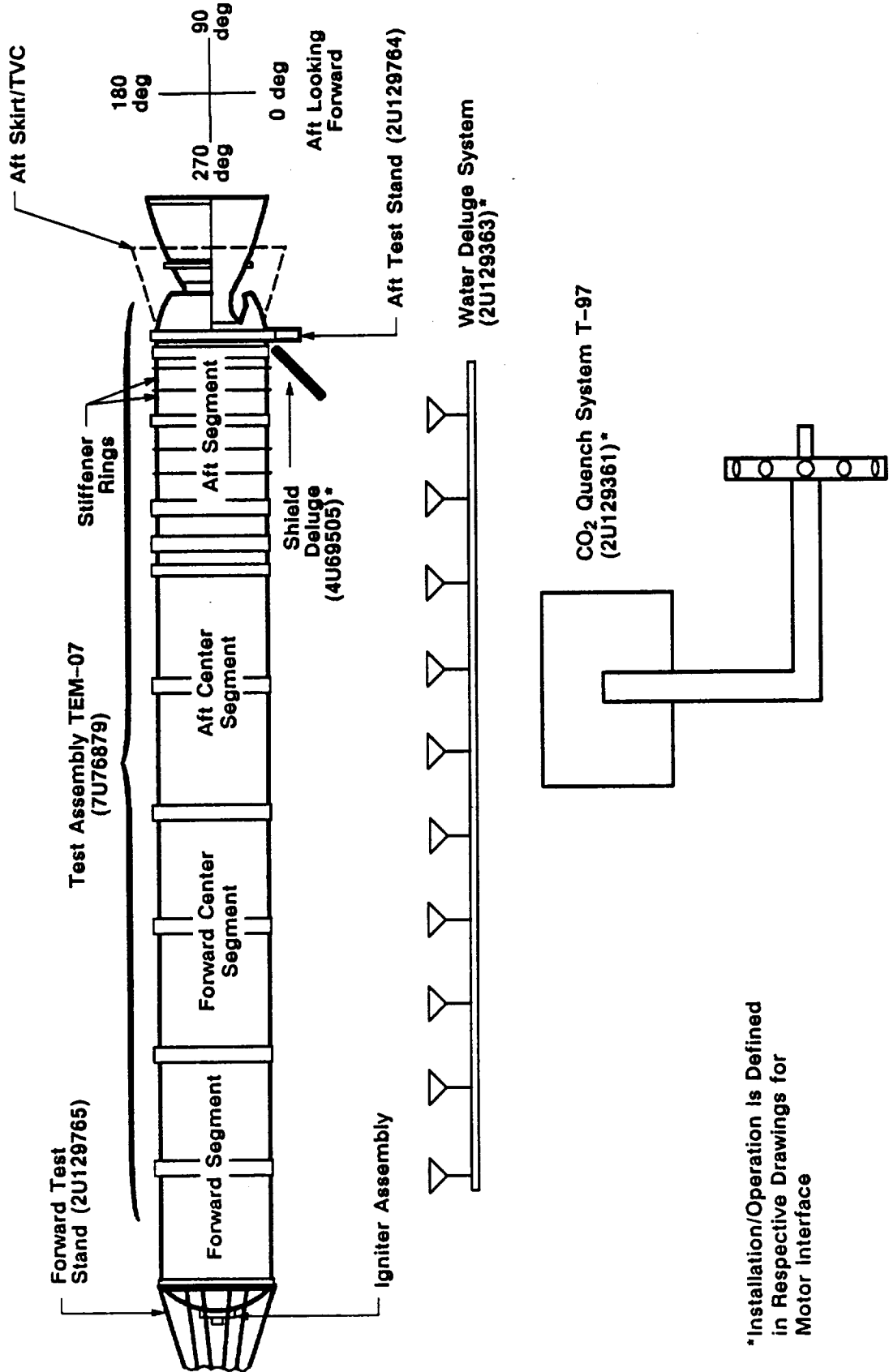
Stiffener rings were installed on both flanges of the aft stiffener cylinder (1U50185-06, S/N 027). These flanges have outer ligament cracks:

- 1) At 240 degrees on aft stub
- 2) At 276 degrees on aft stub (saw cut through)
- 3) At 278 degrees on aft stub
- 4) At 280 degrees on aft stub
- 5) At 282 degrees on aft stub
- 6) At 232 degrees on forward stub
- 7) At 288 degrees on forward stub (not instrumented)

Instrumented outer ligament cracks and instrumented referee holes are illustrated in Figures 1-2, 1-3 and 1-4.

Systems tunnels were removed from the aft center segment and partially removed from the aft segment for this test.

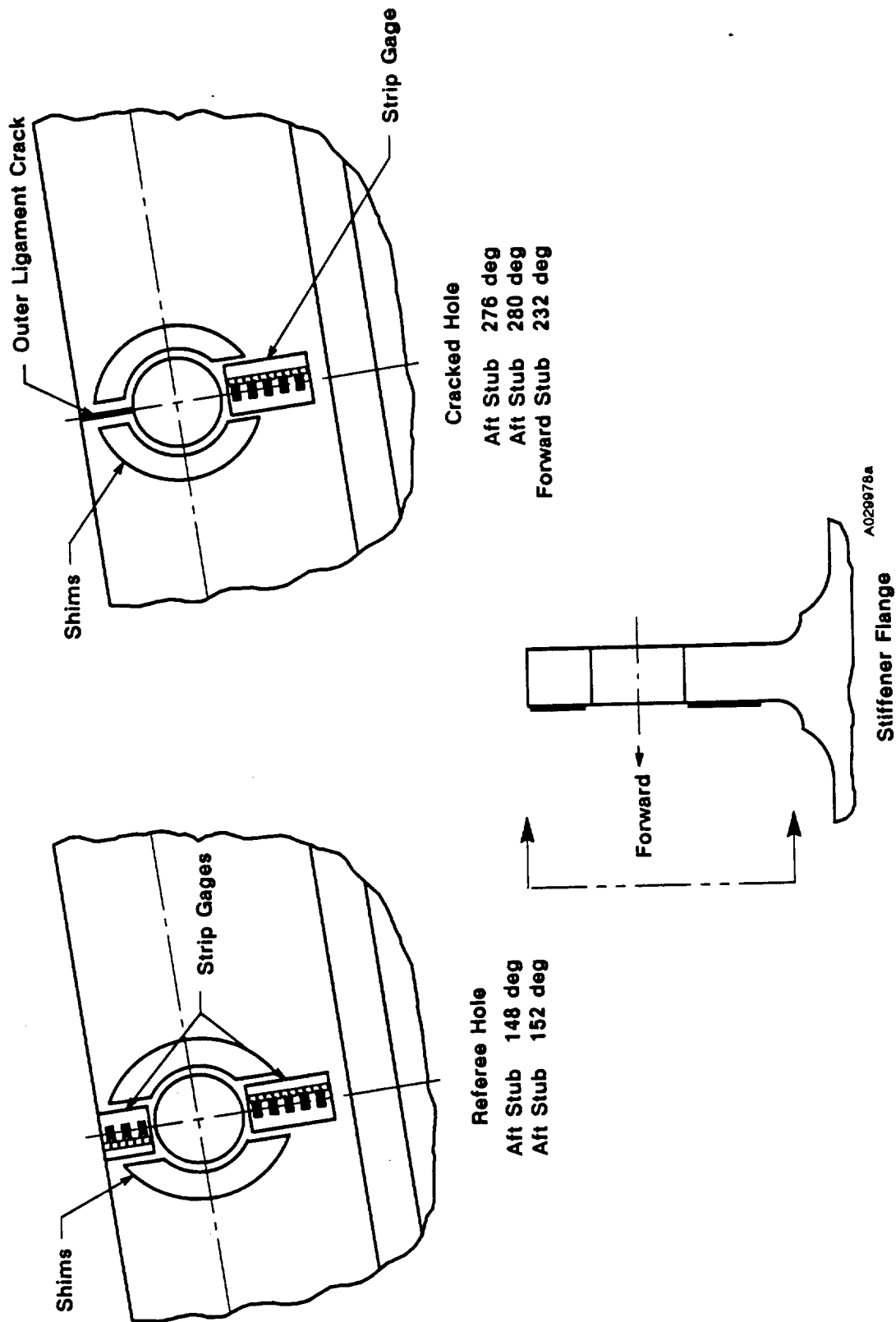
The nozzle to case joint was formed by bolting the HPM nozzle fixed housing into the aft dome with 100 axial bolts. The field joints had a standard HPM insulation configuration as shown in Figure 1-5. The nozzle to case joint had the standard HPM nozzle joint insulation configuration as shown in Figure 1-6.



*Installation/Operation Is Defined
in Respective Drawings for
Motor Interface

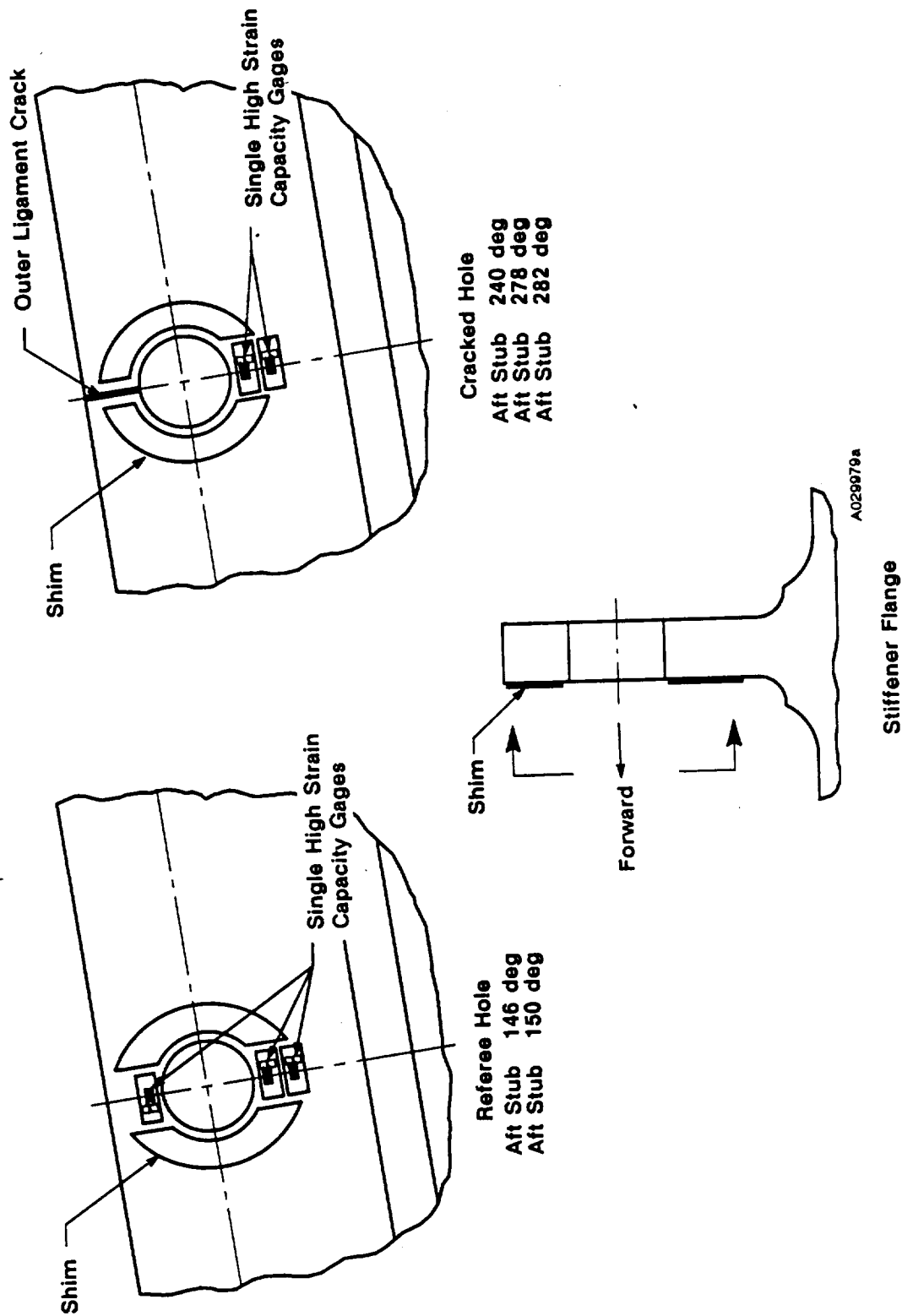
Figure 1-1. TEM-07 Static Test Arrangement

A026864aR1



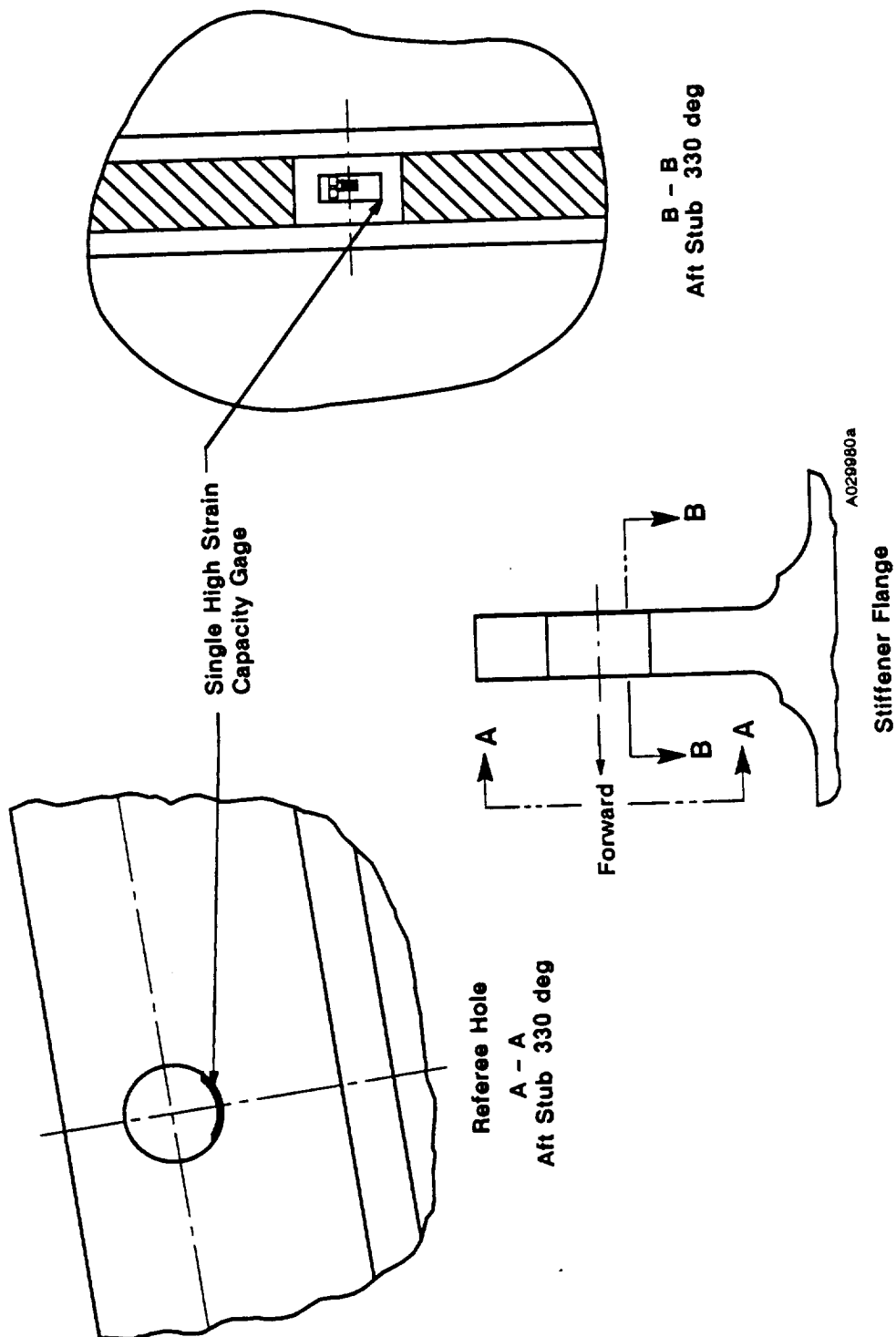
Note: All gages oriented to measure hoop strains

Figure 1-2. Stiffener Stub Outer Cracks and Instrumentation



Note: All gages oriented to measure hoop strains

Figure 1-3. Stiffener Stub Outer Ligament Cracks and Instrumentation



Note: All gages oriented to measure hoop strain

Figure 1-4. Stiffener Stub Outer Ligament Cracks and Instrumentation

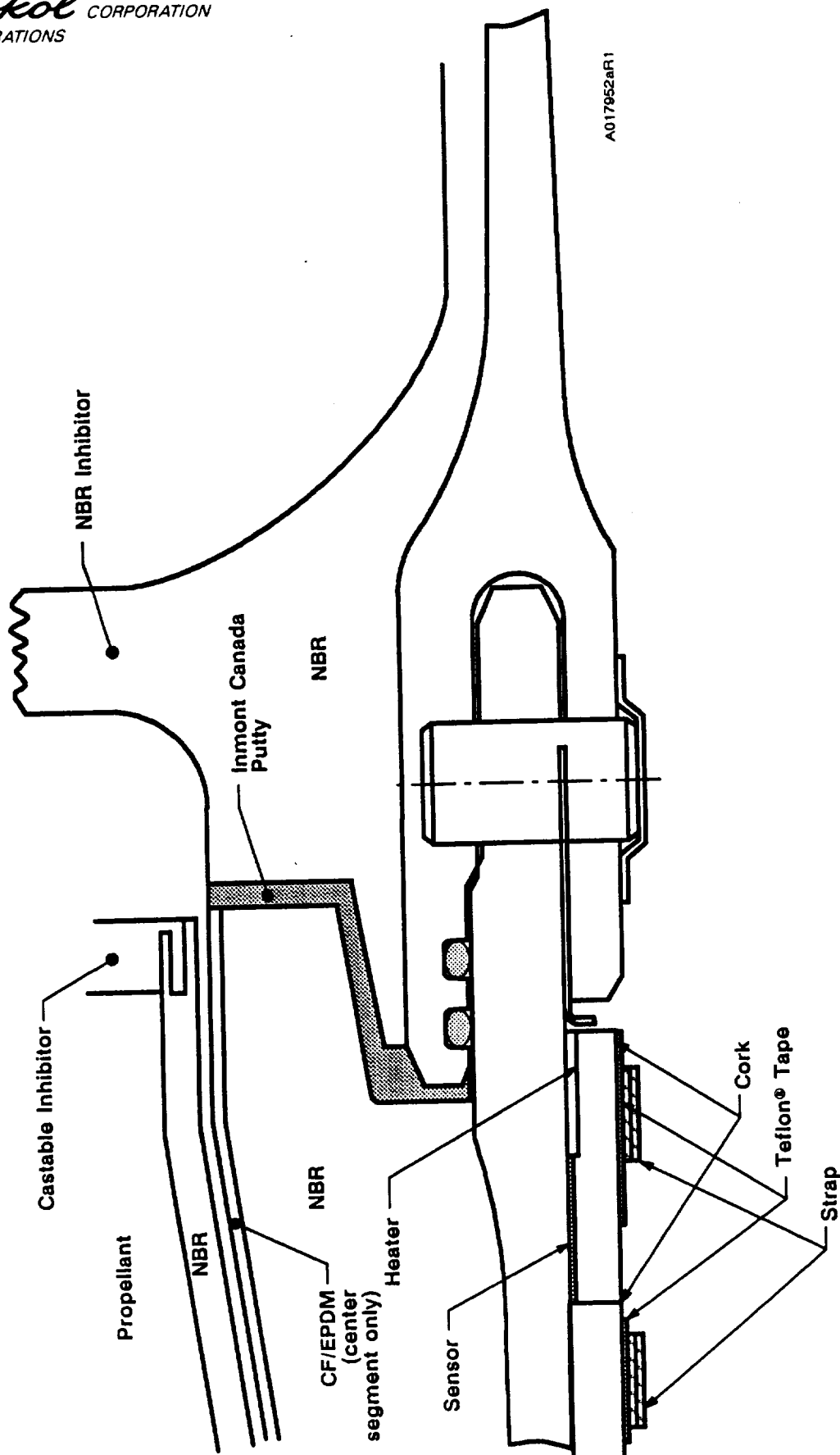


Figure 1-5. TEM-07 Field Joint Configuration

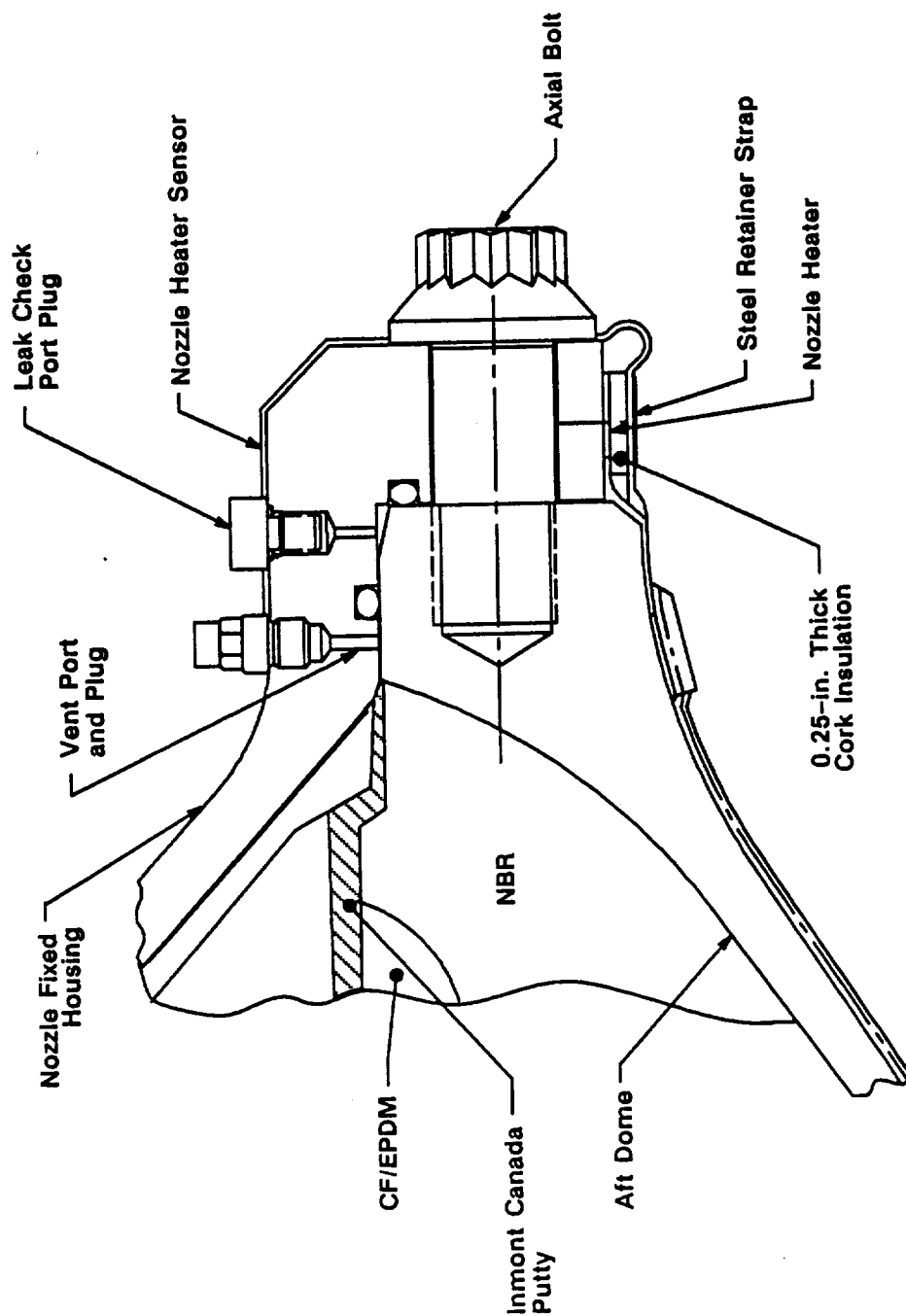


Figure 1-6. TEM-07 (HPM Modified) Nozzle-to-Case Joint Configuration

The assembly and joint configuration were as follows:

- A. Forward segment and forward center segment were mated to form the forward field joint. The forward center segment and aft center segment were mated to form the center field joint. The aft center segment and aft segment were mated to form the aft field joint. The field joints which connected these segments were configured with:
- o Tang and clevis with long pins (Drawing 1U51055), custom-fit shims (Drawing 1U51899), and hat band pin retainers (Drawing 1U82840).
 - o Standard HPM insulation configuration with putty joint filler (STW4-3266) as shown in Figure 1-5.
 - o Primary and Secondary O-rings were Fluorocarbon (STW4-3339).
 - o Leak check port plugs (Drawing 1U100269)
 - o Improved field joint heater (Drawing 1U77252).
 - o Baseline TEM field joint protection system (Drawing 7U77328).
- B. Factory joints were configured with the following:
- o HPM tang and clevis hardware design.
 - o Insulation overlaid and cured over interior of the joint.
 - o HPM pin retainer centered over the short (HPM) pins. Standard shim clips were used between the clevis outer leg and the tang OD.
- C. The nozzle to case joint was configured with:
- o Primary (larger diameter RSRM) and secondary O-ring seals were Fluorocarbon (STW4-3339).
 - o Standard HPM nozzle joint insulation configuration with putty joint filler (STW4-3266) as shown in Figure 1-6.
 - o RSRM configuration ultrasonic preload axial bolts installed in accordance with dwg 7U76882.
 - o MS16142 vent ports at 15, 105, 195 and 285 degrees in the fixed housing (7U76865-02) upstream of the primary O-ring.

- o Adjustable vent port plugs and closure screw (Drawings 1U76425 and 1U50159).
 - o Leak check port plug (Drawing 1U100269)
 - o Redesigned nozzle to case joint heater (7U77118-04)
- D. Igniter to forward dome joint was configured with:
- o Primary and secondary seals of the outer gasket (Drawing 1U51927) are fluorocarbon.
 - o Improved igniter to case joint heater (Drawing 1U77253).
 - o Putty joint filler (STW4-3266).
 - o Ultrasonic bolts (Drawing 1U76598) inner and outer bolt circle

Corrosion protection consisted of full external paint and a film of grease applied as specified in Drawing 7U76881 and STW7-3688 (including O-rings, sealing surfaces, and pin holes).

1.2.2 Internal Insulation/Liner/Inhibitor

The internal insulation system included case acreage insulation, joint insulation and propellant stress relief flaps. The insulation material used for these components was an asbestos silica filled acrylonitrile butadiene rubber (NBR) (STW4-2621). Carbon fiber filled ethylene propylene diene monomer (CF/EPDM) (STW4-2868) was bonded to the NBR in a sandwich type construction under the propellant stress relief flaps in both center segments. CF/EPDM was also used in sandwich construction in the aft dome. The CF/EPDM was installed to reduce the erosion of the insulator near the submerged nozzle in the aft dome and under the stress relief flaps in the center segments.

The liner material specified in STW5-3224 was an asbestos-filled carboxyl terminated polybutadiene (CTPB) polymer which bonded the propellant to the internal insulation in the SRM. The forward facing full web inhibitors were made of NBR. They were located on the forward end of the center and aft segments. The aft facing partial web castable inhibitors were made of a material (STW5-3223) similar in type (CTPB polymer) to the liner. They were HPM configuration and were located on the aft end of the forward and center segments.

Field joints and nozzle to case joint are HPM configuration and were filled with putty and tamped following assembly to repair defects and reduce the potential for blow holes.

1.2.3 Propellant

SRM propellant, TP-H1148 (STW5-3343), is a composite type solid propellant, formulated of polybutadiene acrylic acid acrylonitrile terpolymer binder (PBAN), epoxy curing agent, ammonium perchlorate oxidizer and aluminum powder fuel. Approximately 0.21% by weight (exact amount determined by standardization) of burning rate catalyst (iron oxide) was added to achieve the targeted propellant burning rate of 0.368 in/sec at 625 psia and 60 °F (TWR-19121 and TWR-19838).

The propellant grain design consisted of an eleven-point star with a smooth bore to fin cavity transition region that tapered into a circular perforated (CP) configuration in the forward segment (Drawing 1U52565). The two center segments (Drawing 1U52566) were double-tapered CP configurations and the aft segment (Drawing 1U52757) was a triple-taper CP configuration with a cutout for the partially submerged nozzle.

1.2.4 Ignition System

The SRM ignition system was a modified HPM igniter assembly (Drawing 1U50776). It contained a single nozzle, steel chamber, external and internal insulation, and solid propellant, TP-H1178 (STW5-2833), igniter containing a case bonded 40-point star grain.

The forward mounted solid rocket type igniter (Drawing 1U50776) was modified with a CO₂ quench port. Ultrasonically torqued bolts fastened the igniter adapter to the igniter chamber. A286 bolts in the igniter adapter to case joint were replaced with higher strength MP159 bolts which were ultrasonically preloaded to a higher level.

A Safe and Arm (S&A) device (1U52295-04) which utilizes Krytox grease to lubricate the Barrier-Booster shaft O-rings was installed on the igniter.

Velostat or pink poly plastic sheets were wrapped and tightly sealed around the forward thrust adapter to simulate the thermal protection provided to the igniter and S&A by flight configuration.

1.2.5 Nozzle/TVC

The nozzle assembly (Drawing 7U76738) was a partially submerged convergent/divergent movable design with an aft pivot point flexible bearing (Drawing 1U52840). The phenolic liners were RSRM configuration with exceptions defined by the Low Cost Improvement Program Plan TWR-19524B. All metal hardware was RSRM except for the fixed housing which was HPM modified configuration to mate with the HPM aft segment.

The nozzle incorporated North American Rayon Corporation Corporation rayon into all carbon cloth phenolic liners (Drawings 7U76736, 7U76608, 7U76609, 7U76865, 7U77266, 7U77267, 7U77310).

The nozzle included changes in accordance with Low Cost Improvement Program Plan TWR-19524B and MSFC directives as follows:

- o Minus 50 degree ply angle change on cowl (Drawing 7U76609) second wrap
- o Full cure on CCP first wrap outer boot ring (Drawing 7U76608)
- o Delayed pressure cure on glass cloth phenolic (GCP) inner boot ring (Drawing 7U76608)
- o Bearing protector thickness/location modification (Drawing 7U76864) as shown in Figure 1-7
- o Improved nose to cowl assembly process (Figure 1-8)
- o Boot cavity pressure (Drawings 7U76827, 7U76983) and temperature measurement instrumentation (Figure 1-9)
- o Fixed housing pressure (Drawing 7U76902) measurement instrumentation (Figure 1-9)

The 36 vent holes in the cowl were increased in size from a nominal 0.312 inch diameter to a 0.375 inch diameter to alleviate boot cavity differential pressure. Supporting analyses for this change were documented in TWR-60857, Cowl Vent Hole Study and TEM-02 nozzle boot cavity pressurization. The flexible bearing protector (Drawing 7U76864) was thickened in the belly band region from a 0.67 inch minimum to a 1.0 inch minimum to accommodate any potential for increased erosion due to the larger vent holes.

Four MS-16142 type vent ports were machined into the nozzle fixed housing (7U76865-01) forward of the primary O-ring to facilitate venting of the cavity between the joint putty and the primary O-ring when assembling the nozzle to the case.

The nozzle-to-case joint was assembled with RSRM axial bolts with preload measuring capability. The assembly preload was a nominal 120,000 lbs.

The Linear Shaped Charge was not added to the aft exit cone (Drawing 7U77267) assembly for this test.

The axial test motor included an SRB aft skirt assembly identified on MSFC-NASA Drawing 14A30649-02. The aft skirt assembly contained the TVC subsystem and the heat shield installation.

The Thrust Vector Actuation (TVA) System (Figure 1-10) was comprised of two SRB actuators and two Auxillary Power Units (APU) located in the aft skirt.

The APU Ground Test Controller, APU Manual/Automatic Panel (MAP) and the Ascent Thrust Vector Control units (ATVC) served as the control units for the TVC subsystem.

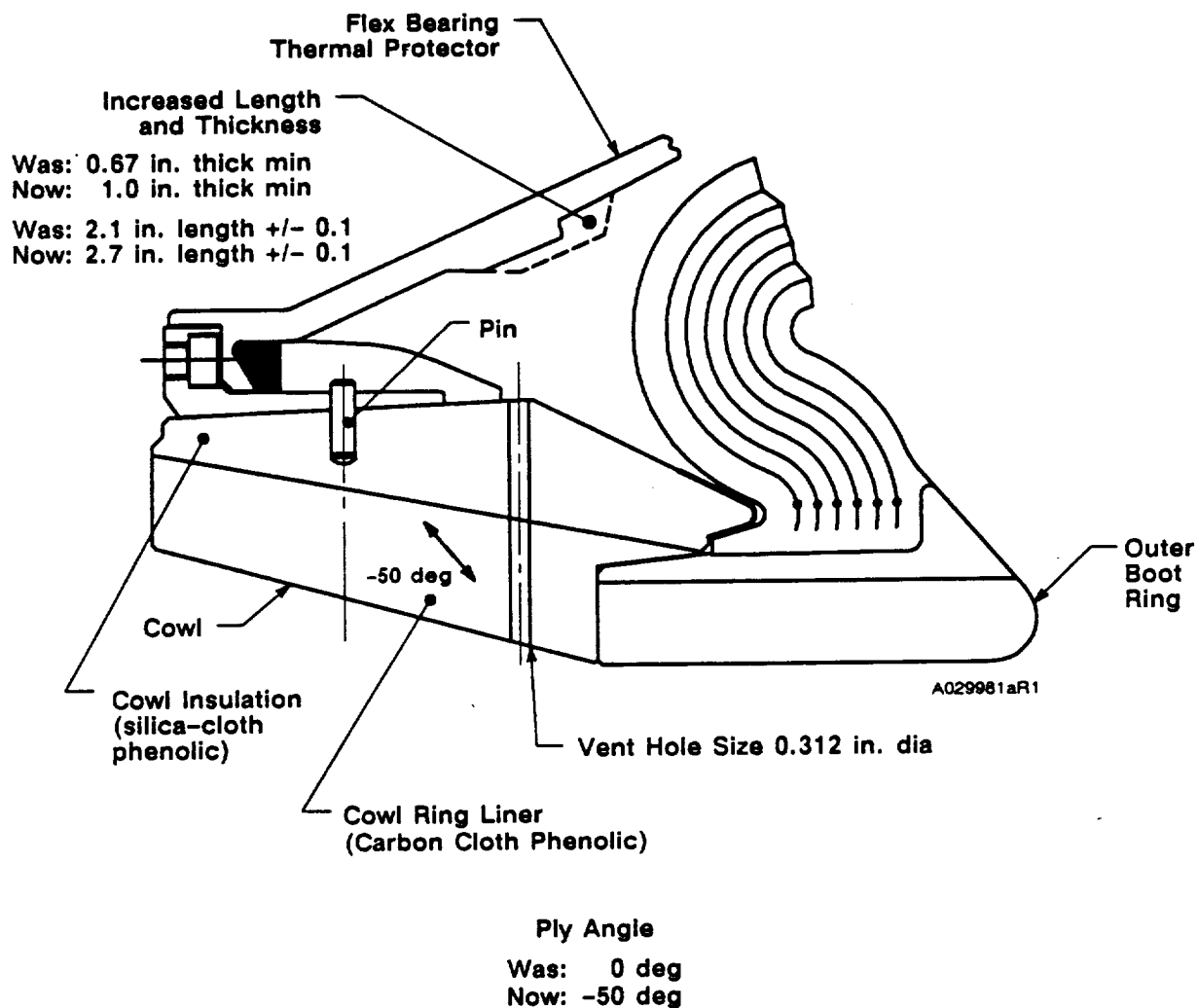
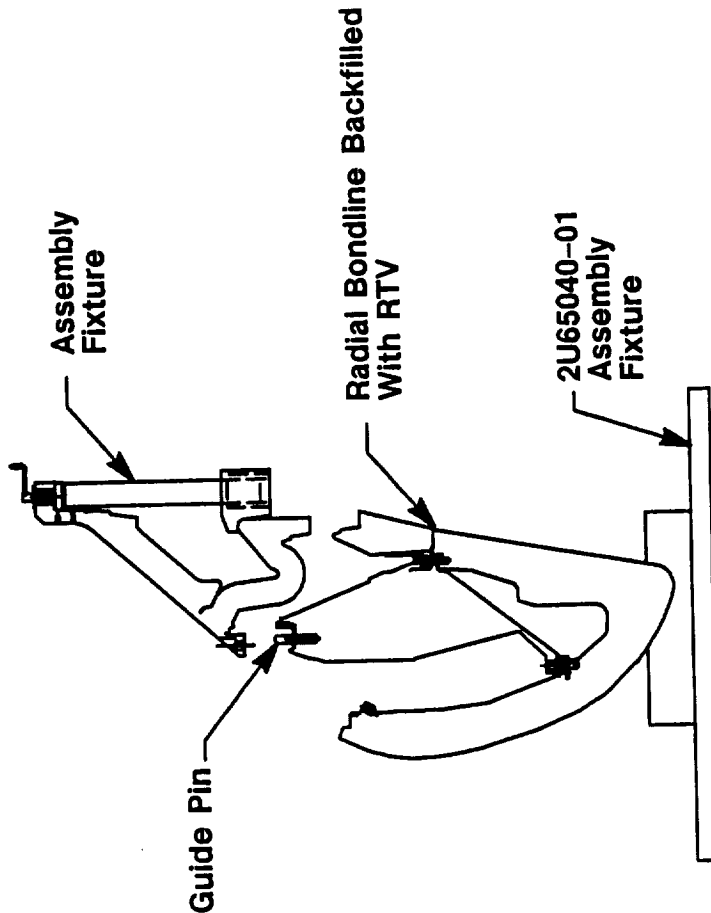


Figure 1-7. Cowl Liner/Flex Bearing Thermal Protector Area Configuration Changes

Improved Assembly Process



Current Assembly Process

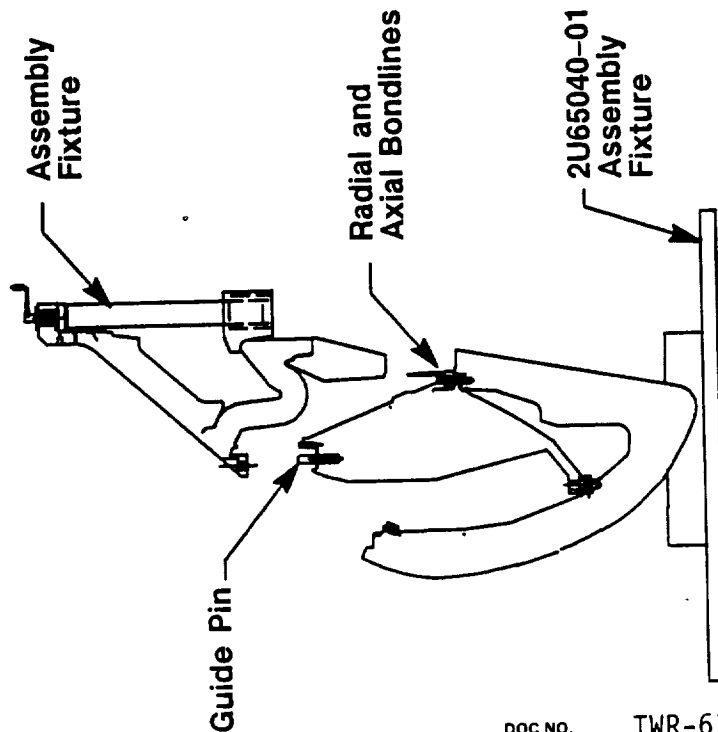
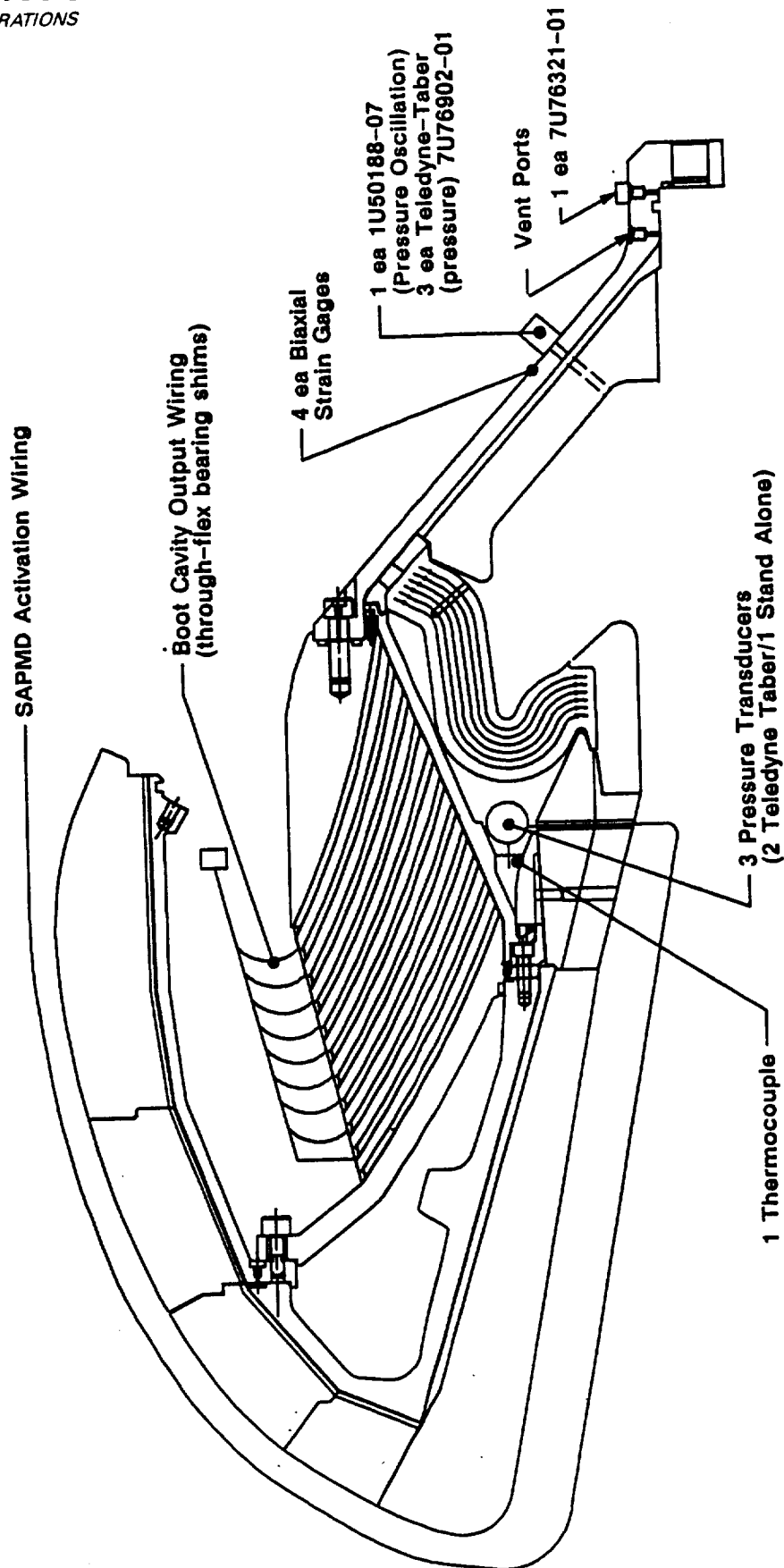


Figure 1-8. Improved Nozzle Cowl Assembly Method



A025667a

Figure 1-9. Fixed Housing and Boot Cavity Instrumentation

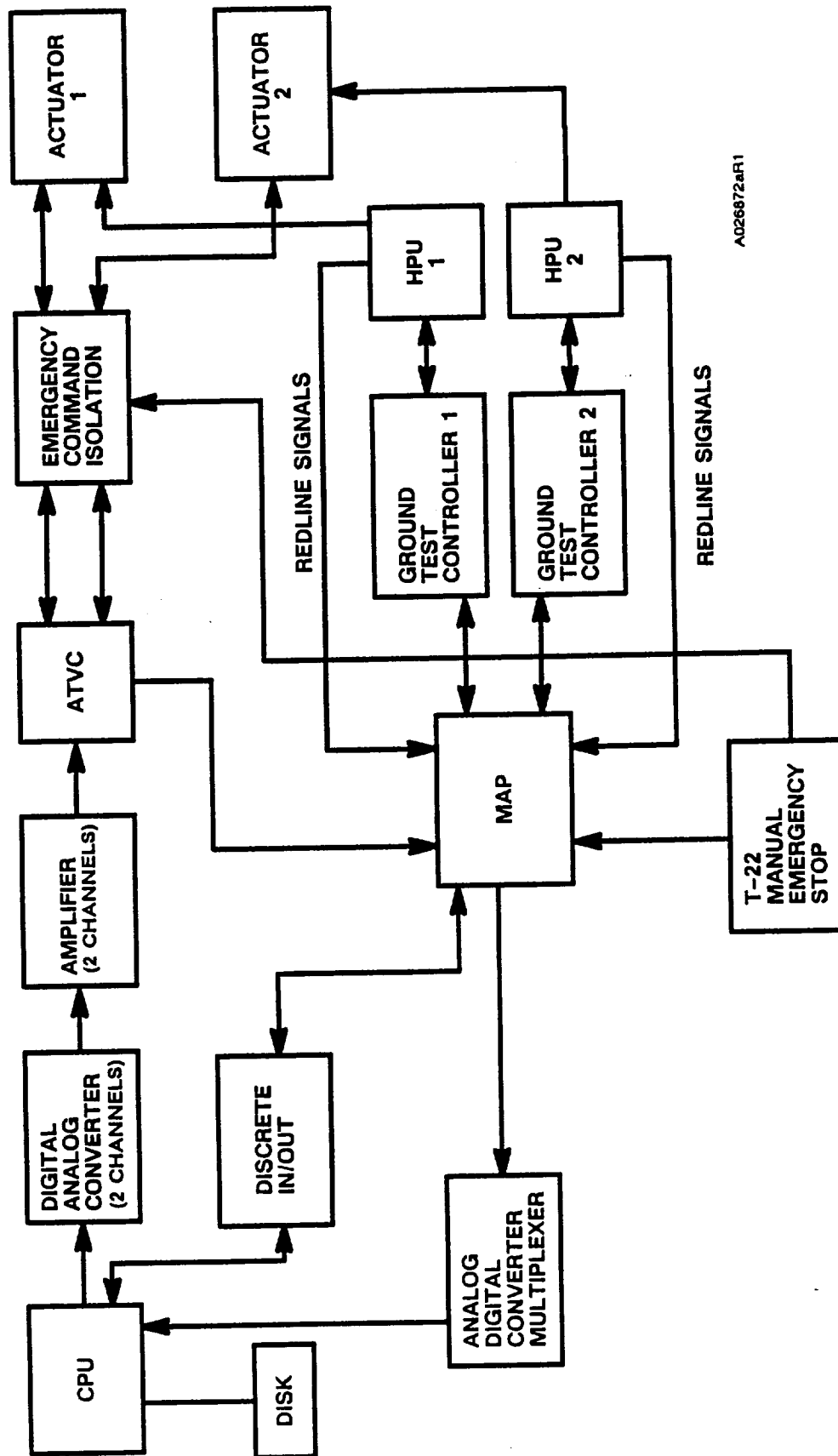


Figure 1-10. Thrust Vector Actuation (TVA) System

1.2.6 Leak Check Port Plugs

Leak check port plugs (1U100269-03) with the Nylock^R locking feature were installed in the leak check ports of all three field joints and the nozzle to case joint.

1.2.7 Adjustable Vent Port Plugs

Adjustable vent port plugs with the Nylok^R locking feature (1U76425-03 and -02) and closure plugs (Drawing 1U50159) were installed in the four RSRM vent ports of the nozzle fixed housing.

1.2.8 Joint Protection Systems

Field Joint Protection Systems Field joint heaters closeout (Drawing 7U77328, static test only) consisted of cork strips retained with Kevlar straps (TEMs 2, 3, 4 and partial 5 and 6). The external joint temperatures were sensed by two sensor assemblies mounted adjacent to the heater. Each assembly contained two resistance temperature detector (RTD) sensors.

Joint Heaters Improved field joint heaters (Drawing 1U77252), igniter to case joint heater (Drawing 1U77253) and nozzle to case joint heater (Drawing 7U77118) were installed as shown in Drawing 7U77328. These heaters consisted of redundant, chemically etched, foil circuits which are superimposed upon one another and laminated in polyamide plastic sheets. The underside Kapton surface of the field joint and nozzle to case joint heaters was coated with a pressure sensitive adhesive. This adhesive provided bonding to the case during assembly. The lead wires extended from the heaters and were terminated in electrical connectors.

Power Cables RSRM joint protection system (JPS) power cables (1U76702-01, 1U76702-02, 1U76703-01, 1U76703-02, 1U76704-01, 1U76704-02, 1U76705-01, 1U76705-02, 1U76706-01 and 1U76706-02) were installed to provide 208 VAC to the RSRM field joint and igniter-to-case joint heaters.

2.0 TEST OBJECTIVES

The TEM-7 test objectives of CTP-0107 Revision A were derived from the objectives of System Test Summary Sheet TGX-21.6 to satisfy the requirements of Contract End Item (CEI) Specification CPW1-3600A, dated 3 August 1987.

Qualification objectives of this test were as follows:

- A. Certify North American Rayon Corporation (NARC) rayon for use in nozzle carbon cloth phenolic (CCP) liners (CPW1-3600A para. 3.2.1.4.13, 3.3.6.1.2.7, 3.3.6.1.2.8).
- B. Certify nozzle inner boot ring cure cycle improvement (CPW1-3600A para. 3.3.6.1.2.8).
- C. Certify nozzle outer boot ring cure cycle improvement (CPW1-3600A para. 3.3.6.1.2.8).
- D. Certify the nozzle cowl ring with an ablative liner ply angle change (from 0 deg to -50 deg) (CPW1-3600A para. 3.2.1.4.13, 3.3.6.1.2.8)
- E. Certify the improved nozzle bearing protector (CPW1-3600A para. 3.3.6.1.2.8).

Other test objectives included:

- F. Recover case and nozzle hardware for RSRM flight and static test programs.
- G. Obtain data on the effect of five year storage of loaded SRM case segments upon motor ignition and performance.
- H. Demonstrate the performance of an improved nose assembly to cowl assembly process for the nozzle (CPW1-3600A para. 3.2.3, 3.2.3.1, 3.3.1.1).
- I. Demonstrate the performance of increased cowl vent hole size (0.375 in. nominal diameter) for reducing boot cavity delta pressure (CPW1-3600A para. 3.3.6.1.2.8).
- J. Obtain additional data on the low frequency chamber pressure oscillations in the motor forward end and correlate with chamber pressure oscillation measurements in the motor aft end.
- K. Obtain additional data on chamber pressure drop down the bore by the use of aft end pressure transducers.

- L. Obtain additional data on cowl boot cavity/aft end (fixed housing) pressurization and temperature.
- M. Obtain additional data on the performance of the aft stiffener segment with known outer ligament cracks in the stiffener stubs.
- N. Obtain thermal radiation data from the nozzle plume for the ASRM program.

3.0 EXECUTIVE SUMMARY

Inspection and instrumentation data indicate that the TEM-7 static test firing was successful overall. Data was gathered at instrumented locations during pretest, test, and post-test operations. The information assembled from the test procedures has supplied valuable knowledge and understanding about the performance of the HPM and RSRM design components utilized in TEM-7.

Damage to the improved nozzle bearing protector and flex bearing resulted in failure to demonstrate acceptable performance of increased cowl vent hole size (0.375 in. nominal diameter).

The separation of the nozzle fixed housing phenolic insulation from the metal fixed housing did not cause any noticeable performance problems. The aft end pressure transducers and strain gages provided valuable data which will be helpful in the investigation of this anomaly.

Investigations are being conducted to understand these anomalies and the phenomena which caused them. The final test report, TWR-17659, will contain conclusions and recommendations for resolution of these conditions.

4.0 INSTRUMENTATION

4.1 INTRODUCTION

TEM-7 instrumentation measurements consisted of forward and aft end chamber pressure; igniter chamber pressure; forward and aft pressure chamber pressure oscillations; stiffener stub strains; nozzle components temperatures and strain; temperature for deluge control; nozzle deflections; nozzle boot cavity temperature and pressure; plume radiation measurements; test stand water deluge pressure; and timing. Boot cavity temperature and pressure and aft end chamber pressure measurements were made for a second time on the TEM program. New improved stand-alone units with thermocouples were used for the first time. TEM-7 was instrumented to gather data on cracked stiffener stub holes as a follow up on data gathered on FSM-1. The metal component parts on the nozzle using NARC material were instrumented with temperature sensors and strain gages. Plume radiation measurements were taken again to enhance data gathered on FSM-1.

4.1 OBSERVATIONS

Forward pressure measurements were nominal, but aft end pressure measurements dropped off unexpectedly at T+2 seconds. The pressure transducers were heat effected as a gas path developed in the fixed housing insulation liner. Strain gages near the pressure transducers confirmed the unbond which occurred to the fixed housing insulation. The data from pressure gages and strain gages gave a time history of the unbonding sequence. All other strain gages and temperature sensors on the nozzle components performed and recorded no anomalies.

The instrumented stiffener stub holes strain gages all recorded data except for the lone referee strain gage mounted inside a stiffener stub hole.

The installed pressure transducers in the boot cavity and thermocouple were erratic. One pressure transducer recorded data until T+20 seconds and the other failed. The thermocouple data were erratic throughout the firing, but did demonstrate the increased temperature into the boot cavity resulting from increased vent hole diameters.

Temperature data were nominal. The ambient temperature was 43.7 °F and the propellant mean bulk temperature was 65 °F at T-0 (ignition). Joint and case temperature sensors all performed nominally.

Aft skirt and nozzle positioning measurements all performed as expected.

One of the twenty-two radiometers failed prior to the firing, but all other sensors provided very good data for plume radiation studies.

5.0 PHOTOGRAPHY

Photographic coverage was required to document the test, test configuration, instrumentation, and any anomalous conditions which may have occurred. The TEM-7 photographs and video tapes are available from the Thiokol Corporation Photographic Services Department.

5.1 STILL PHOTOGRAPHY

Still color photographs of the test configuration were taken before, during, and after the test. Photographs were taken of joints each 45 deg minimum and at anomalous conditions.

5.2 MOTION PICTURES

Color motion pictures of the test were taken with nine high-speed cameras, two real-time documentary cameras, and four video cameras. Documentary motion pictures are recorded on roll 8330, high-speed motion pictures on roll 8331, and videotape on T0118 through T-0121. Cameras are listed in Table 5-1. The camera setup is shown in Figure 5-1.

Table 5-1. Photography and Video Coverage

<u>Camera</u>	<u>Station</u>	<u>Location</u>	<u>Type</u>	<u>Coverage</u>
1	7	Thrust Block	HS	Igniter Port
2	1	No. Fwd. Barricade	HS	Center Fwd & Center Joints
3	1	No. Fwd. Barricade	Vid	Overall Motor & Plume
4	2	No. Aft Barricade	HS	Center Aft & N/C Joints
5	2	No. Aft Barricade	Doc	Aft Case, Nozzle & Plume
6	2	No. Aft Barricade	HS	Nozzle, 200 ft Plume
7	3	So. Aft Barricade	Doc	Overall Motor & Plume
8	3	So. Aft Barricade	Vid	Aft Case, Noz., Plume, Deluge
9	4	So. Center Barricade	Vid	Aft Joint, Nozzle, Plume
10	4	So. Center Barricade	HS	Nozzle, 200 ft Plume
11	4	So. Center Barricade	HS	Center Aft & N/C Joints
12	5	So. Fwd. Barricade	HS	Center Fwd & Center Joints
13	7	Thrust Block	HS	Igniter Port
14	7	Thrust Block	Vid	Top of Case, Nozzle & Plume
15	7	Thrust Block	HS	Top of Case, Nozzle & Plume

CODE:

HS	-	9 each	300 PPS
Doc	-	2 each	24 PPS
Video	-	4 each	Real Time

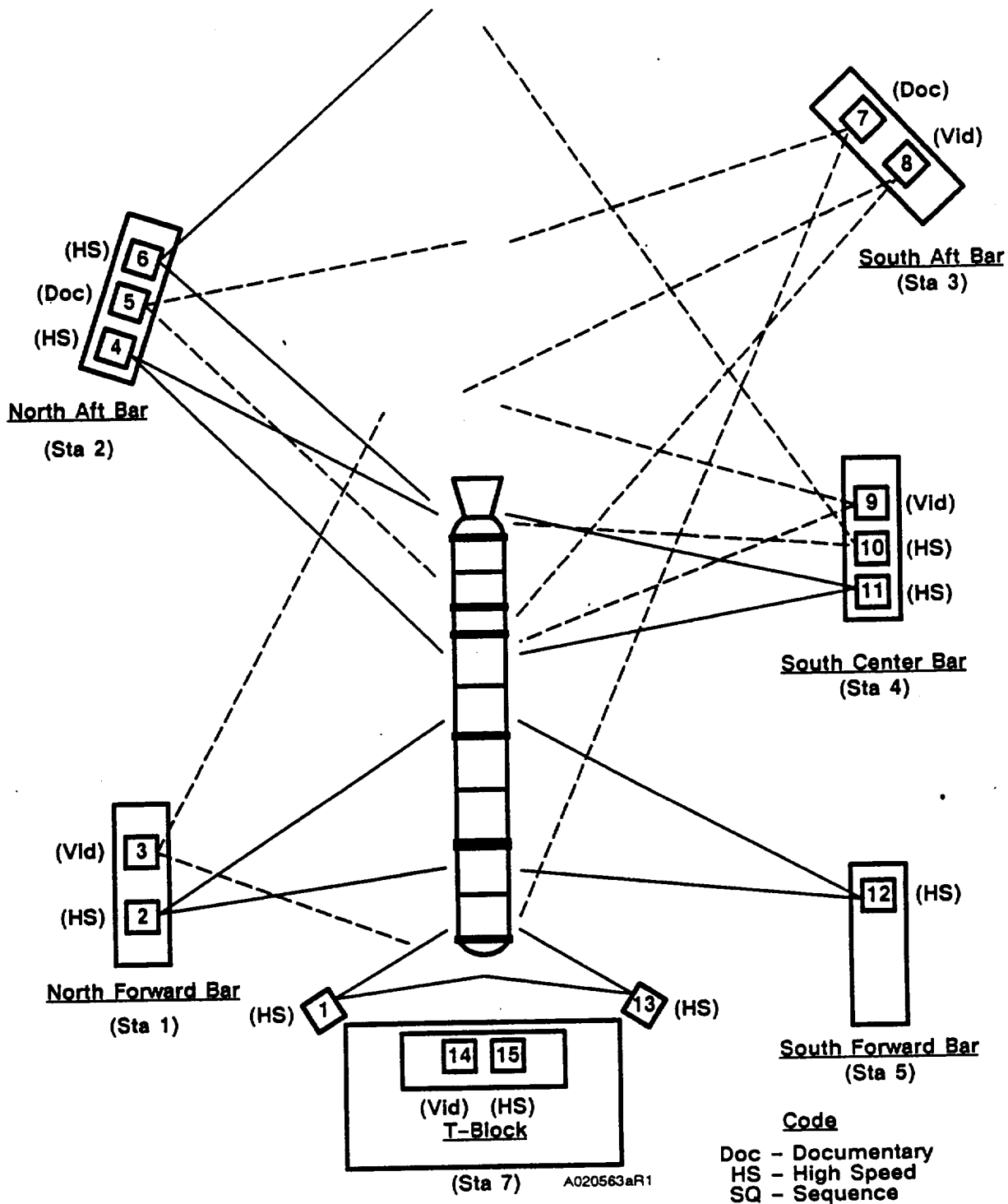


Figure 5-1. T-97 Photography Coverage--TEM-07

6.0 TEST RESULTS

6.1 CASE PERFORMANCE

6.1.1 Introduction

Case assembly procedures proved adequate, and chamber pressure was contained during the static test.

6.1.2 Observations

6.1.2.1 Forward Field Joint

The TEM-7 forward field joint was disassembled on 16 January 1991. Light corrosion was observed in and around the leak check port hole and on the case at the joint heater region at 280 through 294 degrees. Typical pin hole slivers were found intermittently around the circumference of the clevis and tang pin holes. This is caused by installation of the pins at assembly. No anomalous conditions were observed.

6.1.2.2 Center Field Joint

The TEM-7 center field joint was disassembled on 14 January 1991. The condition of the joint was nominal. No corrosion was observed on the tang or clevis joints. Typical pin hole slivers were found intermittently around the circumference of the clevis and tang pin holes. This is caused by installation of the pins at assembly. The leak check plug and port were in nominal condition.

6.1.2.3 Aft Field Joint

The TEM-7 aft field joint was disassembled on 10 January 1991. No corrosion was observed on the tang or clevis joints. Pin hole slivers were found at 48, 50, 86, 88 and 228 degrees. This is caused by installation of the pins at assembly. Before port hole assessment the joint had shifted approximately 0.5 inch (pinholes were misaligned by approximately 0.5 inch at 0 degrees). The putty apparently extruded into the through hole when the joint shifted because no trace of putty was found on the clevis between the primary and secondary O-rings. A preliminary PFAR was submitted since this condition is outside the engineering limits.

6.1.2.4 Cracked Stiffener Stub Holes

Special Issue (TWR-61209 Paragraph 3.2.1 Item 1)

All seven cracked stiffener stub holes were visually examined for new cracks and/or deformation. On several holes (240, 278 and 280 degrees) deformation was noted to exist on the aft face of the flange (near the hole). It was determined that this condition was a result of a previous usage and not a result of this test. No new cracks were detected by visual inspection. A gouge was found on the 240 degree hole on the aft flange. The gouge was located at approximate center of the flange cross section and raised metal exists.

6.2 CASE INTERNAL INSULATION PERFORMANCE

6.2.1 Introduction

The four TEM-7 segments had been insulated and cast with propellant more than five years before the TEM-7 static test.

Field Joint Assembly The case insulation of the three HPM-configuration field joints consisted of asbestos-silica-filled NBR (Figure 6-1). Prior to mating, the joints were inspected per STW7-2831, REV NC, the flight motor insulation criteria for the HPM joints. Putty was applied to the clevis joints per STW7-3746, as shown in Figure 6-2, and the joints were mated. After mating, each joint (Figure 6-3) was inspected from the bore for discontinuities and the putty was tamped.

Nozzle-to-Case Joint Assembly. The putty layup for the nozzle-to-case joint, shown in Figure 1-6, was performed to the dimensions of STW7-3745, as were previous TEMs. Figure 6-4 shows the putty layup used throughout the HPM program. The TEM-7 nozzle was mated to the aft segment with no apparent anomalies. Because of inaccessibility, the nozzle-to-case joint was not inspected or tamped as the field joints were.

Similar to TEM-5 and TEM-6, the nozzle-to-case joint incorporated four vent ports in the fixed housing. The vent ports were left open during assembly to exhaust entrapped air from within the joint. This concept was intended to reduce the potential for O-ring damage from gas flow through putty blowholes.

Prefire Inspection/Joint Putty Tamping. A prefire bore inspection was performed to assess the putty flow/layup of each field joint. The inspection occurred after the chocks were removed and the final leak check had been performed. This did not include the nozzle-to-case joint, which was inaccessible during this operation. The putty in the field joints was inspected for grease, discontinuities, bubbles, blowholes, etc.

All volcanoes, bubbles, and possible bubbles were tamped closed with a putty tamping tool. No grease contamination was found in any of the joint putty and the field joint putty condition was nominal. The overall prefire insulation condition of TEM-7 was similar to previous TEMs.

6.2.2 Observations

From an insulation standpoint, TEM-7 performed as expected. The performance in all three field joints and nozzle-to-case joint was excellent; no gas penetration to the seals was observed. The joints functioned within the HPM experience.

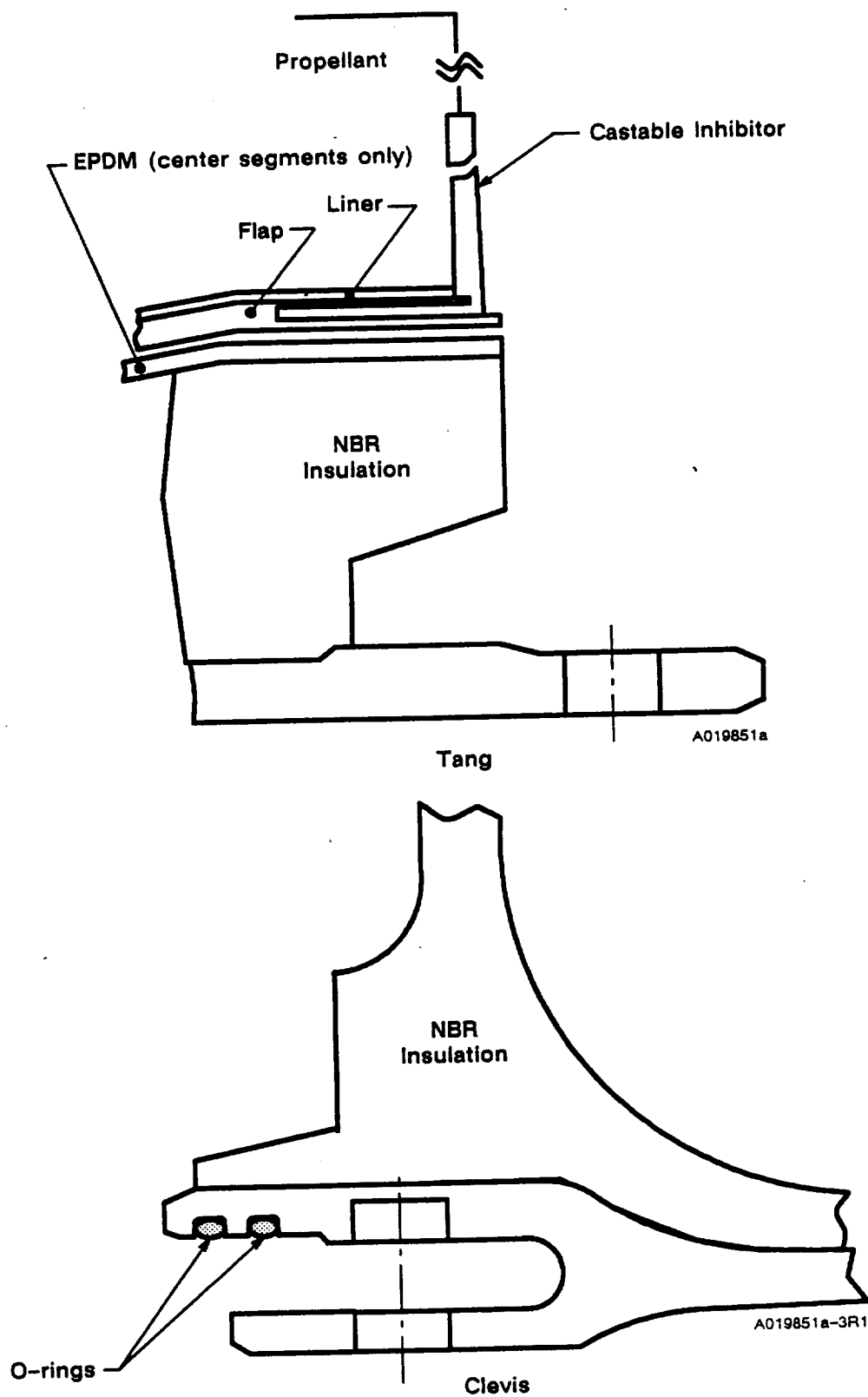


Figure 6-1. HPM Field Joint

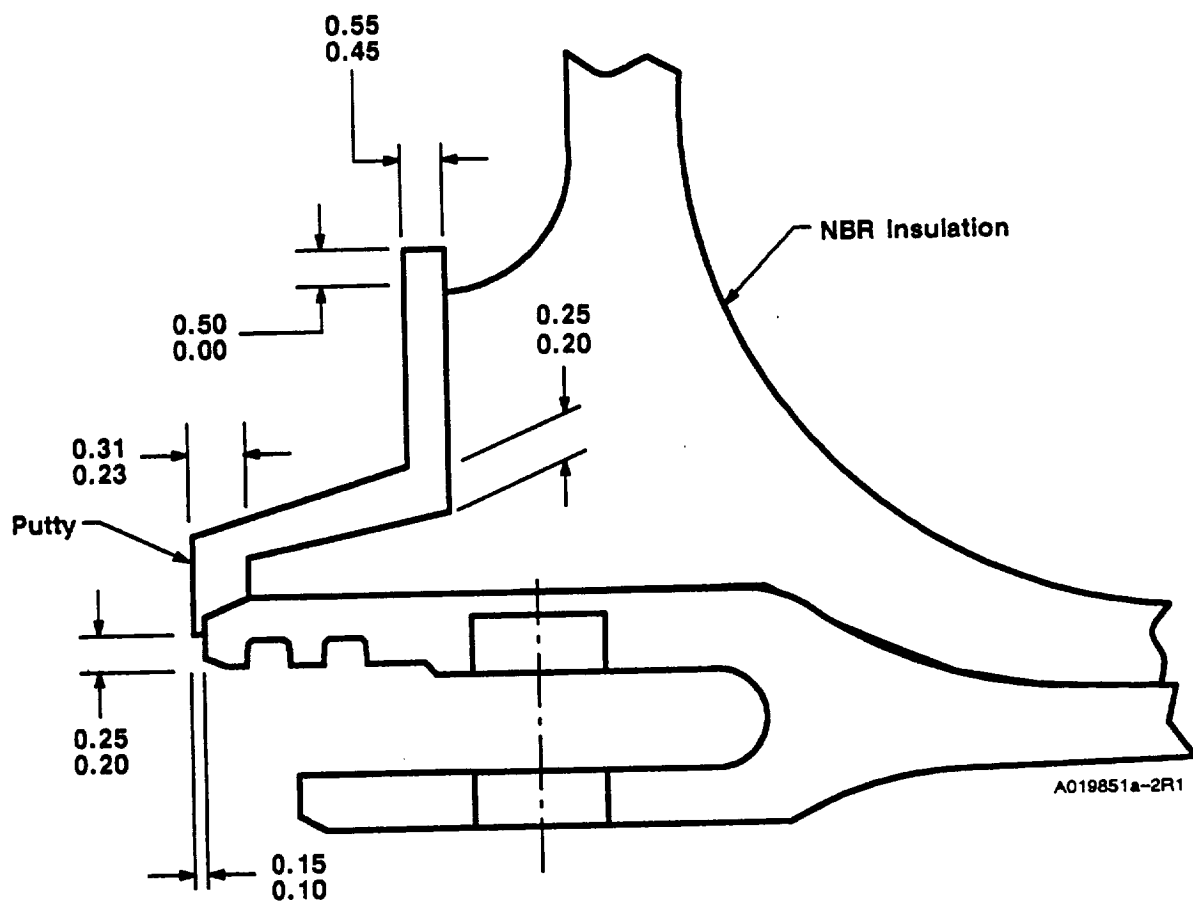


Figure 6-2. Clevis Joint Filler Putty Layup

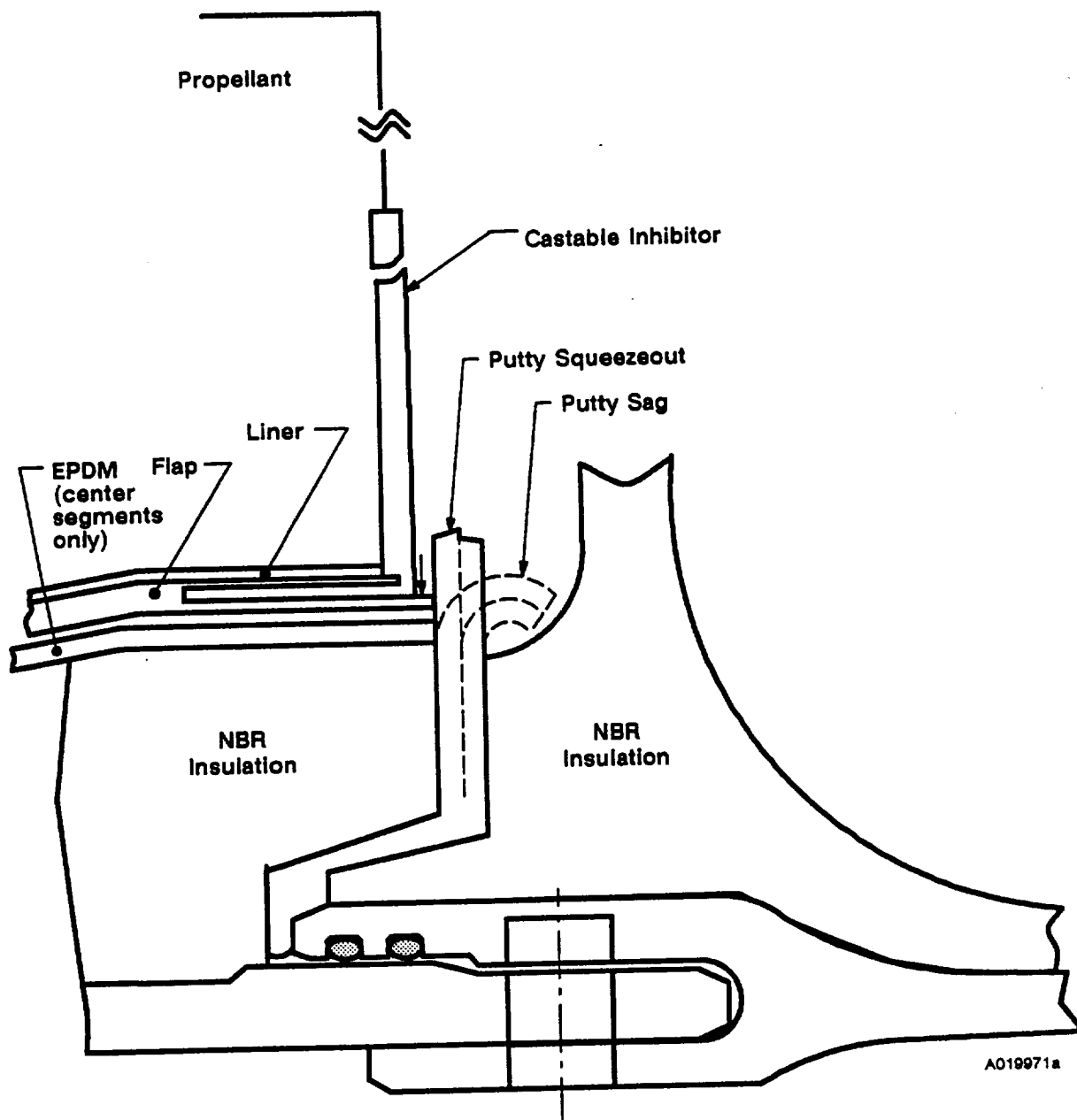


Figure 6-3. Assembled HPM Field Joint

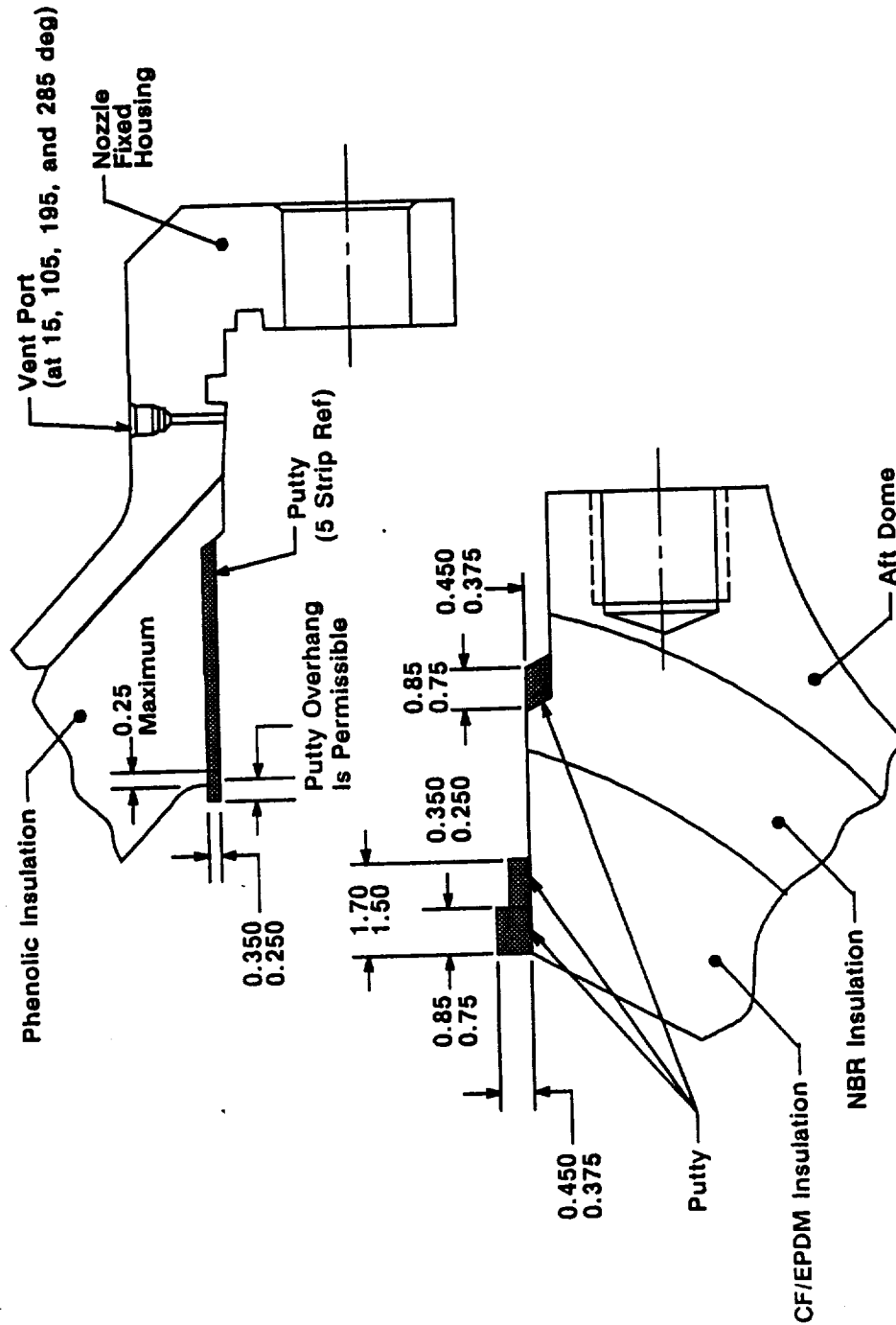


Figure 6-4. TEM-7 (HPM modified) Case-to-Nozzle Joint Configuration—Putty Layout

Postfire Internal Insulation Inspection An internal walkthrough inspection was performed. The internal acreage insulation, center and aft segment NBR inhibitors, and stress relief flaps (center and forward segments) appeared to be in normal condition from the walkthrough inspection. A small amount of castable inhibitor remaining attached to the forward center segment flap. Castable inhibitor remained attached intermittently full circumference to the forward segment flap. Two large pieces of castable inhibitor were found laying loose in the middle of the forward and forward center segments. A more detailed inspection of the flaps and inhibitors was performed when the remaining field joints were disassembled. The slag pool extended the full length of the aft segment and 39 inches into the aft center segment. The size of the slag pool and the amount of slag appeared to be typical of previous static test TEM motors. The final slag weight in the aft segment was 1813 lbs.

Aft Field Joint Insulation The aft field joint was disassembled and inspected on 10 January 1991. The joint insulation and putty were in normal condition showing normal heat effects, charring, and erosion. The putty exhibited a constant olive green color with normal tack. The putty failure at disassembly was 15% adhesive (tang side) and 85% cohesive. One terminated blowhole was present at 155 degrees measuring 2.1 inches circumferentially by 0.65 inch radially. The blowhole terminated approximately 0.10 inch inboard of the insulation ramp. The gas penetration was between the tang insulation and the putty. Heat effects with slight erosion to the NBR insulation were present on the tang side of the joint in the region of the blowhole. Heat affected and eroded putty were present on the clevis side. The terminated blowhole is within the experience of the HPM design field joints and had no adverse effect on joint performance. No clevis or tang edge separations were detected. The aft center segment stress relief flap and the aft segment NBR inhibitor were in normal condition. The flap was eroded normally back to the flap bulb full circumference. The NBR inhibitor was eroded uniformly showing approximately 8-10 inches remaining. No tears were present on either the flap or inhibitor.

Center Field Joint Insulation The center field joint was disassembled and inspected on 14 January 1991. The joint insulation and putty were in normal condition showing normal heat effects, charring, and erosion. Gas penetrated into the bondline 0.80 inch maximum outboard of the remaining material on the clevis side from 280 deg.-0 deg.-74 deg. Gas did not reach the step in the insulation. The putty exhibited a consistent olive green color with normal tack. The putty failure at disassembly was 2% adhesive and 98% cohesive. No clevis or tang edge separations were detected. The forward center segment stress relief flap and the aft center segment NBR inhibitor were in normal condition. The entire flap remained from 270 deg.-0 deg.-90 deg. The NBR inhibitor was eroded uniformly showing approximately 20-25 inches remaining. No tears were present on either the flap or inhibitor.

Forward Field Joint Insulation The forward field joint was disassembled and inspected on 16 January 1991. The joint insulation and putty were in normal condition showing normal heat effects, charring, and erosion. Gas penetrated slightly into the joint bondline between the clevis insulation and the putty from 262 deg.-280 deg. The average depth of the gas penetration was 0.30 inch (0.40 inch max.) outboard of the remaining material. Heat affected NBR on the clevis side and heat affected putty on the tang side were present in this region. The putty exhibited a consistent olive green color with normal tack. The putty failure at disassembly was 2% adhesive and 98% cohesive. The tang insulation on this joint had several prefire edge separations over 0.50 inch in axial depth (0.75 inch max). These separations were repaired before joint assembly. No clevis or tang edge separations were detected upon postfire inspection indicating the repair procedure was adequate. The forward segment stress relief flap and the forward center segment NBR inhibitor were in normal condition. The entire flap remained full circumference with heat affected and slightly blistered NBR underneath. Castable inhibitor was present intermittently. The NBR inhibitor was eroded uniformly with approximately 25-30 inches remaining. No tears were present on either the flap or inhibitor.

Nozzle-to-Case Joint Insulation The nozzle-to-case joint was disassembled and inspected on 15 January 1991. The joint insulation and putty were in normal condition showing normal heat effects and sooting at the forward edge of the bondline. There was no evidence that gas had penetrated the joint insulation bondline (putty). The putty exhibited a consistent olive green color with normal tack. The putty failure at disassembly was 5% adhesive and 95% cohesive. Three voids in the putty were found on the fixed housing at the step extending forward. The largest void was located at 186 deg. measuring 2.2 inches circumferentially by 0.7 inch axially.

6.3 SEALS/LEAK CHECK PERFORMANCE

6.3.1 Introduction

After each pressure vessel joint was assembled, a leak test was performed to determine the integrity of the seals. The leak tests consisted of a joint volume determination and a pressure decay test. The volume and pressure information was combined with temperature and time data, collected during the test, and used in the calculation of a leak rate expressed in terms of standard cubic centimeters per second (scs). Each leak test has a maximum leak rate allowed.

Some specifications require only a maximum pressure decay over time. This method has been determined as sufficient based on the small, constant volumes, and the equivalent leak rates, which are conservative when using all worst-case variables.

Table 6-1 lists all joints leak tested on TEM-07, corresponding leak test specifications, and the equipment used. The leak tests will be discussed in detail in Section 6.3.1.3. The case factory joints were tested after the original assembly. This report does not discuss the results of those tests. The majority of the nozzle internal joints (joints 1 through 4) were of RSRM configuration and tested to the accompanying requirements. Nozzle internal joint 5 was a combination of HPM and RSRM hardware and could not be leak tested since it only contained a single O-ring.

Table 6-1. TEM-7 Seal Leak Testing

<u>Joint</u>	<u>Specification</u>	<u>Equipment</u>
Case Field Joints	STW7-3682	8U76902
Nozzle-to-Case Joint	STW7-3682	2U129714
Nozzle Joint 1	STW7-3475	8U76248
Nozzle Joint 2	STW7-3476	2U129714
Nozzle Joint 3	STW7-3477	2U129714
Nozzle Joint 4	STW7-3478	2U129714
Ignition System		
Inner Gasket	STW7-3632	2U126714
Outer Gasket	STW7-3632	2U129714
Special Bolt Installation	STW7-3632	2U129714
S&A Joint	STW7-3633	8U76500
Transducer Assembly	STW7-2853	2U65686
Barrier-Booster	STW7-2913	2U65848

6.3.2 Observations

The case field joint leak test results are shown in Table 6-2. The TEM field joints were tested at lower pressures (185 psig) than RSRM field joints (1,000 psig) because of their configuration. These joints were tested with and without the assembly stands (chocks) in place. This was done since previous HPM motors showed the potential for leaking after the stands were removed. The results of the leak tests for the field joints were acceptable.

The field joint tests were performed with a variation of the 8U75902 Ground Support Equipment leak test system. For testing of the TEM motors, the equipment was modified to include a pressure relief valve to preclude the possibility of over-pressurizing the joint.

Table 6-2. TEM-7 Case Field Joint Leak Test Results

Pressure (psig)	Maximum Leak Rate (sccs)	Actual Leak Rates (sccs), Prechock/Postchock		
		FWD	CTR	AFT
185	0.1	0.0121/ 0.0084	0.0023/ 0.0101	0.0128/ 0.0089
30	0.0082	0.0005/-0.0002	-0.0002/ 0.0000	0.0003/-0.0001

The ignition system leak test results are shown in Table 6-3. The tests were performed with the new leak test equipment as shown in Table 6-1. The equipment was identical to that used to test most of the RSRM joints. All results were within the limits.

Table 6-3. TEM-7 Igniter and S & A Leak Test Results

Joint Seal	Allowable Leak Rate (sccs), HI/LO*	Actual Leak Rate (sccs), HI/LO
Inner	0.10 / 0.0082	0.0043 /-0.0002
Outer	0.10 / 0.0082	0.0070 /-0.0005
Transducer Installation	0.10 / 0.0082	0.0085 /-0.0001
OPT **	10 psi/10 min/ 1 psi/10 min	1.0 / 0.0 2.0 / 0.0 3.0 / 0.0 2.0 / 0.0
Barrier- Booster	1 psi / 10 min	N/A
S & A	0.10 / 0.0082	0.0040 /-0.0001

N/A Not available

* HI = 1000 psig, LO = 30 psig

** OPTs tested at 1024 psig and 30 psig, leak rate units are psi/10 min.

Table 6-4 lists the results of the TEM-7 nozzle-to-case joint leak test. This joint was tested at a maximum pressure of 185 psig. This differs from the RSRM nozzle-to-case joint leak tests which are performed at 920 psig. The TEM-7 nozzle-to-case leak test was performed after the first torque sequence, when the axial bolts are torqued to 25 ft.-lb. This procedure prevented the occurrence of a metal-to-metal seal between the fixed housing and the aft dome when the axial bolts were fully torqued. All leak test results were within the allowable limits.

The 2U129714 equipment was used to test the TEM-7 nozzle-to-case joint. This is the new equipment used to test all RSRM nozzle-to-case joints starting with 360L006A.

Table 6-4. TEM-7 Nozzle-to-Case Leak Test Results

Pressure (psig)	Allowable Leak Rate (sccs)	Actual Leak Rate (sccs)
185	0.072	0.0091
30	0.0082	0.0000

The nozzle internal joint leak test results are shown in Table 6-5. The tests were performed with the new leak test equipment as shown in Table 6-1. The equipment was identical to that used to test most of the RSRM joints. All results were within the limits.

Table 6-5. TEM-7 Nozzle Internal Joint Leak Test Results

JOINT #	MAX TEST PRESSURE	*ALLOWABLE LEAK RATE, HI/LO (sccs)	ACTUAL LEAK RATE HI/LO (SCCS)
(# 1)	83	0.029/0.0082	0.0025/0.0006
(# 2)	920	0.084/0.0082	0.0007/-0.0003
(# 3)	740	0.070/0.0082	0.0010/-0.0008
(# 4)	144	0.053/0.0082	0.0032/ 0.0002

6.3.2.1 Forward Field Joint

The TEM-7 forward field joint was disassembled on 16 January 1991. Putty was observed in contact intermittently with the primary O-ring for approximately 60 percent of the joint. Putty in contact with the primary O-ring is a typical condition. The grease on the O-rings and sealing areas was as prescribed in STW7-3688. No anomalous conditions were observed.

6.3.2.2 Center Field Joint

The TEM-7 center field joint was disassembled on 14 January 1991. The condition of the joint was nominal. No hot gas or soot reached the primary O-ring. No damage was found on the primary or secondary O-rings while in the groove. The grease on the O-rings and sealing areas was as prescribed in STW7-3688. Putty was found over the full circumference up to, but not past, the primary O-ring. The leak check plug and port were in nominal condition.

6.3.2.3 Aft Field Joint

The TEM-7 aft field joint was disassembled on 10 January 1991. No hot gas or soot reached the primary O-ring. There was no evidence of damage to the O-rings while in the groove. The grease on the O-rings and sealing areas was as prescribed in STW7-3688. Putty was found in the leak check through hole obstructing all but a very small portion of the hole. Before port hole assessment the joint had shifted approximately 0.5 inch (pinholes were misaligned by approximately 0.5 inch at 0 degrees). The putty apparently extruded into the through hole when the joint shifted because no trace of putty was found on the clevis between the primary and secondary O-rings. A preliminary PEAR was submitted since this condition is outside the engineering limits.

6.3.2.4 Nozzle-to-Case Joint

The TEM-7 nozzle-to-case joint was disassembled on 15 January 1991. Zinc chromate putty was observed up to but not past the primary O-ring around the entire circumference, and no blowholes were observed. Two scratches that could be felt with a 5-mil brass shim stock were found on the aft dome boss secondary sealing surface at 89 degrees and 75.6 degrees. A preliminary PEAR was submitted on the scratches. No other anomalies were observed.

6.3.2.5 Internal Nozzle Joint, Forward Exit Cone-to-Aft Exit Cone (Joint 1)

The post-fire evaluation of the TEM-7 aft exit cone-to-forward exit cone joint was conducted on 3 January 1991. The sealing surfaces were visually inspected and found to be in good condition with no evidence of damage, corrosion, or excess grease coverage. No damage was found on the primary or secondary O-rings. RTV backfill was found up to the primary seal but not past the primary O-ring. No pressure path was found through the RTV rubber.

6.3.2.6 Igniter

6.3.2.6.1 S&A Removal

The Safety and Arming Device was removed on 17 December 1990. No anomalous conditions were found during the evaluation of the Safe and Arm sealing surfaces and gasket. Heavy soot was found on the gasket aft face, over the full circumference, up to the primary seal. Cadmium plating was missing inward of the gasket aft face primary seal, 0.020 inch from the seal cushion at 175 degrees. No soot was found on the gasket forward face to the primary seal. Heavy soot was found on the retainer inside diameter over the full circumference. No damage to the gasket seals or the Safe and Arm sealing surfaces were found.

6.3.2.6.2 S&A Disassembly

The TEM-7 Safe and Arm Device was disassembled on 20 December 1990. One anomalous condition was observed during the disassembly assessment. A small axial scratch was found at 300 degrees on the primary seal surface of the Barrier-Booster (B-B) housing bore. the scratch was less than 0.1 inch in length and could be felt with a 0.005 inch thick brass shim. A preliminary PEAR was submitted on the scratch and presented to the Ignition Team.

Typical soot was observed to reach the rotor shaft forward primary O-ring. Soot was also observed to reach both SII primary O-rings. However, no soot or blow-by was observed past any seal. There was no evidence of damage to the rotor shaft or the SII O-rings.

Typical circumferential galling was found on the land between the primary and secondary seal surfaces of both SII ports. This is an acceptable condition per the barrier-booster refurbishment specification.

Special Issue (TWR-61209 Paragraph 3.2.3 Item 1)

An assessment was made at disassembly to determine if any contamination was present in the SII port leak test through holes (Ref. DR #400579). No contamination was found.

6.3.2.6.3 Igniter Operational Pressure Transducers

No anomalous conditions were found on the OPTs or the O-rings. No damage to the transducer threads or sealing surfaces was found. Each secondary O-ring had typical puncture marks caused by the removal tool.

6.3.2.6.4 Igniter Special Bolts

No damage was found on the primary O-rings and no damage to the bolt threads or sealing surfaces was observed.

6.3.2.6.5 Igniter Pressure Transducer

The secondary O-ring had a typical puncture mark caused by the removal tool. No damage was found on the primary O-ring. No damage to the plug threads or sealing surfaces was observed.

6.3.2.7 Aft End Pressure Transducers

Four aft end pressure transducers on the fixed housing were heat affected. The findings from the heat affected pressure transducers that were presented to the RPRB on 1-9-91 were confirmed in the M-53 Metalography lab. Two of the four primary seals were heat affected which was caused by heating of the transducers and not direct gas impingement. The other two primary seals were not heat affected. The worst case heat affected pressure transducer burned through from inside to outside at the primary O-ring groove. It was also plugged with aluminum slag. No heat effects were found on any secondary O-ring. The secondary O-ring on the aft end OPT type pressure transducer was damaged during assembly due to a grease overfill condition. Details of the lab work will be included in the final report.

Two preliminary PFARs were written. One on the OPT secondary O-ring overfill condition and another on the heat affected primary O-rings on two transducers.

6.4 NOZZLE ASSEMBLY PERFORMANCE

6.4.1 Introduction

TEM-7 was the first full scale static test for qualification of North American Rayon Corporation (NARC) rayon in all nozzle carbon cloth phenolic (CCP) liners. Two additional full scale nozzles will be statically tested for qualification of the NARC rayon as outlined in the second source rayon program plan, TWR-18965. Low cost nozzle improvements, previously demonstrated on the TEM-6 static test, to be qualified on TEM-7 included a change in the carbon cloth phenolic (CCP) liner ply angle of the cowl, improved inner and outer boot ring phenolic cure cycles, and an improved flexible bearing protector design.

Detailed observations and discussions of nozzle subassemblies and components are contained in the TEM-7 Nozzle Quick-Look Report, TWR-61490. Additional nozzle data will be contained in the TEM-7 Final Test Report, TWR-17659, after all post test nozzle hardware activities and evaluation of data are complete.

6.4.2 Observations

6.4.2.1 Nozzle Fixed Housing

After the fixed housing phenolic insulation was separated from the metal fixed housing, the phenolic showed char and sooting around each instrumentation through hole on the phenolic to metal bond surface. There were small slag deposits in the immediate vicinity of the holes. The metal housing also was sooted around the holes on the corresponding surfaces. The entire remaining surface which mates with the phenolic insulation was severely rusted. A small area around one hole was cleaned of soot and rust which revealed erosion to the housing. Surface hardness measurements 0.2 inch around is 32 R_c and should be 44 R_c . Unbond investigation results will be reported in TWR-61585.

The differences between TEM-6 and TEM-7 were:

1.
 - o The TEM-6 fixed housing phenolic insulation was installed during the HPM program.
 - o The TEM-7 fixed housing phenolic insulation was North American Rayon Corporation (NARC) specifically installed for one of three full scale motor test qualifications.
2.
 - o The instrumentation through holes were drilled through the TEM-6 fixed housing and insulation with the phenolic insulation already bonded in place.
 - o On TEM-7 the fixed housing instrumentation holes were drilled through the metal fixed housing without the insulation. The phenolic insulation was then bonded to the fixed housing. After cure of the bondline, the instrumentation holes were drilled through the phenolic insulation.

6.4.2.2 Flexible Bearing Protector

Two areas, at 280 degrees and 330 degrees, were burned through the bearing protector. At the 280 degree location, the flex bearing rubber eroded approximately 0.15 inch. Locations from 230 degrees through 0 degree to 10 degrees eroded more than 0.4 inch. The difference between TEM-6 and TEM-7 were:

- o The TEM-6 cowl vent holes were flight configuration, i.e. 5/16 (0.312) inch diameter.
- o The TEM-7 cowl vent holes were increased in size to 3/8 (0.375) inch diameter (Figure 1-7).
- o The belly band region of the TEM-7 bearing protector was increased to 1.0 inch minimum thickness (Figure 1-7).
- o The TEM-7 nozzle was vectored.

6.4.2.3 Internal Joints Backfill

Joint #1 - Aft Exit Cone/Forward Exit Cone Assembly The RTV extended below the char line all the way to the primary O-ring, full depth for 360 degrees. There were no blowpaths present. There were no voids of any significant size.

Joint #2 - Nose Inlet/Cowl Assembly The RTV extended below the char line all the way to the bearing flange, full depth for 360 degrees. The RTV also extruded into the gap intermittently between the bearing flange and the nose cap. There were no blowpaths present. There were no voids of any significant size.

Joint #3 - Nose Inlet/Throat Assembly The RTV extended below the char line all the way to the first 90 degree bend, 75% of the RTV went to the second 90 degree bend. There was one area for about 30 degrees that went past the second bend for about one quarter of an inch. The fill edge was a smooth line, not heavily scalloped. There were no blowpaths present. There were no voids of any significant size.

Joint #4 - Throat/Forward Exit Cone Assembly The RTV extended below the char line the complete circumference of the joint. Scalloping of the RTV was present, with evidence of grease interfering with the flow of RTV into the joint. Grease was found on the phenolics at 22-42, 220-225 and 275-300 degrees. A Postfire Anomaly Record (PFAR) has been written on this condition. The RTV reached the primary O-ring except where grease was present on the phenolics. No blowpaths were present in the RTV. There were no voids of any significant size.

Joint #5 - Aft End Ring/Fixed Housing The RTV reached the O-ring at 210 through 215 degrees. The RTV did extend past the O-ring footprint at 210 degrees on the fixed housing. A PFAR has been written on this condition. It appears that the RTV did not inhibit the sealing action of the O-ring. The only evidence of RTV across the footprint was a red stain on the O-ring. No RTV adhered to the fixed housing seal surface. Intermittent voids were present in the RTV from the assembly process but no blowpaths were present. Grease did not interfere with the RTV fill in the joint.

6.4.2.4 Internal Joints Conditions

Joint #2 - Nose Inlet/Forward End Ring/Cowl Erosion and heat effect was present on the flex bearing elastomer pad #8 at 280 and 330 degrees. This corresponds to the bearing protector burn-through areas. An eroded area at 280 degrees measured 0.560 inch long by 0.280 inch wide by 0.160 inch deep. The heat effected area at 330 degrees measured 0.880 inch long by 0.380 inch wide. The erosion and heat effect did not appear to impinge on the surrounding shims.

A light coat of grease was present on the joint metal surfaces except where corrosion was present. Light to medium corrosion was found on the forward face of the forward end ring flange. The corrosion extended from the surface outer edge to the inboard side of the through holes from 348 through 0 to 36 degrees and from 84 to 210 degrees. Minor scratches caused by jacking screws during disassembly were located in four equally spaced locations on the nose-inlet housing aft surface. No bondline separations were observed on this joint.

Joint #3 - Nose Inlet/Throat A light coat of grease was present on the joint metal surfaces. No corrosion or metal damage was observed. No bondline separations were observed on this joint.

Joint #4 - Throat/Forward Exit Cone Assembly Grease coverage on the joint metal surfaces was nominal. No corrosion or damage to the metal components was present. No bondline separations were present on the throat housing assembly. Metal-to-adhesive separations were observed on the forward exit cone assembly. The separation extended the complete circumference of the bondline with a maximum radila width of 0.050 inch.

Joint #5 - Aft End Ring/Fixed Housing Bearing protector burn-through areas were found at 280 and 330 degrees. A PFAR has been written on this condition. Also, areas of deep erosion were found at 230 through 0 to 90 degrees. The depth of erosion ranged from 0.28 to 0.88 inch. The thickness of the TEM-7 bearing protector was 1.0 inch at the burn-through and eroded areas as compared to the RSRM thickness of 0.75 inch in the same location. The burn-through and eroded areas were in line with the cowl vent holes.

The diameter of cowl vent holes were enlarged by 0.060 inch for the TEM-7 nozzle.

Grease coverage on the joint metal surfaces was nominal. No corrosion or metal damage was observed. Typical even sooting on the flexible boot inside diameter was present.

No bondline separations were observed at this joint, but the inner boot ring had sheared along the glass plies and moved forward approximately 0.030 inch. The shearing of the ring was associated with the fixed housing insulation separation that was detected at nozzle-to-case demate.

6.4.3 TEM-07 Nozzle Strain Gage Response Summary

The TEM-07 nozzle metal parts were RSRM configuration except for the fixed housing which was HPM design. Preliminary review of data from various strain gages indicates expected performance, except for the fixed housing assembly. Also of note is a positive shift of approximately 60 to 130 micro in/in at station 1839.0 (nose inlet assembly) on all four circumferentially located hoop strain gages.

Not all strain data has been evaluate to date. Hoop and meridional stains have been reviewed for gages at the following axial locations:

<u>Station</u>	<u>Assembly</u>
1865.0	Forward Exit Cone
1839.39	Throat
1839.0	Nose Inlet
1842.5	Nose Inlet
1867.0	Fixed Housing

Strain data on the forward exit cone and throat were compared to both RSRM predicted values and previously observed actuals. Data showed nominal performance.

Strain data from Station 1842.5 (near the nose inlet housing aft end) on the nose inlet assembly was comparable to previous test measurements. Meridional stain at station 1839.0 was normal and very close to predicted values. The hoop strain at station 1839.0 followed a normal profile except in was shifted in the positive direction approximately 60 to 130 micro in/in. This data is preliminary, and the cause of this shift should be more thoroughly investigated.

Strain data at station 1867.0 on the fixed housing shows an anomalous occurrence at approximately 2 seconds into motor burn. Postfire analysis on this problem is ongoing and will be fully documented in the final test report for TEM-07.

6.4.4 Nozzle TVC Performance

The TVC system performed as planned and followed the specified duty cycle.

6.5 IGNITION SYSTEM PERFORMANCE

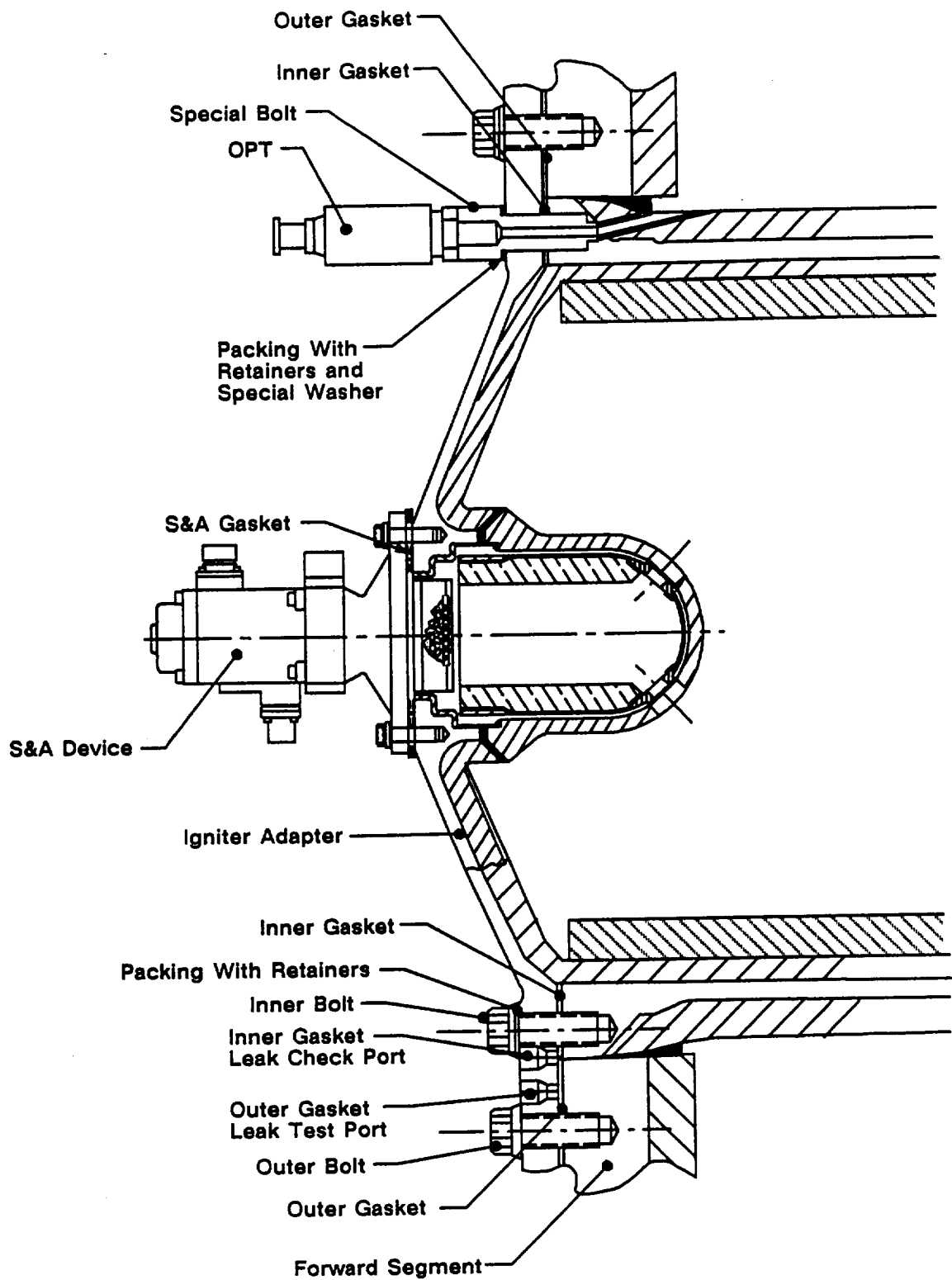
6.5.1 Introduction

The SRM ignition system consisted of a modified HPM igniter assembly containing a single nozzle, steel chamber, external and internal insulation, and a solid propellant igniter containing a case bonded 40-point star grain (Figures 6-5 and 6-6). The ignition system was modified with a CO2 quench port.

A Safe and Arm (S&A) device utilizing Krytox grease to lubricate the barrier-booster shaft O-rings was installed on the igniter (Figure 6-7).

6.5.2 Observations

S&A Cycle Times. Performance of the Krytox^R grease on the B-B shaft was excellent. S&A cycle times were within the engineering requirements of 2.0 sec or less at 24 Vdc (TWR-17656 Table III).



A026375a

Figure 6-5. Ignition System Components and Seals

REVISION _____

DOC NO.	TWR-61561	VOL
SEC	PAGE	49

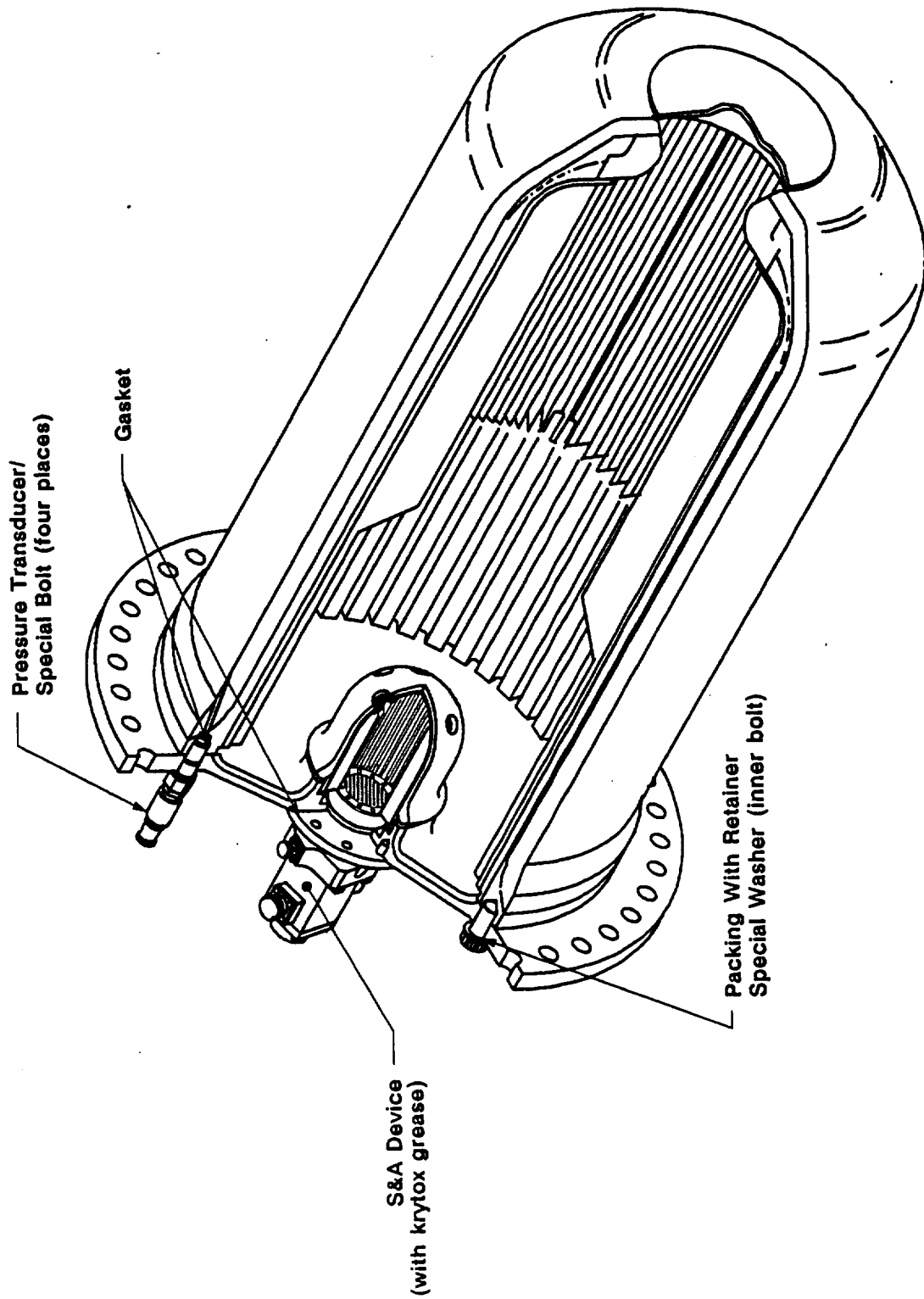


Figure 6-6. Standard HPM Igniter System

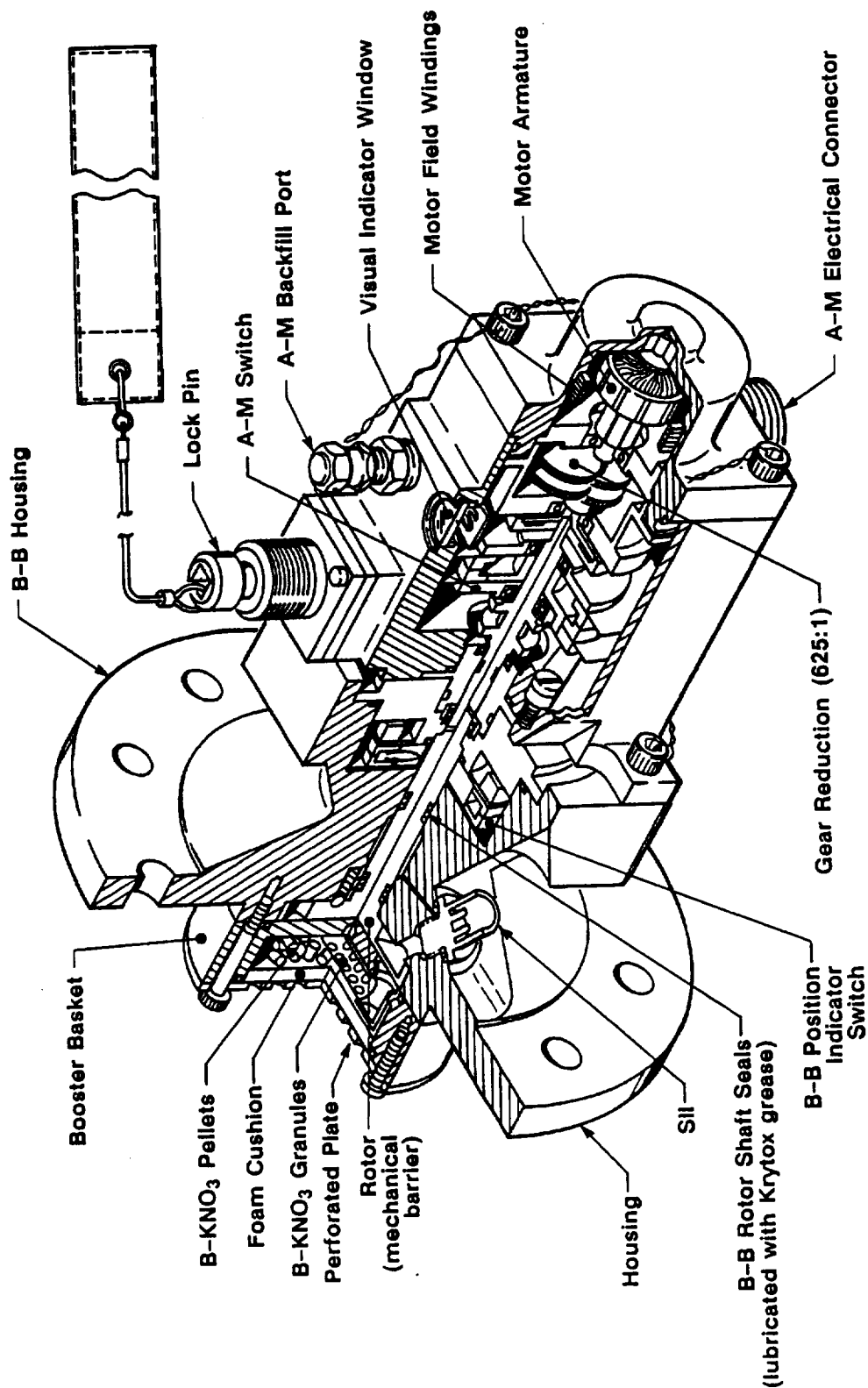


Figure 6-7. S&A Device Configuration

6.6 JOINT PROTECTION SYSTEMS PERFORMANCE

6.6.1 Introduction

Field joint heater closeout consisted of cork strips retained with Kevlar¹ straps. The external joint temperatures were sensed by two sensor assemblies mounted adjacent to the heater. Improved field joint heaters (Drawing 1U77252), igniter to case joint heater (Drawing 1U77253) and nozzle to case joint heater (Drawing 7U77118) were installed in accordance with Drawing 7U77328. These heaters consisted of redundant, chemically etched, foil circuits which were superimposed upon one another and laminated in polyamide plastic sheets. The underside Kapton surface of the field joint and nozzle to case joint heaters were coated with a pressure sensitive adhesive. This adhesive provided bonding to the case during assembly. The lead wires extended from the heaters and were terminated in electrical connectors.

6.6.2 Observations

The Joint protection systems performed within specifications and maintained the joint temperatures within the required temperature range at the time of motor ignition.

A post-test inspection with the FJPS still on the motor revealed no evidence of damage.

6.7 BALLISTICS/MASS PROPERTIES PERFORMANCE

6.7.1 Introduction

The SRM propellant, TP-H1148, was a composite type solid propellant, formulated of polybutadiene acrylic acid acrylonitrile terpolymer binder (PBAN), epoxy curing agent, ammonium perchlorate oxidizer and aluminum powder fuel. A small amount of burning rate catalyst (iron oxide) was added to achieve the desired propellant burn rate.

The propellant grain design consists of a forward segment with an eleven point star that transitions into a tapered circular perforated (CP) configuration, two center segment double tapered CP configurations, and an aft segment triple taper CP configuration with a cutout for the partially submerged nozzle.

6.7.2 Objectives

The primary test objectives from Section 2.0 regarding ballistics/mass properties were:

- G. Obtain data on the effect of five year storage of loaded SRM case segments upon motor ignition and performance.
- J. Obtain additional data on the low frequency chamber pressure oscillations in the motor forward end and correlate with chamber pressure oscillation measurements in the motor aft end.
- K. Obtain additional data on chamber pressure drop down the bore by the use of aft end pressure transducers.

6.7.3 Conclusions/Recommendations

The TEM-7 ballistic performance was within expected limits. The TEM-7 ballistic performance compared well with previous TEM performance and HPM historical data. The aft end pressure gauges provided very little useful ballistics data due to the aft end anomalous condition. The five year storage of loaded case segments did not appear to effect motor performance. The measured slag weight in the aft segment was 1813 lbm.

The TEM-7 motor exhibited chamber pressure oscillations similar to previously tested Space Shuttle HPMs. The 1-L mode oscillations were typical for an HPM. In general, HPM 1-L mode amplitudes are lower than those for RSRMs. The magnitudes of the TEM-7 oscillations were among the lowest experienced in HPMs. The aft end pressure oscillations could not be analyzed due to lack of data.

6.7.4 Observations

A comparison of TEM-7 performance with predicted values and with the nominal HPM performance revealed few differences. The predicted burn rate for TEM-7 was 0.370 in./sec at 625 psia and 60 °F, the target burn rate was 0.368 in./sec and the delivered burn rate was 0.371 in./sec. Predicted and measured performance compared well and was within the current HPM Specifications.

Table 6-6 is a summary of the measured ballistic and nozzle performance data. Figure 6-8 is a comparison of measured and predicted pressure-time histories. The measured and predicted performance compared well for this motor. Thrust was not measured for this static test, only reconstructed thrust based on nominal thrust to pressure ratios is available.

Figures 6-9 and 6-10 contain plots of the analytical reconstruction of the TEM-7 performance. The analytical model calculated the motor burn rate and Surface Burn Rate Error (SBRE) factor. The calculated burn rate of 0.3709 in./sec at 625 psia and 60 °F was approximately 0.3% above the predicted value of 0.3697, well within burn rate variation. The calculated SBRE table compared well with the nominal HPM table as expected, since the propellant grain geometry was the same.

Figure 6-11 shows measured aft end chamber pressure with reconstructed head-end pressure and the corresponding aft-end pressure data. The reconstruction is forced to match the head-end pressure, not aft end pressure. The TEM-6 motor provided good insight to the measured aft end pressure and the reconstructed aft end data shown in Figure 6-11 is believed to be accurate for TEM-7.

The actual TEM-7 aft end pressure data is scattered. At 2 seconds in burn the pressure data rapidly decreases and then recovers to a point. After each gauge recovers from the initial pressure drop, all consistently lag head end pressure. Post flight inspection did reveal plugged port holes and heat affected transducers. As shown in the figure, all aft end pressure readings maintained a higher than ambient pressure after the test. Gauge PNNAR006 drops below the other aft end gauges as was seen on TEM-6.

The ballistics code shows the reconstruction of PSN to be higher than actual measured data, but the reconstruction of pressure at axial location 1577 in. (aft segment factory joint) is very close to measured aft-end pressure. The ballistics model is a 1-D code that does not accurately model the flow field in the aft end of the aft segment (the 1-D model shows a pressure recovery after location 1577 in.). Previous strain gauge data has shown no increase in pressure in this region and thus the pressure at the factory joint models the aft end pressure very well.

A. AMBIENT CONDITIONS

DATE & TIME AT FIRE PULSE	13.0 - 12 - 11 - 1990	
AMBIENT TEMPERATURE	44.00	DEG F
MEASURED MEAN BULK TEMPERATURE	65.00	DEG F
MEASURED AMBIENT PRESSURE	12.28	PSIA

B. WEIGHT DATA

TOTAL LOADED PROPELLANT WEIGHT	1109826.0	LBS
TOTAL EXPENDED WEIGHT	1114176.0	LBS
UNEXPENDED PROPELLANT RESIDUE	2000.0	LBS
EXPENDED INERT WEIGHT		
A FORWARD SEGMENT	718.0	LBS
B FORWARD CENTER SEGMENT	598.0	LBS
C AFT CENTER SEGMENT	962.0	LBS
D AFT SEGMENT (INCLUDING NOZZLE FROM FIELD JOINT FORWARD)	4072.0	LBS
E TOTAL EXPENDED INERTS	6350.0	LBS
TOTAL EXPENDED PROPELLANT WEIGHT	1107826.0	LBS

C. NOZZLE DATA

INITIAL THROAT AREA	2280.3	SQ IN
FINAL THROAT AREA	249.3	SQ IN
WEB TIME AVERAGE THROAT AREA	2378.5	SQ IN
ACTION TIME AVERAGE THROAT AREA	2306.9	SQ IN
TOTAL TIME AVERAGE THROAT AREA	2307.1	SQ IN
INITIAL EXIT AREA	1750.5	SQ IN
FINAL EXIT AREA	1761.8	SQ IN
TOTAL TIME AVERAGE EXIT AREA	1764.2	SQ IN
WEB TIME AVERAGE THROAT RADIAL EROSION RATE	0.00972	IN/SEC
ACTION TIME AVERAGE THROAT RADIAL EROSION RATE	0.00910	IN/SEC
TOTAL TIME AVERAGE THROAT RADIAL EROSION RATE	0.00905	IN/SEC
INITIAL EXPANSION RATIO	7.7123	
WEB TIME AVERAGE EXPANSION RATIO	7.4138	
ACTION TIME AVERAGE EXPANSION RATIO	7.3878	
ACTION TIME AVERAGE NOZZLE EFFICIENCY	0.97292	
TOTAL TIME AVERAGE NOZZLE EFFICIENCY	0.97305	

K 01

THIokol CORPORATION SRM STATIC TEST TEN-7 11 DECEMBER 1990 S

D. TIME AND BALLISTIC DATA

TIME AT FIRST INDICATION OF HEAD END PRESSURE	0.029	SEC
IGNITION DELAY TIME	-0.023	SEC
TIME AT 90% MAX IGNITER PRESSURE	0.052	SEC
IGNITION INTERVAL TIME	0.235	SEC
IGNITION RISE TIME	0.208	SEC
TIME WHEN HEAD END CHAMBER PRESSURE	0.235	SEC
ACHIEVES 565.5 PSIA DURING IGNITION	120.951	SEC
TIME AT LAST INDICATION OF HEAD END PRESSURE	109.049	SEC
TIME AT WEB BISECTOR	108.813	SEC
WEB TIME	120.203	SEC
ACTION TIME	120.922	SEC
TOTAL TIME	0.512	SEC
TAILOFF THRUST DECAY TIME		
MAXIMUM CHANGE IN THRUST OVER TEN MILLISECONDS	271759.	LB
DURING IGNITION	1840.	PSIA
MAX IGNITER PRESSURE	933.20	PSIA
MAX MEASURED HEAD END PRESSURE	0.652	SEC
TIME AT MAX HEAD END PRESSURE	3165676.	LB
MAXIMUM THRUST	16,504	SEC
TIME AT MAX THRUST		
MAXIMUM THRUST CORRECTED TO VACUUM	3381797.	LB
MAXIMUM THRUST CORRECTED TO SEA LEVEL	3123085.	LB
MAXIMUM STAGNATION PRESSURE	863.7	PSIA
WEB TIME AVERAGE HEAD END CHAMBER PRESSURE	680.58	PSIA
ACTION TIME AVERAGE HEAD END CHAMBER PRESSURE	632.04	PSIA
WEB TIME AVERAGE NOZZLE STAGNATION PRESSURE	663.86	PSIA
ACTION TIME AVERAGE NOZZLE STAGNATION PRESSURE	616.82	PSIA
INITIAL THRUST	2942746.	LB
INITIAL THRUST CORRECTED TO VACUUM	3158717.	LB
INITIAL THRUST CORRECTED TO SEA LEVEL	2900184.	LB
WEB TIME AVERAGE THRUST	2443689.	LB
WEB TIME AVERAGE THRUST CORRECTED TO VACUUM	2660180.	LB
ACTION TIME AVERAGE THRUST	2259933.	LB
ACTION TIME AVERAGE THRUST CORRECTED TO VACUUM	2471540.	LB
CHARACTERISTIC EXHAUST VELOCITY	5079.31	FT/SEC

L 01

THIOL CORPORATION SRM STATIC TEST TEN-7 11 DECEMBER 1990 S

E. IMPULSE DATA

MEASURED TOTAL IMPULSE	271.792	MILLION LB-SEC
TOTAL IMPULSE CORRECTED TO VACUUM	297.302	MILLION LB-SEC
MEASURED IMPULSE AT 20 SEC	61.497	MILLION LB-SEC
20 SEC IMPULSE CORRECTED TO VACUUM	65.814	MILLION LB-SEC
MEASURED IMPULSE AT 60 SEC	162.382	MILLION LB-SEC
60 SEC IMPULSE CORRECTED TO VACUUM	175.353	MILLION LB-SEC
WEB TIME IMPULSE	265.906	MILLION LB-SEC
WEB TIME IMPULSE CORRECTED TO VACUUM	289.462	MILLION LB-SEC
ACTION TIME IMPULSE	271.653	MILLION LB-SEC
ACTION TIME IMPULSE CORRECTED TO VACUUM	297.067	MILLION LB-SEC
SPECIFIC IMPULSE	243.940	SEC
SPECIFIC IMPULSE CORRECTED TO VACUUM	266.836	SEC
WEB TIME SPECIFIC IMPULSE	245.379	SEC
WEB TIME SPECIFIC IMPULSE CORRECTED TO VACUUM	267.117	SEC
ACTION TIME SPECIFIC IMPULSE	243.981	SEC
ACTION TIME SPECIFIC IMPULSE CORRECTED TO VACUUM	266.824	SEC
PROPELLANT SPECIFIC IMPULSE	245.336	SEC
PROPELLANT SPECIFIC IMPULSE CORRECTED TO VACUUM	268.367	SEC

F. PRESSURE INTEGRAL DATA

TOTAL TIME PRESSURE INTEGRAL	76024.1	LB/SG IN-SEC
WEB TIME PRESSURE INTEGRAL	74056.6	LB/SG IN-SEC
ACTION TIME PRESSURE INTEGRAL	75982.6	LB/SG IN-SEC

A 02

THIKOL CORPORATION SRM STATIC TEST TEM-7 11 DECEMBER 1990 S

CORRECTED TO 40. DEGREES

D. TIME AND BALLISTIC DATA

TIME AT FIRST INDICATION OF HEAD END PRESSURE	0.031	SEC
TIME WHEN HEAD END CHAMBER PRESSURE	0.247	SEC
ACHIEVES 503.5 PSIA DURING IGNITION	124.320	SEC
TIME AT LAST INDICATION OF HEAD END PRESSURE	112.186	SEC
TIME AT WEB BISECTOR	111.940	SEC
WEB TIME	123.572	SEC
ACTION TIME	906.10	PSIA
MAX MEASURED HEAD END PRESSURE	0.670	SEC
TIME AT MAX HEAD END PRESSURE	3283433	LB
MAXIMUM THRUST CORRECTED TO VACUUM	838.6	PSIA
MAXIMUM STAGNATION PRESSURE	660.67	PSIA
WEB TIME AVERAGE HEAD END CHAMBER PRESSURE	613.84	PSIA
ACTION TIME AVERAGE HEAD END CHAMBER PRESSURE	644.44	PSIA
WEB TIME AVERAGE NOZZLE STAGNATION PRESSURE	599.06	PSIA
ACTION TIME AVERAGE NOZZLE STAGNATION PRESSURE	2582354	LB
WEB TIME AVERAGE THRUST CORRECTED TO VACUUM	2400403	LB
ACTION TIME AVERAGE THRUST CORRECTED TO VACUUM		

E. IMPULSE DATA

TOTAL IMPULSE CORRECTED TO VACUUM	296.831	MILLION LB-SEC
20 SEC IMPULSE CORRECTED TO VACUUM	63.837	MILLION LB-SEC
60 SEC IMPULSE CORRECTED TO VACUUM	170.935	MILLION LB-SEC
WEB TIME IMPULSE CORRECTED TO VACUUM	289.068	MILLION LB-SEC
ACTION TIME IMPULSE CORRECTED TO VACUUM	296.622	MILLION LB-SEC
SPECIFIC IMPULSE CORRECTED TO VACUUM	266.413	SEC
WEB TIME SPECIFIC IMPULSE CORRECTED TO VACUUM	266.705	SEC
ACTION TIME SPECIFIC IMPULSE CORRECTED TO VACUUM	266.412	SEC
PROPELLANT SPECIFIC IMPULSE CORRECTED TO VACUUM	267.940	SEC

**** 02***

THIOL CORPORATION SRM STATIC TEST TEM-7 11 DECEMBER 1990 S

CORRECTED TO 60. DEGREES

D. TIME AND BALLISTIC DATA

TIME AT FIRST INDICATION OF HEAD END PRESSURE	0.029	SEC
TIME WHEN HEAD END CHAMBER PRESSURE		
ACHIEVES 563.5 PSIA DURING IGNITION	0.238	SEC
TIME AT LAST INDICATION OF HEAD END PRESSURE	121.619	SEC
TIME AT WEB BISECTION	109.649	SEC
WEB TIME	109.411	SEC
	120.864	SEC
ACTION TIME	927.72	PSIA
MAX MEASURED HEAD END PRESSURE	0.656	SEC
TIME AT MAX HEAD END PRESSURE		
MAXIMUM THRUST CORRECTED TO VACUUM	3361900.	LB
MAXIMUM STAGNATION PRESSURE	858.6	PSIA
WEB TIME AVERAGE HEAD END CHAMBER PRESSURE	676.60	PSIA
ACTION TIME AVERAGE HEAD END CHAMBER PRESSURE	628.38	PSIA
WEB TIME AVERAGE NOZZLE STAGNATION PRESSURE	659.98	PSIA
ACTION TIME AVERAGE NOZZLE STAGNATION PRESSURE	613.25	PSIA
WEB TIME AVERAGE THRUST CORRECTED TO VACUUM	2644611.	LB
ACTION TIME AVERAGE THRUST CORRECTED TO VACUUM	2457255.	LB

E. IMPULSE DATA

TOTAL IMPULSE CORRECTED TO VACUUM	297.197	MILLION LB-SEC
20 SEC IMPULSE CORRECTED TO VACUUM	65.402	MILLION LB-SEC
60 SEC IMPULSE CORRECTED TO VACUUM	174.446	MILLION LB-SEC
WEB TIME IMPULSE CORRECTED TO VACUUM	289.350	MILLION LB-SEC
ACTION TIME IMPULSE CORRECTED TO VACUUM	296.993	MILLION LB-SEC
SPECIFIC IMPULSE CORRECTED TO VACUUM	266.741	SEC
WEB TIME SPECIFIC IMPULSE CORRECTED TO VACUUM	267.033	SEC
ACTION TIME SPECIFIC IMPULSE CORRECTED TO VACUUM	266.740	SEC
PROPELLANT SPECIFIC IMPULSE CORRECTED TO VACUUM	268.270	SEC

THIOL CORPORATION SRM STATIC TEST TEN-7 11 DECEMBER 1990 S

CORRECTED TO 90. DEGREES

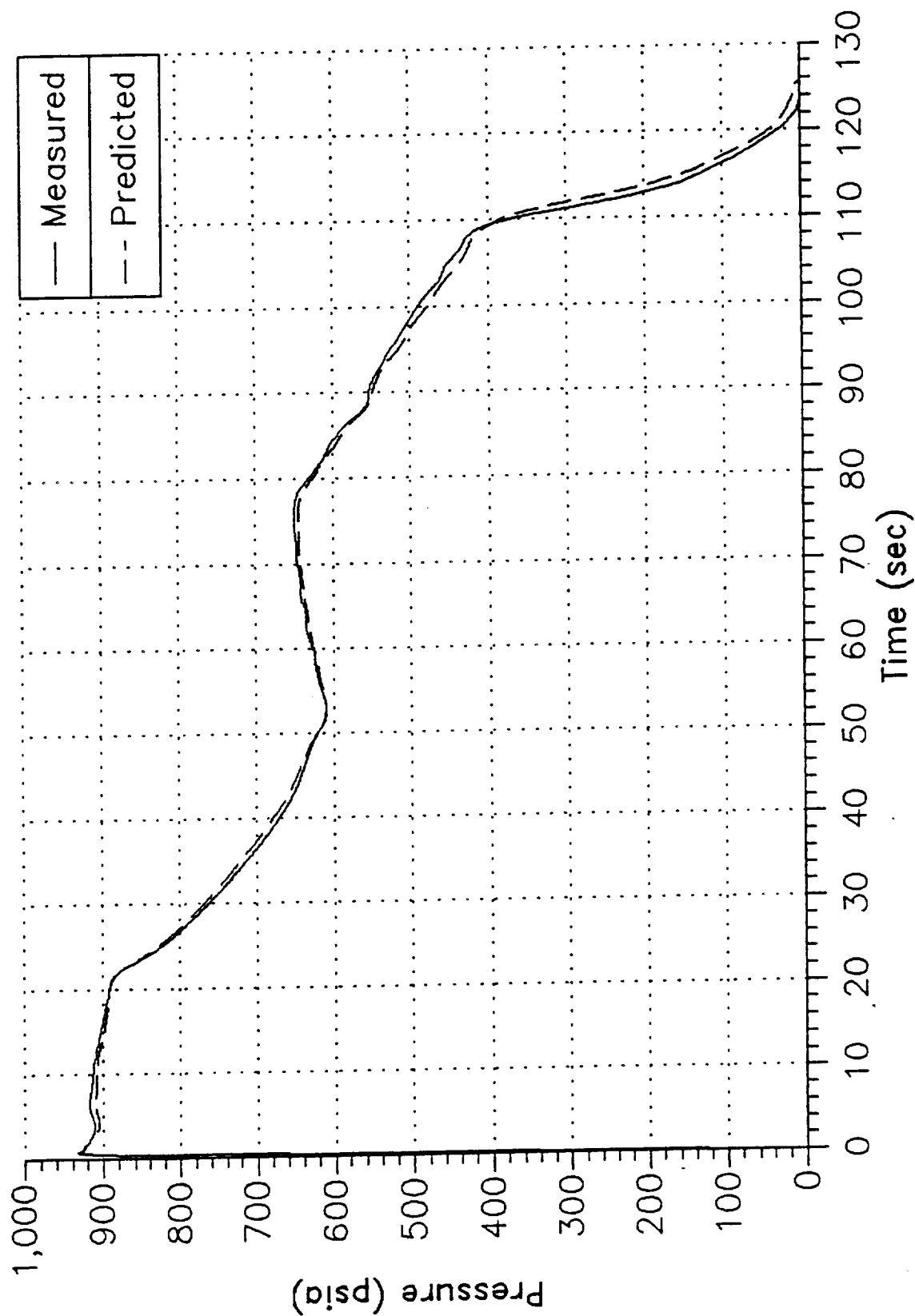
D. TIME AND BALLISTIC DATA

TIME AT FIRST INDICATION OF HEAD END PRESSURE	0.026	SEC
TIME WHEN HEAD END CHAMBER PRESSURE	0.224	SEC
Achieves 583.5 PSIA DURING IGNITION	117.670	SEC
TIME AT LAST INDICATION OF HEAD END PRESSURE	106.040	SEC
TIME AT WEB BISECTOR	105.815	SEC
WEB TIME	116.931	SEC
ACTION TIME	961.12	PSIA
MAX MEASURED HEAD END PRESSURE	0.634	SEC
TIME AT MAX HEAD END PRESSURE	3483113.	LB
MAXIMUM THRUST CORRECTED TO VACUUM	289.5	PSIA
MAXIMUM STAGNATION PRESSURE	700.99	PSIA
WEB TIME AVERAGE HEAD END CHAMBER PRESSURE	650.74	PSIA
ACTION TIME AVERAGE HEAD END CHAMBER PRESSURE	683.77	PSIA
WEB TIME AVERAGE NOZZLE STAGNATION PRESSURE	635.08	PSIA
ACTION TIME AVERAGE NOZZLE STAGNATION PRESSURE	2739954.	LB
WEB TIME AVERAGE THRUST CORRECTED TO VACUUM	2544695.	LB
ACTION TIME AVERAGE THRUST CORRECTED TO VACUUM		

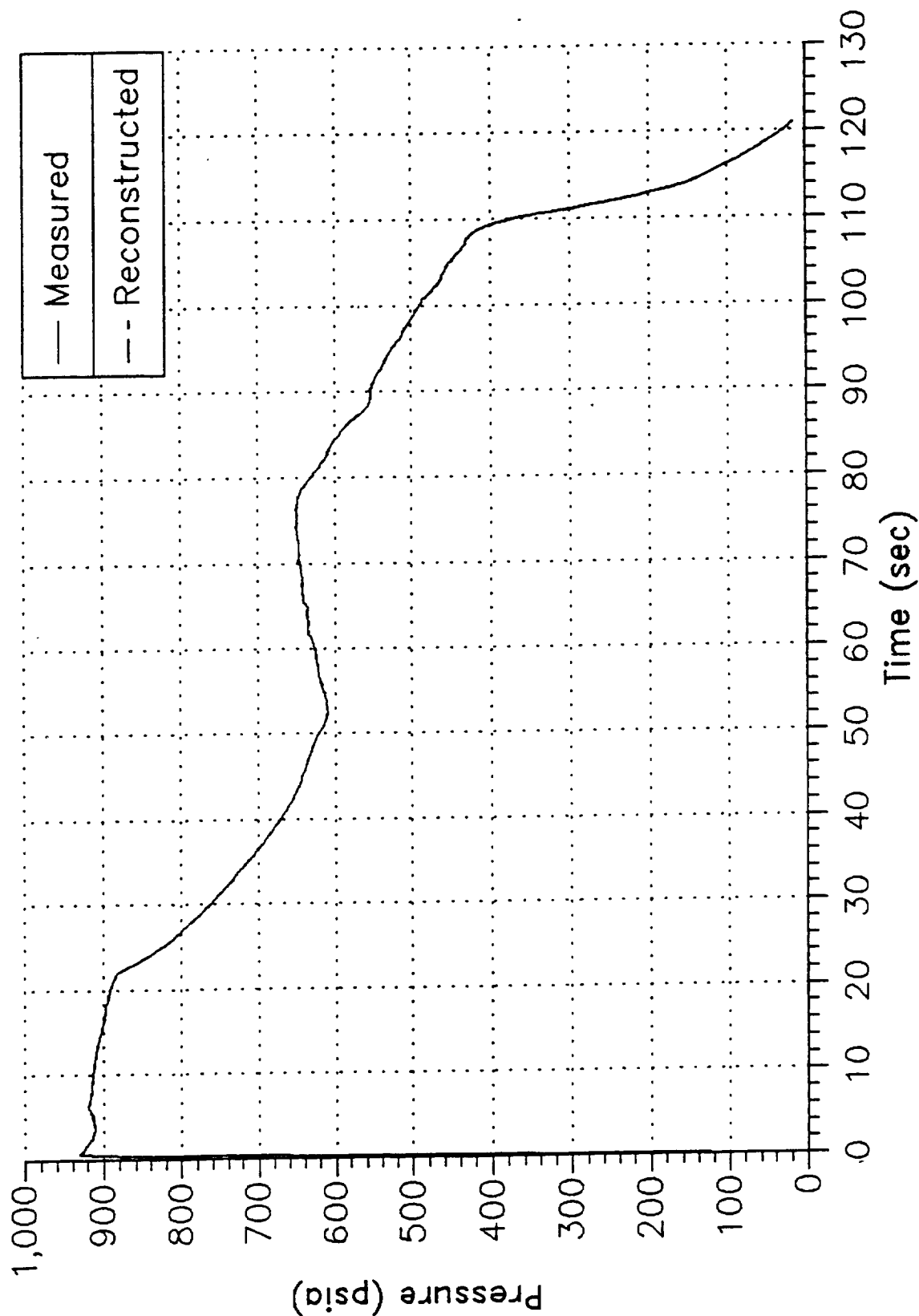
E. IMPULSE DATA

TOTAL IMPULSE CORRECTED TO VACUUM	297.744	MILLION LB-SEC
20 SEC IMPULSE CORRECTED TO VACUUM	67.820	MILLION LB-SEC
60 SEC IMPULSE CORRECTED TO VACUUM	179.915	MILLION LB-SEC
WEB TIME IMPULSE CORRECTED TO VACUUM	289.929	MILLION LB-SEC
ACTION TIME IMPULSE CORRECTED TO VACUUM	297.552	MILLION LB-SEC
SPECIFIC IMPULSE CORRECTED TO VACUUM	267.232	SEC
WEB TIME SPECIFIC IMPULSE CORRECTED TO VACUUM	267.523	SEC
ACTION TIME SPECIFIC IMPULSE CORRECTED TO VACUUM	267.231	SEC
PROPELLANT SPECIFIC IMPULSE CORRECTED TO VACUUM	268.764	SEC

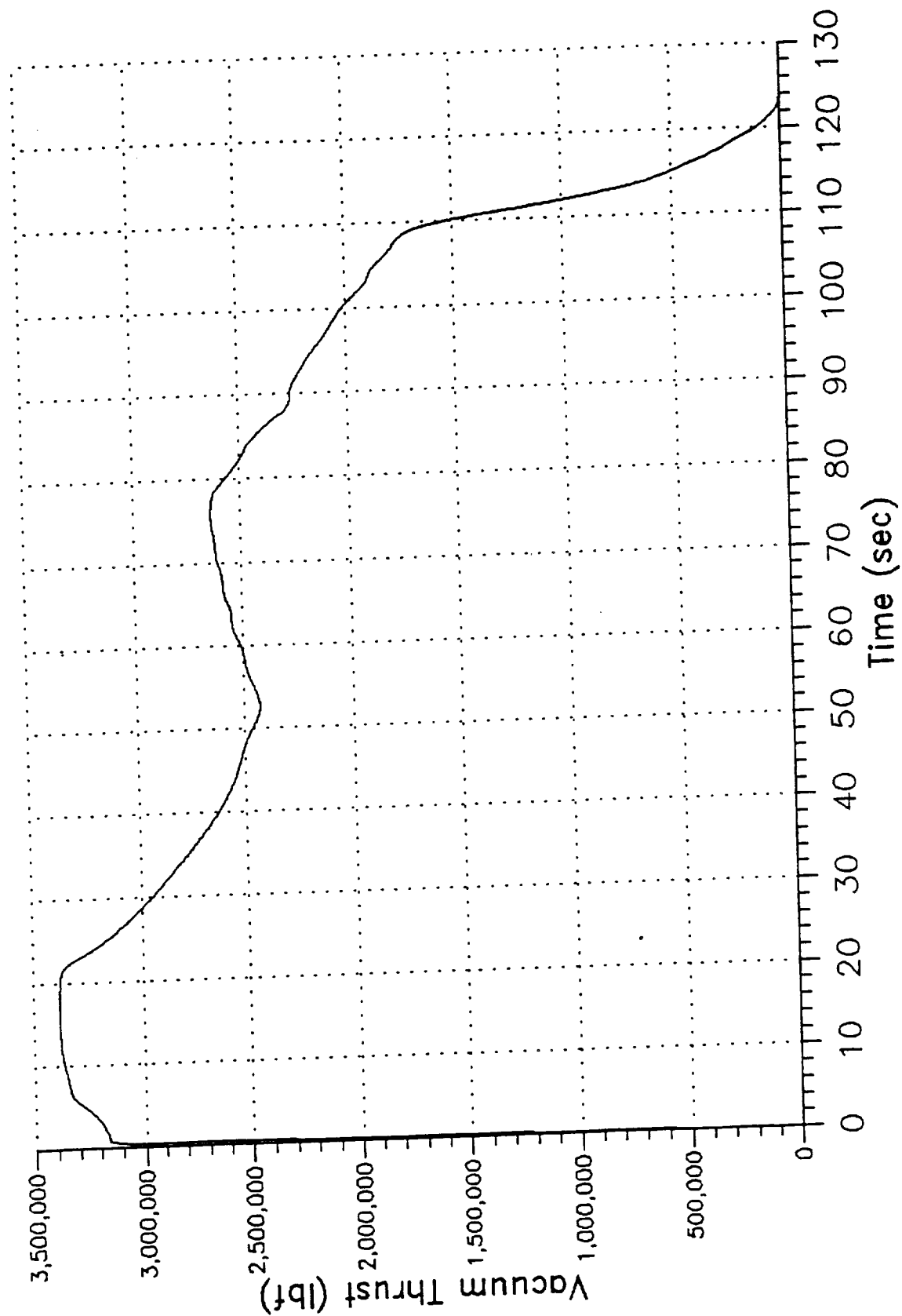
TEM-7 Predicted and Measured Pressure at 65 Deg. F



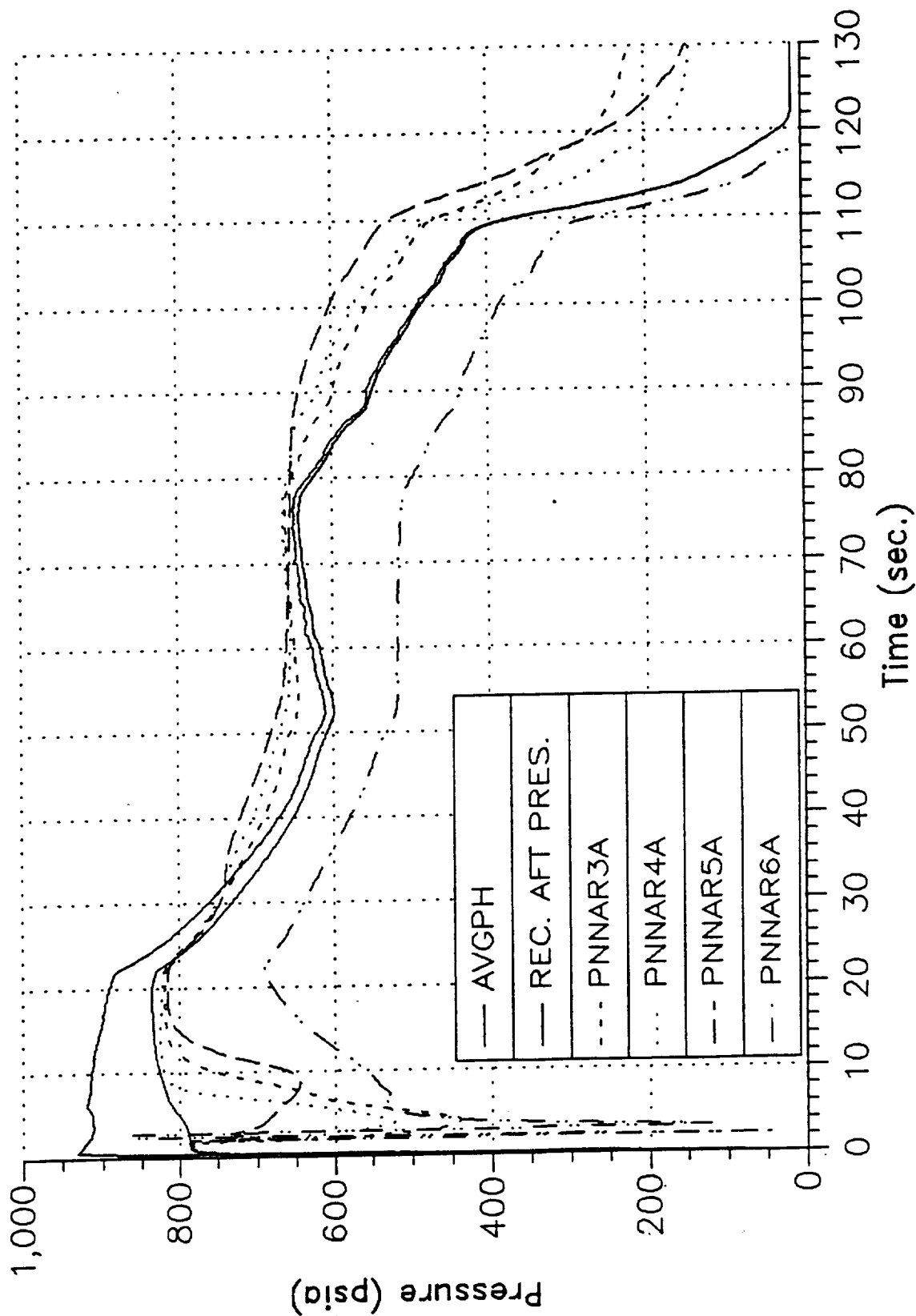
TEM-7 Reconstructed and Measured Pressure at 65 Deg. F



TEM-7 Reconstructed Vacuum Thrust at 65 Deg. F



TEM-7 Comparison of Reconstructed and Measured Aft-End Pressure



All aft end gauges were acoustically quiet (due to partial plugging) and no oscillation analysis could be made.

The motor average subscale burn rates, full-scale motor burn rates (determined from post-test curve matching) and resulting scale factors for SRM-15 to SRM-24, used to predict the TEM-7 burn rate are listed in Table 6-7. The full-scale motor burn rates were determined from post-test curve matching in which the analytical model was forced to match the measured motor performance. The mean scale factor was 1.0175 with a sigma 0.00440 and a coefficient of variation of 0.432 percent.

A plot of the measured data comparing the ignition transients of the TEM static tests is shown in Figure 6-12. The TEM-7 transient was very similar to previously measured motor ignition performance. The TEM-7 maximum pressure rise rate was 80.62 psi/10-msec. The historical three point average pressure rise rate is 90.07 psi/10-msec with a variation of 6.80 psi/10-msec. TEM-7 was the second lowest measured pressure rise rate but was within 2 standard deviations from the population average. A summary table showing the historical pressure rise rates, thrust rise rates and ignition intervals is shown in Table 6-8. A summary of the TEM-7 ignition events is shown in Table 6-9.

The TEM-7 igniter grain configuration was identical to the HPM flight and static test igniter design. The igniter was cast from propellant batch number D760006 using TP-H1178 propellant. The delivered maximum mass flow rate was 330.0 lbm/sec at 65 °F for the TEM-7 igniter (65 °F is the assumed PMBT for the igniter). The TEM-7 igniter performance characteristics were within the expected ranges. Comparison of the TEM-7 igniter performance at 80 °F with the igniter limits at 80 °F is shown in Figure 6-13. The TEM-7 is within the limits at 80 °F.

A comparison of the igniter pressure versus motor head-end and nozzle stagnation pressure for the first 1.4 seconds of motor operation is shown in Figure 6-14. The slight mismatch between igniter and head-end chamber pressure values from 0.6 to 1.4 seconds is within allowed transducer error. A plot of head-end and nozzle stagnation pressure for the full duration of the static test is shown on Figure 6-15. These curves are characteristic of the ratio of the head-end to nozzle stagnation pressures from previous SRM static test motors.

Table 6-7. Burn Rate Data Comparison Subscale to Full-Scale

AT 625 PSIA, 60 °F

<u>MOTOR</u>	<u>SRM TARGET</u>	<u>BURN RATE</u>			<u>SCALE FACTOR</u>
		<u>5" CP STD.</u>	<u>SRM PRED.</u>	<u>SRM DEL.</u>	<u>5" CP STD.</u>
SRM-15A	0.368	0.366	0.370	0.3701	1.0112
SRM-15B	0.368	0.366	0.370	0.3709	1.0134
SRM-16A	0.368	0.365	0.369	0.3684	1.0093
SRM-16B	0.368	0.365	0.369	0.3688	1.1040
SRM-17A	0.368	0.363	0.367	0.3680	1.0138
SRM-17B	0.368	0.362	0.366	0.3694	1.0204
SRM-18A	0.368	0.362	0.367	0.3693	1.0202
SRM-18B	0.368	0.363	0.368	0.3690	1.0165
SRM-19A	0.368	0.364	0.369	0.3703	1.0173
SRM-19B	0.368	0.364	0.369	0.3704	1.0176
SRM-20A	0.368	0.368	0.373	0.3742	1.0168
SRM-20B	0.368	0.366	0.371	0.3744	1.0230
SRM-21A	0.368	0.367	0.370	0.3737	1.0183
SRM-21B	0.368	0.365	0.368	0.3744	1.0258
SRM-22A	0.368	0.362	0.365	0.3675	1.0152
SRM-22B	0.368	0.362	0.365	0.3697	1.0213
SRM-23A	0.368	0.364	0.367	0.3713	1.0201
SRM-23B	0.368	0.364	0.367	0.3721	1.0223
SRM-24A	0.368	0.360	0.365	0.3678	1.0217
SRM-24B	0.368	0.361	0.366	0.3674	1.0177

AVERAGE SCALE FACTOR = 1.0175, SIGMA = 0.00440, %CV = 0.432

ETM-1	0.368	0.365	0.372	0.3681	1.0085
DM-8	0.368	0.360	0.366	0.3677	1.0214
DM-9	0.368	0.362	0.368	0.3691	1.0196
QM-6	0.368	0.360	0.366	0.3665	1.0181
QM-7	0.368	0.358	0.364	0.3657	1.0215
PVM-1	0.368	0.360	0.366	0.3677	1.0214
TEM-1	0.368	0.362	0.368	0.3659	1.0116
TEM-2	0.368	0.362	0.368	0.3664	1.0122
TEM-3	0.368	0.362	0.368	0.3672	1.0155
TEM-4	0.368	0.362	0.369	0.3681	1.0160
TEM-5	0.368	0.362	0.368	0.3654	1.0105
TEM-6	0.368	0.361	0.367	0.3667	1.0166
FSM-1	0.368	0.364	0.370	0.3701	1.0165
TEM-7	0.368	0.363	0.370	0.3709	1.0208

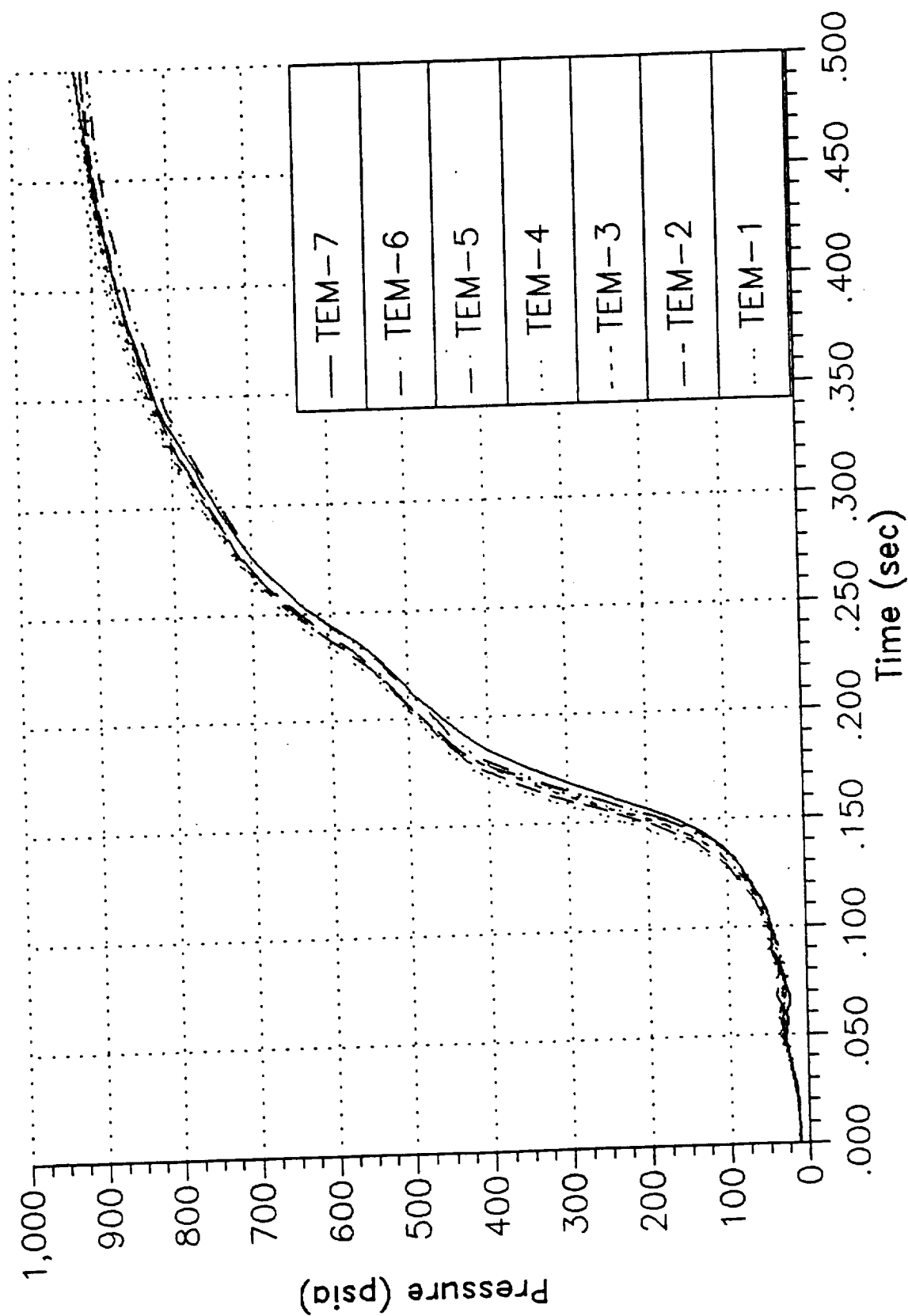
Table 6-8. Historical Three Point Average Thrust and Pressure Rise Rate Data

MOTOR	OCCURRENCE TIME	PRESSURE RISE RATE	OCCURRENCE TIME	THRUST RISE RATE	IGNITION INTERVAL
<u>STATIC TEST</u>					
DM-2	0.1480	85.30	0.1480	245,380	0.2330
QM-1	0.1560	86.38	0.1560	246,128	0.2362
QM-2	0.1640	93.58	0.1720	234,950	0.2391
QM-3	0.1560	94.45	0.1520	245,615	0.2287
QM-4	0.1505	91.96	0.2225	234,438	0.2192
ETM-1A	0.1520	86.72	0.1560	230,023	0.2279
DM-8	0.1680	77.00	0.1760	257,272	0.2424
DM-9	0.1640	81.00	0.1720	275,525	0.2436
QM-6	0.1480	87.40	0.1520	211,476	0.2321
QM-7	0.1480	99.60	N/A	N/A	0.2230
PVM-1	0.1520	92.80	0.1520	294,664	0.2338
TEM-01	0.1520	85.13	0.1520	238,583	0.2255
QM-8	0.1720	72.30	N/A	N/A	0.2517
TEM-2	0.1520	94.40	0.1520	288,772	0.2280
TEM-3	0.1520	88.51	N/A	N/A	0.2272
TEM-4	0.1480	81.52	0.1520	279,764	0.2283
TEM-5	0.1560	87.12	N/A	N/A	0.2299
TEM-6	0.1600	84.49	0.1520	273,946	0.2342
FSM-1	0.1520	97.06	0.1440	250,453	0.2278
<u>FLIGHT MOTORS</u>					
SRM-1A	0.1530	87.58			0.2373
SRM-1B	0.1500	91.57			0.2358
SRM-2A	0.1530	90.74			0.2348
SRM-2B	0.1660	90.27			0.2345
SRM-3A	0.1500	91.05			0.2308
SRM-3B	0.1500	89.68			0.2271
SRM-5A	0.1530	95.10			0.2361
SRM-5B	0.1660	84.43			0.2380
SRM-6A	0.1530	92.72			0.2342
SRM-6B	0.1470	88.22			0.2329
SRM-7A	0.1500	99.90			0.2282
SRM-7B	0.1500	99.32			0.2276
SRM-8A	0.1530	106.29			0.2224
SRM-8B	0.1500	91.06			0.2196
SRM-9A	0.1530	92.31			0.2303
SRM-10A	0.1530	92.89			0.2373
SRM-10B	0.1500	84.56			0.2342
SRM-13B	0.1410	98.85			0.2115
RSRM-1A	0.1501	99.0			0.2296
RSRM-1B	0.1596	80.5			0.2310
RSRM-2A	0.1564	87.3			0.2390
RSRM-2B	0.1501	100.2			0.2342
	NUMBER	43		11	35
	AVERAGE	90.07		246,732	0.2321
	STANDARD DEVIATION	6.80		22,627	0.0076
	% COEFFICIENT OF VARIATION	7.55		9.17	3.27
TEM-7	0.1600	80.62	N/A	N/A	0.2359

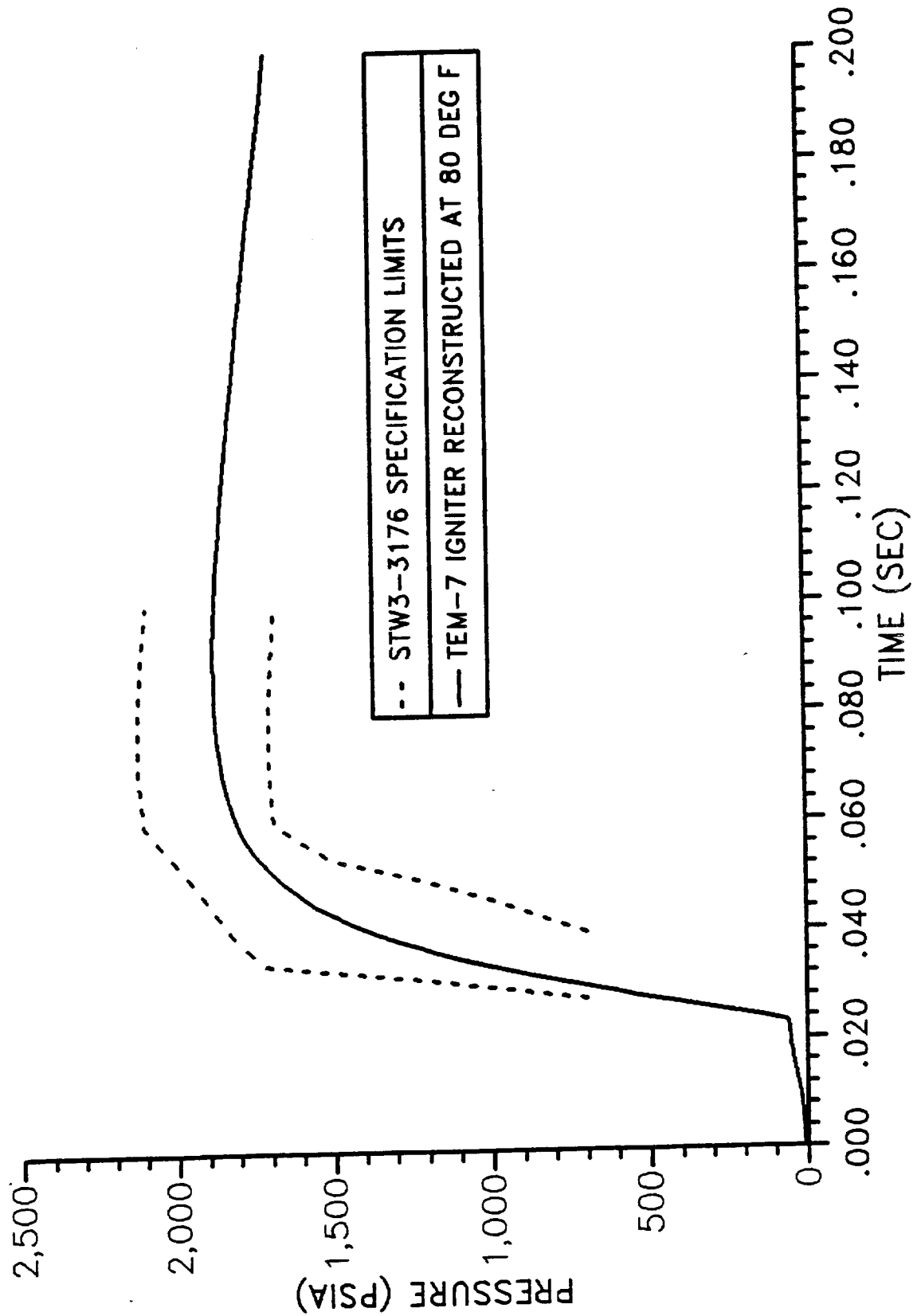
Table 6-9. Measured SRM Ignition Performance Data at 65 °F

PARAMETER	TEM-7	SPECIFICATION REQUIREMENT
MAXIMUM IGNITER MASS FLOW RATE (LBM/SEC)	330.0	N/A
IGNITION TRANSIENT (SEC) (0 TO 563.5 PSIA)	0.2359	0.170 - 0.340
MAXIMUM PRESSURE RISE RATE (PSI/10-MSEC)	80.6	109
PRESSURE LEVEL AT START OF MAXIMUM RISE RATE (PSIA)	231	N/A
TIME SPAN OF MAXIMUM PRESSURE RISE (MSEC)	160 - 170	N/A
EQUILIBRIUM PRESSURE 0.6 SEC (IGNITION END) (PSIA)	931	N/A
TIME TO FIRST IGNITION (SEC) (BEGIN PRESSURE RISE)	0.029	N/A

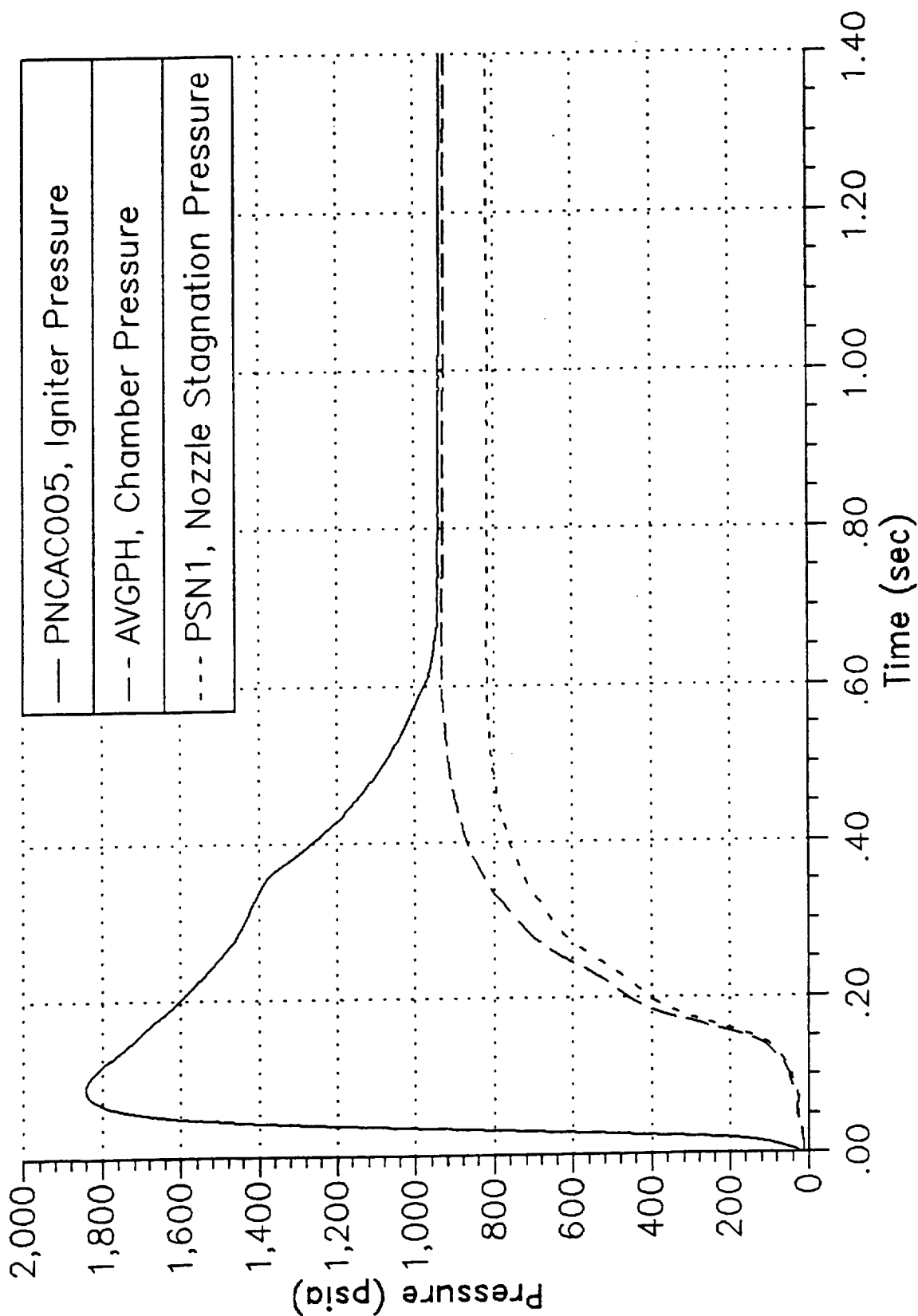
Measured Head-End Pressure Transients



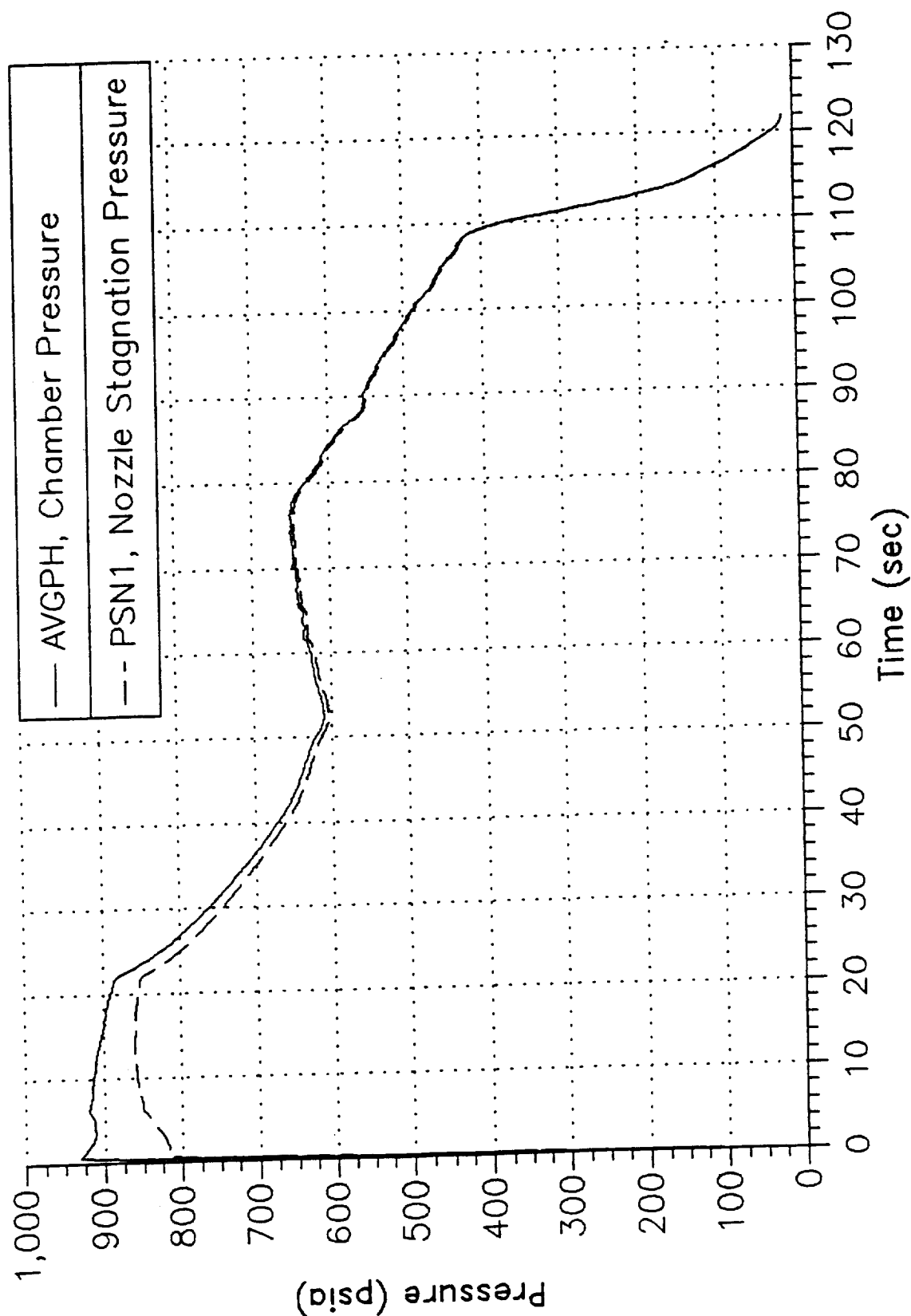
TEM-7 IGNITER RECONSTRUCTED AT 80 DEG F
IN SPECIFICATION LIMITS



TEM-7 Igniter Pressure vs. Head-End and Nozzle Stagnation Pressure



TEM-7 Measured Head-End and Nozzle Stagnation Pressure Time Histories



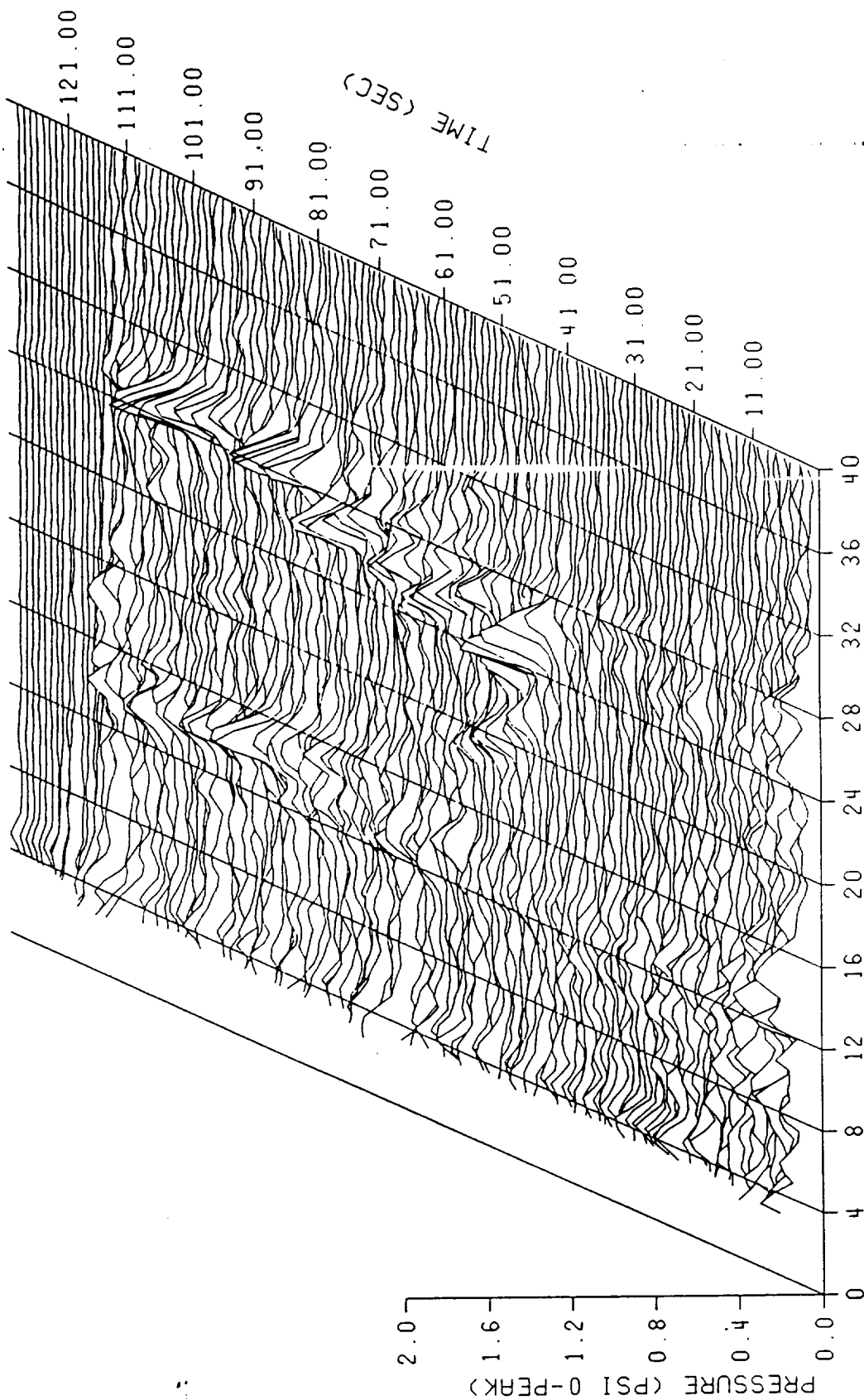
TEM-7 was instrumented with 3 pressure transducers for head-end pressure measurement (PNCAC001-PNCAC003) and 1 gauge for igniter pressure measurement (PNCAC005). The signal from the head-end OPT data channel (PNCAC001) was split to provide both A-C coupled data (for chamber pressure oscillation data) and mean pressure. TEM-7 was also instrumented with 4 aft end pressure gauges (PNNAR003-PNNAR006) and again the aft end OPT data channel (PNNAR006) was split to provide both oscillatory aft end chamber pressure data and mean data. However, aft end data was not useful for dynamic analysis on this test. In addition, the mean pressure data channels are used to calculate dynamic pressure and to verify the accuracy of the A-C coupled data.

Data acquired from gauge PNCAC001 are displayed in a waterfall plot format in Figure 6-16. The first longitudinal (1-L) and second longitudinal (2-L) acoustic modes can be observed at about 15 and 30 Hz, respectively. This waterfall plot is fairly typical of HPM designs. The magnitudes on this static test were among the lowest experienced on HPMs.

Figures 6-10 and 6-11 describe the running, instantaneous, peak-to-peak oscillation amplitudes of the 1-L and 2-L acoustic modes respectively for the TEM-7 motor head-end pressure. This type of analysis is more representative of instantaneous oscillations than are the time averaged oscillations presented in a waterfall plot.

When using waterfall plots to compare static test motor oscillation amplitudes, it is important to remember that this format uses an averaging method of analysis. This presents no difficulty for steady state signals but has an attenuating effect on transient signals. Since most of the data obtained from a solid rocket motor are transient, any oscillation magnitudes referred to as maxima are, in fact, not true but averaged values over a given time slice. These numbers are, nonetheless, very useful for comparison. Table 6-10 shows such a comparison for recent static test motors and the flight motors. This table contains the most recent data. DM-6 and DM-7 were Filament Wound Case (FWC) motors.

A comparison of TEM-7 thrust data at 60 °F and a burn rate of 0.368 in./sec at 625 psia and 60 °F with the CEI Specification CPW1-3300, dated 15 January 1986, thrust-time limits at 0.368 in./sec is shown on Figure 6-19. The TEM-7 performance was within average population limits. Note that the limits are for the average of the historical SRM population not an individual motor. The historical motor population is well within the limits. None of the individual motor performance tolerances and limit parameters were exceeded. The TEM-7 ignition performance satisfied the ignition interval and the maximum pressure rise rate requirements as shown in Table 6-9.

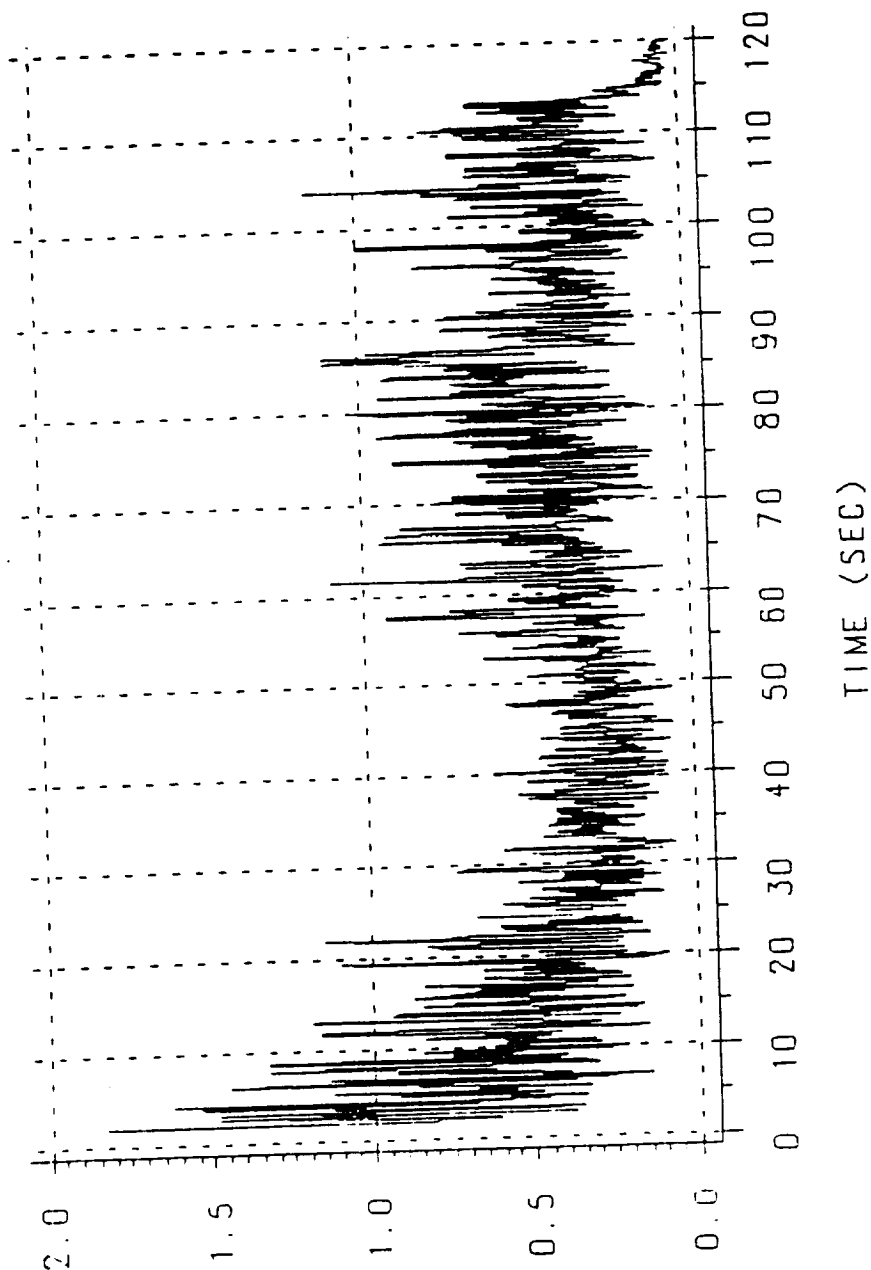


SHUTTLE TEM-7 PNCAC001 FM, 750 HZ 1-L, 2-L 2000 S/S

START TIME = 1.00000 SEC
 END TIME = 129.000 SEC
 TIME SLICE = 2.00000 SEC
 SAMPLE RATE 2000. SPS

TIME INCREMENT = 1.00000 SEC
 X SKEW VALUE = 0.035000 IN.
 Y SKEW VALUE = 0.075000 IN.

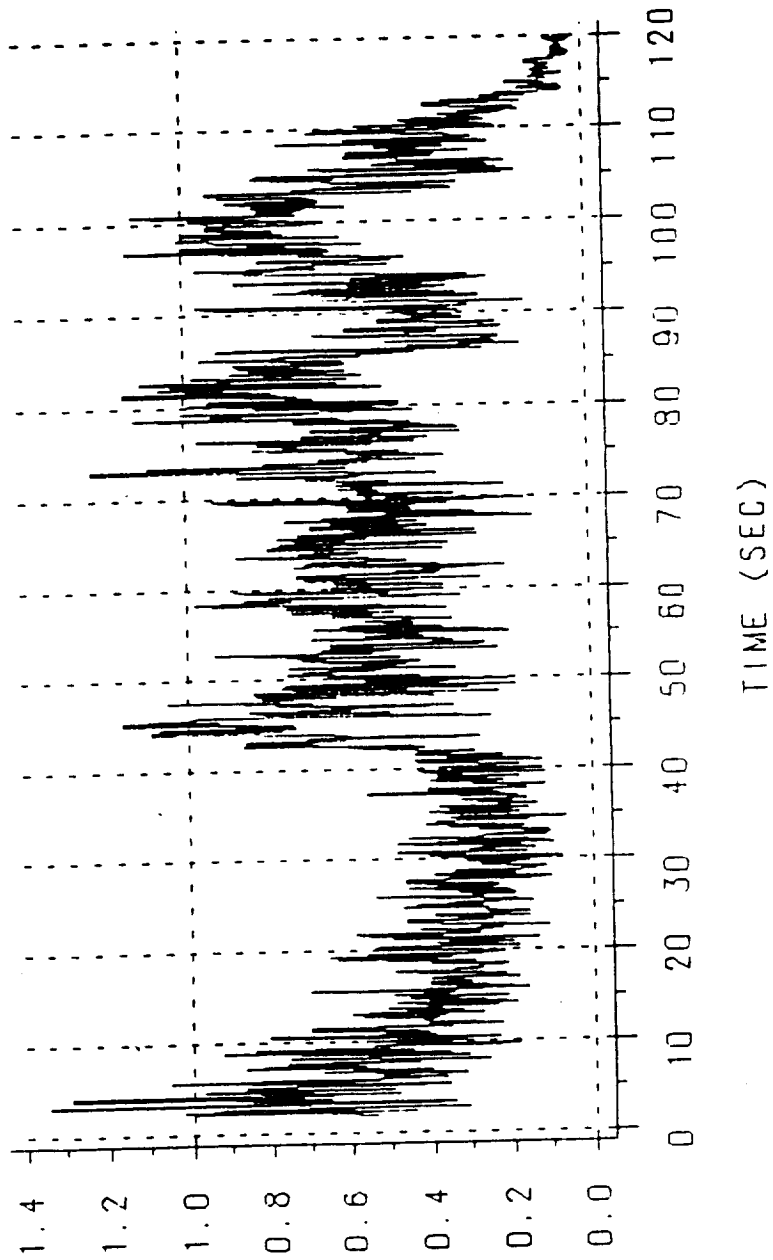
MAXIMUM OSCILLATION AMPLITUDES
PNCAC001 1-L ACOUSTIC MODE 2000 SPS



PRESSURE (PSI P-P)

TEST — TEM-7 250 PT

MAXIMUM OSCILLATION AMPLITUDES
PNCAC001 2-L ACOUSTIC MODE 2000 SPS



PRESSURE (PSI P-P)

TEST — TEM-7 250 PT

TEM-7 Reconstructed Thrust Compared to CEI Specification Limits

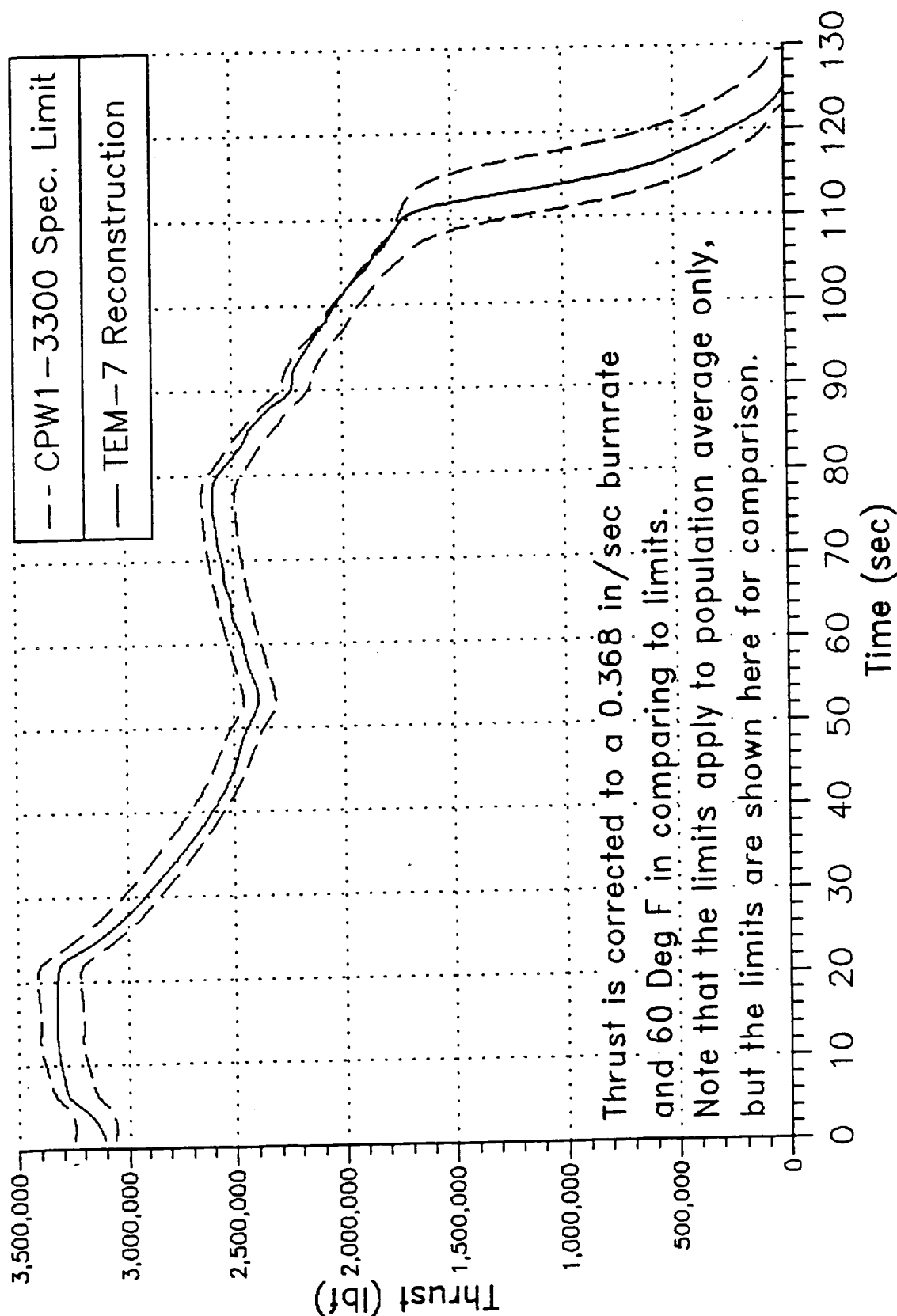


Table 6-10

MAXIMUM PRESSURE OSCILLATION AMPLITUDE COMPARISON

<u>MOTOR</u>	<u>SOURCE OF MEASUREMENT</u>	<u>MODE</u>	<u>TIME OF MEASUREMENT</u>	<u>FREQUENCY (HZ)</u>	<u>MAX PRESSURE (PSI 0-TO-PEAK)</u>
TEM-7	Waterfall PNCAC002	1-L	85	15.5	0.45
		2-L	100	29.5	0.53
FSM-1 *	Waterfall PNCAC001	1-L	100	14.0	0.64
		2-L	79	29.5	0.74
TEM-6	Waterfall PNCAC001	1-L	92	15.0	0.41
		2-L	98/99	29.5	0.67
TEM-6 (Aft)	Waterfall PNNAR005	1-L	92	15.0	0.31
		2-L	98/99	29.5	0.44
TEM-5	Waterfall PNCAC005	1-L	81	16.0	0.46
		2-L	100	29.5	0.57
TEM-4	Waterfall	1-L	115	14.5	0.37
		2-L	87	29.5	0.96
TEM-3	Waterfall	1-L	106	15.0	0.36
		2-L	102	30.0	0.58
STS-29 (left)	Waterfall AC OPT	1-L	86	15.5	0.31
		2-L	89	28.0	0.44
STS-29 (right)	Waterfall AC OPT	1-L	85	15.5	0.38
		2-L	83	29.5	0.54
TEM-2	Waterfall	1-L	78	16.0	0.43
		2-L	100	29.5	0.68
QM-8 *	Waterfall (P000002)	1-L	104	14.5	1.32
		2-L	55	27.5	0.47
TEM-1	Waterfall	1-L	79	15.5	0.37
		2-L	95	29.5	0.78
STS-27 (left)	Waterfall AC OPT	1-L	82	15.5	0.37
		2-L	82	29.5	0.60
STS-27 (right)	Waterfall AC OPT	1-L	82	15.5	0.57
		2-L	83	29.5	0.72
STS-26 (left)	Waterfall AC OPT	1-L	79	16.0	0.70
		2-L	95	29.5	0.87
STS-26 (right)	Waterfall AC OPT	1-L	83	15.0	0.54
		2-L	94	30.0	0.47
PVM-1 *	Waterfall	1-L	99	14.5	1.23
		2-L	79	29.5	0.77
QM-7 *	Waterfall P000001	1-L	93	14.5	1.40
		2-L	79	29.5	0.95
QM-6 *	Waterfall	1-L	107	14.5	1.05
		2-L	85	29.5	0.53

* RSRM static test motors.

** Filament wound case (FWC) HPM motors.

Table 6-10 (cont)
MAXIMUM PRESSURE OSCILLATION AMPLITUDE COMPARISON

<u>MOTOR</u>	<u>SOURCE OF MEASUREMENT</u>	<u>MODE</u>	<u>TIME OF MEASUREMENT</u>	<u>FREQUENCY (HZ)</u>	<u>MAX PRESSURE (PSI 0-TO-PEAK)</u>
DM-9 *	Waterfall	1-L	107	14.5	0.81
		2-L	96	30.0	0.64
DM-8 *	Waterfall	1-L	78	16.0	0.58
		2-L	97	29.5	0.62
ETM-1A	Waterfall	1-L	84	15.5	0.45
		2-L	101	29.5	0.61
DM-7 **	Waterfall	1-L	77	15.5	0.90
		2-L	96	29.0	0.62
DM-6 **	Waterfall	1-L	76	15.5	0.51
		2-L	86	29.0	0.78
QM-4	Waterfall	1-L	81	15.5	0.31
		2-L	80	29.5	0.30

* RSRM static test motors.

** Filament wound case (FWC) HPM motors.

6.8 STATIC TEST SUPPORT EQUIPMENT

6.8.1 Introduction

The deluge system and related instrumentation were similar to previous TEMs. Deluge system nozzle arrangement is shown in Figure 1.2.8-1.

6.8.2 Observations

The deluge system performed as designed.

7.0 APPLICABLE DOCUMENTS

<u>Drawings</u>	<u>Title</u>
Unnumbered	TEM-7 Drawing Tree
1U50159	Plug, Leak Check Port, Nozzle
1U50185	Case Segment, Stiffener
1U50188	Transducer, Motional Pickup Pressure
1U50776	Igniter, Rocket Motor, Test Configuration
1U51055	Pin Straight Headless
1U51899	Retainer, Pin Field Joint, SRM
1U51927	Gasket - Outer
1U52295	S/A Device
1U52565	Segment, Rocket Motor, Fwd (Thermal Protection)
1U52566	Segment, Rocket Motor, Center (Thermal Protection)
1U52757	Segment, Rocket Motor, Aft (Thermal Protection)
1U52840	Flex Bearing Assembly
1U76425	Adjustable Vent Port Plug
1U76598	Bolt, Machine, Ultrasonic
1U76702	Cable Assembly, Power, Electrical-Heater, Fwd Dome
1U76703	Cable Assembly, Power, Electrical, Branched-Heater, Fwd Segment
1U76704	Cable Assembly, Power, Electrical, Branched-Heater, Fwd Ctr Segment
1U76705	Cable Assembly, Power, Electrical, Branched-Heater, Aft Ctr Segment

1U76706	Cable Assembly, Power, Electrical-Heater, Aft Segment
1U77252	Heater - Field Joint
1U77253	Heater - Igniter to Case Joint
1U82840	Band Pin Assembly Retainer
1U100269	Plug, Machine Thread
2U65040	Assembly Fixture - Nozzle
2U129361	CO ₂ Quench System T-97
2U129363	Water Deluge System
2U129760	Static Test Arrangement
2U129764	Aft Test Stand Ass'y Sequence T-97
2U129765	Forward Test Stand Sequence
4U69505	Shield, Deluge System
7U76608	Boot Assy, Flexible Bearing, Nozzle
7U76609	Cowl, Flexible Boot, Nozzle
7U76736	Exit Cone Assy, Fwd Section
7U76738	Nozzle Assembly, Final
7U76827	Boot Cavity Pressure Transducer Assy
7U76864	Bearing Protector, Flexible
7U76865	Housing Assembly, Modified - Nozzle, Fixed .
7U76879	Test Assembly, TEM
7U76881	Motor Assy, Test, TEM
7U76882	Nozzle Assembly Segment, TEM
7U76899	Igniter/Fwd Segment Assy, TEM
7U76902	Transducer Assy, Pressure
7U76983	Insulated SAPMD

7U77118	Heater - Field Joint, Nozzle and Igniter, Refurbished
7U77266	Nose Inlet Assembly
7U77267	Exit Cone Assy, Aft - Modified
7U77310	Throat - Inlet Assy, Nozzle
7U77328	Joint Protection Systems, Technical Evaluation Motor

Specifications

Title

CPW1-3600A	Prime Equipment Contract End Item Detail Specification (CEI)
STW4-2621	Insulation, Acrylonitrile Butadiene Rubber (NBR), Asbestos and Silicon Dioxide-Filled
STW4-2868	Thermal Insulation, Ethylene Propylene Diene Monomer (EPDM) - Neoprene Rubber, Carbon Fiber - Filled
STW4-3266	Putty and Caulking or Glazing Compounds, Other
STW4-3339	Rubber, Fluorocarbon, Elastomer; High Temperature and Compression Set Resistant
STW5-2833	TP-H1178 Propellant, Solid Rocket Motor, Igniter Space Shuttle Project
STW5-3223	Inhibitor, UF-3267, Solid Rocket Motor, Space Shuttle Projects
STW5-3224	Liner, Solid Rocket Motor, Space Shuttle Project.
STW5-3343	Propellant, Solid Rocket Motor, TP-H1148
STW7-2831 No Change	Inspection and Process Finalization Criteria, Insulated Components, Space Shuttle Solid Propellant Rocket Motor
STW7-2853	Leak Test, Pressure Transducer Assemblies, Space Shuttle Project SRM

STW7-2913	Procedure, Leak Test of Barrier-Booster Redundant Seals
STW7-3475	Leak Testing, Forward-to-Aft-Exit-Cone Joint, Space Shuttle Redesigned Solid Rocket Motor
STW7-3476	Leak Testing, Forward-End-Ring-to-Nose-Inlet Housing Joint, Space Shuttle Redesigned Solid Rocket Motor
STW7-3477	Leak Testing, Nose-Inlet-to-Throat Support Housing Joint, Space Shuttle Redesigned Solid Rocket Motor
STW7-3478	Leak Testing, Throat-Support-Housing-to-Forward-Exit-Cone Joint, Space Shuttle Redesigned Solid Rocket Motor
STW7-3632	Leak Test, Inner and Outer Igniter Joints, Space Shuttle Project Solid Rocket Motor
STW7-3633	Leak Test, S & A
STW7-3682	Leak Testing, Field and Case to Nozzle Joints
STW7-3688	Grease Application and O-Ring Installation, Field and Case to Nozzle Joints
STW7-3745	Putty, Aft Segment and Nozzle Assembly Joint, Application of
STW7-3746	Putty, Vacuum Seal, Field Joint Assembly, Application of

Documents

Title

TWR-17656	TEM-07 Flash Report
TWR-17659	Technical Evaluation Motor No. 6 (TEM-6) Final test Report
TWR-18965	Program Plan for Development and Qualification of a Second Source Rayon Supplier (1650 Denier)
TWR-19121	Predicted Ballistic Performance Characteristics for TEM-7

TWR-19524B	Program Plan for Low Cost Nozzle Improvements
TWR-19838	Technical Evaluation Motor 7 (TEM-07) Performance Information Summary
TWR-60273	TEM Postfire Engineering Evaluation Plan
TWR-60857	Cowl Vent Hole Diameter Study and TEM-2 Nozzle Boot Cavity Pressurization
TWR-61209	Postfire Hardware Special Issues TEM-7
TWR-61231	TEM-7 Seals Squeeze and Temperature Requirements
TWR-61490	TEM-7 Nozzle Quick-Look Report
TWR-61585	TEM-07 Fixed Housing Unbond Investigation